Technische Universiteit Delft

IAF Assignment Optimization for Amsterdam Airport Schiphol

Max Aalberse

TU Delft

IAF Assignment Optimization for Amsterdam Airport Schiphol

by

Max Aalberse

to obtain the degree of Master of Science
at the Delft University of Technology,

Student number: 4279611

Thesis committee:	Prof. dr. ir. J.M. (Jacco) Hoekstra,	TU Delft, supervisor
	F. (Ferdinand) Dijkstra	KDC Mainport Schiphol, supervisor
	Dr. A. (Alessandro) Bombelli	TU Delft, examiner
	Dr. O.A. (Alexei) Sharpanskykh	TU Delft, examiner

TU Delft

Contents

Abbreviations

AAS	Amsterdam Airport Schiphol
ADEP	Aerodrome of Departure
AROT	Arrival Runway Occupancy Time
ATC	Air Traffic Control
ATM	Air Traffic Management
BADA	Base of Airdraft Data
DBS	Distance Based Separation
DEST	Destination
ECMWF	European Centre for Medium-Range Weather Forecasts
ERA5	Fifth Generation ECMWF Atmospheric Reanalysis
Entry COP	Entry Co-Opereation Point
GA	Genetic Algorithm
HRSL	High Resolution Settlement Layer
IAF	Initial Approach Fix
ICAO	International Civil Aviation Organization
ICAO_ACT	ICAO Aircraft Type Designation
MIP	Mixed Integer Programming
MMO	Maximum Operating Speed Limit
MTOW	Maximum Take-off Weight
MVA	Minimum Vectoring Altitude
MZFW	Maximum Zero Fuel Weight
NAS	New And Separation Scenario
NWS	New Without Separation Scenario
OEW	Operational Empty Weight
PDE	Partial Differential Equation
ROD	Rate of Descend
SEL	Sound Exposure Level
SESAR	Single European Sky ATM Research
STAR	Standard Terminal Arrival Route
SUA	Special Use Airspace
TAS	True Airspeed
TBS	Time Based Separation
netCDF	Network Common Data Form
nextGen	Next Generation Air Transportation System

Nomenclature

$\dot{m}_{fuel_t}$	Fuel Flow at Time t	[kg/s]
η	Thrust Specific Fuel Consumption	[kg/(min*kN)]
Ψ	Factor of Importance of Emission and Noise Objective	[-]
ρ	Air Density	[kg/m^3]
C_d	Drag Coefficient	[-]
C_l	Lift Coefficient	[-]
$C_{d0_{approach}}$	Approach Configuration Zero Drag Coefficient	[-]
$C_{d0_{cruise}}$	Cruise Configuration Zero Drag Coefficient	[-]
$C_{d2_{approach}}$	Approach Configuration Lift Induced Drag Coefficient	[-]
$C_{d2_{cruise}}$	Cruise Configuration Lift Induced Drag Coefficient	[-]
$C_{d_{ap}}$	Approach Configuration Drag Coefficient	[-]
$C_{d_{cr}}$	Cruise Configuration Drag Coefficient	[-]
C_{f1}	Fuel Flow Constant 1	[-]
C_{f2}	Fuel Flow Constant 2	[-]
C_{f3}	Fuel Flow Constant 3	[-]
C_{f4}	Fuel Flow Constant 4	[-]
$C_{fcruise}$	Cruise Fuel Flow Factor	[-]
D	Drag	[N]
f_{ap}	Fuel Use during Approach	[kg/min]
f_{cr}	Fuel Flow During Cruise	[kg/s]
f_{min}	Minimum Fuel Flow	[kg/min]
f_{nom}	Nominal Fuel Use	[kg/min]
g_0	Gravity Constant	[m/s^2]
H_p	Geopotential Pressure Altitude	[m]
m	Mass	[kg]
S	Wing Surface	[m^2]
T_{HR}	Thrust	[N]
$V_{TAS_{kts}}$	True Airspeed	[kts]
W	Weight	[kg]
α_i	Amount of Time Aircraft i is Assigned to Land Early	[s]

β_i	Amount of Time Aircraft i is Assigned to Land Late	[s]
δ_{ij}	Decision Variable for Order Assignment	[-]
$\dot{x}$	East Speed Component	[m/s]
$\dot{y}$	North Speed Component	[m/s]
γ_{ij}	Decision Variable for Runway Assignment	[-]
μ_1	Minimum Distance Between Approaching Aircraft	[s]
μ_2	Aircraft Runway Occupancy Time	[s]
θ	Heading Angle	[degrees]
$AROT$	Aircraft Runway Occupancy Time	[s]
c	Communication Buffer	[s]
C_{DELAY}	Normalization Constant for Delay Objective	[-]
$C_{EMISSION}$	Normalization Constant for Emission Objective	[-]
C_{NOISE}	Normalization Constant for Noise Objective	[-]
E_i	Earliest Arrival Time for Aircraft i	[s]
F_i	Emission Objective	[kg]
g_i	Penalty Landing Early	[-]
h_i	Penalty Landing Late	[-]
L_A	A-Weighted Sound Level	[dB]
L_i	Latest Arrival Time for Aircraft i	[s]
L_{DEN}	Day-Evening-Night Average Sound Level	[dB]
M	Large Number	[-]
M_{cruise}	Cruise Speed Mach Number	[-]
MMO	Maximum Operating Speed Limit Mach Number	[-]
$MTOW$	Maximum Take-Off Weight	[kg]
MVA	Minimum Vectoring Altitude	[ft]
$MZFW$	Maximum Zero Fuel Weight	[kg]
n	Approach Path Length	[NM]
$OBJ_{L_{DEN}}$	Noise Objective	[dB]
OEW	Operational Empty Weight	[kg]
P	Amount of Aircraft in Optimization	[-]
p_{e_0}	Reference Sound Pressure	[Pa]
p_e	Sound Pressure	[Pa]
POP	Population Constant	[-]
Q	Amount of IAF in Optimization	[-]

R	Amount of Runways in Optimization	[-]
ROD	Rate of Descend	[ft/s]
S_{ij}	Minimum Separation Aircraft Landing on Same Runway	[s]
s_{ij}	Minimum Distance Between Approaching Aircraft	[NM]
s_{ij}	Minimum Separation Aircraft Landing on Different Runway	[s]
SEL	Sound Exposure Level	[dB]
SPL	Sound Pressure Level	[dB]
T_0	Time Step Size	[s]
T_i	Target Assigned Landing Time	[s]
T_{ij}	Time Based Separation Between two Approaching Aircraft	[s]
T_{ref}	Evaluated Time Span	[s]
V	Speed	[kts]
$V_{TAS_{approach}}$	True Approach Speed	[kts]
$V_{TAS_{cruise-Mcruise}}$	True Cruise Speed at Cruise Altitude	[kts]
$V_{TAS_{cruise-MMO}}$	True Maximum Operating Speed at Cruise Altitude	[kts]
w_i	Day-Evening-Night Penalty for Sound Event	[-]
W_x	East Wind Component	[-]
W_y	North Wind Component	[-]
W_{nofuel}	Estimated No Fuel Weight	[kg]
x_i	Assigned Arrival Time for Aircraft i	[s]
y_i	Fraction of Time Between E_i and L_i	[-]
z_{irq}	Decision Variable for Runway/IAF Assignment	[-]

List of Figures

List of Tables

I

Paper

IAF Assignment Optimization for Amsterdam Airport Schiphol

M.D.N. Aalberse
Supervised by: Prof. dr. ir. J.M. Hoekstra (TU Delft), F. Dijkstra (KDC Mainport Schiphol)

ABSTRACT – During the COVID-19 pandemic people living close to the airport got accustomed to less flights, and therefore less noise disturbance. Now the amount of traffic is increasing again and so is the noise disturbance.
For this research specifically the optimizing task of distributing of arriving aircraft over the IAF is addressed, as often the shortest transition routes from an IAF towards the runway go over densely populated areas, but flying via another IAF results in longer flying times and thus more CO_2 emissions. A tool that is able to quantitatively make a trade-off between noise and emission is required to provide a basis for the distribution of aircraft over the IAF.
In this research the feasibility and effects of using an expanded version of the aircraft landing problem to create the IAF Selection Optimization tool is studied, including the effects of different settings for the tool. As a case study Amsterdam Airport Schiphol is used, as it is a busy airport that lies close (11km) to the city center of Amsterdam.
In this paper first the methodology of the IAF Selection Optimization tool is explained, and afterwards the working of the tool is discussed by running various scenarios for three different days from 2019 at AAS.
For all scenarios an optimal and feasible solution was found by the tool, based on the input variables selected for each scenario. It could therefore be concluded that the IAF Selection Optimization tool provides a means to optimally distribute aircraft based over the IAF based on a quantitative trade-off.
KEYWORDS: Initial Approach Fix (IAF), Mixed Integer Programming (MIP), Aircraft Landing Problem, Air Traffic Control (ATC), Amsterdam Airport Schiphol (AAS), Noise, Emission.

1. Introduction

Over the years the amount of flights has increased generally each year, as people got accustomed to the benefits of flight. Along with the increase of the amount of flight hours come the negative aspects of flight, such as environmental impact and noise disturbance. With the challenges of global warming the environment is always a great factor in aviation, and with the recent decrease in flights due to the COVID-19 pandemic people got accustomed again to less flights and less noise, which in turn increased the discussions about noise disturbance around airports. Especially now the amount of flights are already back to pre-COVID numbers, or are quickly going there [1].

The issue addressed in this research is the balance between noise disturbance for residents surrounding a busy airport and the emissions aircraft emit into the air by flying a certain route. Special focus hereby is on the transition routes aircraft travel from the Initial Approach Fix towards the runway and the selection of the IAF. Often the shortest routes from the IAF to the runway cross heavily populated areas at a limited altitude, thus inflicting a great deal of noise disturbance on them. Flying around these areas increases flight time and thus has a greater impact on the environment and operational cost of airlines.

Much research has been performed on the runway allocation problem, but this has not been combined with an IAF selection optimization. To address the previous stated problems the IAF selection optimization will aim to provide a tool that is able to optimize between noise and emission based on their respective importance. Since the respective importance is different for each of the stakeholders this will be an input for the tool. This results in the following research goal:
The goal of this study is to research the feasibility and effectiveness of an IAF selection tool that is able to optimally distribute aircraft over the IAF based on a quantitative trade-off between noise disturbance and CO2 emissions.

As case study Amsterdam Airport Schiphol has been chosen since it is a one of the busiest airports in the world in terms of total passengers (#12 in 2019) and lies close to densely populated areas, being only 11 kilometers away from the city center of Amsterdam.

First the case study at AAS will be described, followed by the methodology. The methodology consists of two parts; the method selection, and the IAF selection tool supported by the the route optimization tool. A block diagram of the tool can be found in figure 1.1. Afterwards the results of this study are discussed, and finally the conclusion and recommendations are presented.

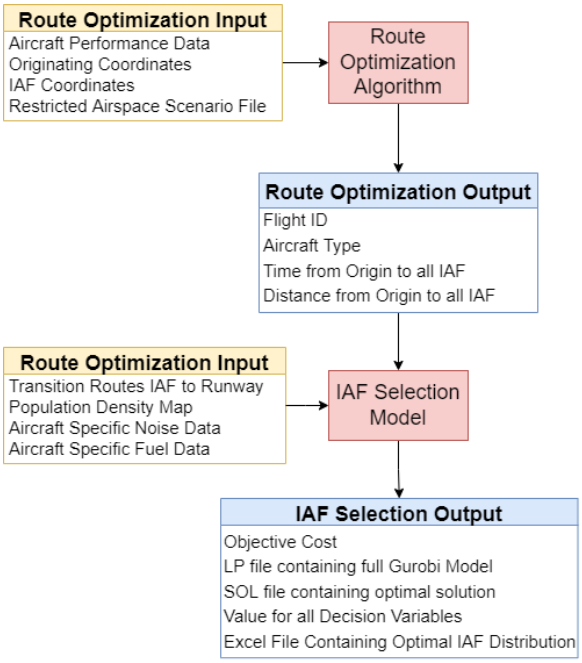

Figure 1.1: Block Diagram of IAF Selection tool

Case Study Amsterdam Airport Schiphol

Amsterdam Airport Schiphol (AAS) is the biggest airport of The Netherlands and the 3rd largest airport of Europe in terms of passengers with 71.7 million passengers in 2019 [2]. AAS has 6 runways, of which 5 are mainly used for commercial aviation and 1, the Oostbaan, mainly for general aviation [3]. Since general aviation is not handled in the same way as commercial traffic, both the Oostbaan as well as general aviation are not taken into account in this research. An overview of the runways is seen in figure 1.2.

Figure 1.2: Runway layout Amsterdam Airport Schiphol [4].

For this research several proposed changes to the Dutch airspace and its effect on AAS are taken into account [5][6]. Currently AAS has 3 Initial Approach Fixes, namely ARTIP in the North-East, RIVER in the South-West, and SUGOL in the North-West of AAS. A fourth IAF is considered in the South-East of AAS, and therefore taken into account in this research.

To get to the IAF aircraft first need to enter the Dutch airspace. This is done by flying over one of the Entry Co-Ordination Points (Entry COP) and to follow one of the Standard Terminal Arrival Routes (STAR) to the IAF. Each IAF has a designated set of Entry COP from which the IAF can be reached [7]. Since the fourth IAF does not exist yet STARs for this IAF needed to be estimated.

To get from the IAF towards the runway aircraft have to fly a transition route. Currently all runways have a transition route from (almost) all IAFs. With the restructuring of the Dutch airspace it is planned to make a strict East-West separation [6]. This would mean that, with a runway configuration of 18C and 18R for landing, aircraft entering the Dutch airspace from the East would always land on runway 18C and aircraft entering from the West on runway 18R. The reason this is done is to accommodate for so called tubes, fixed routes that aircraft must fly in to go from the IAF to the runway. The benefit of these tubes is a lower workload for the Air Traffic Controller by limiting the amount of routes and conflict areas, and a higher airspace capacity. It also provides the possibility to use curved approaches which could decrease the noise disturbance around the airport, as it would be better possible to fly around some densely populated areas and thus replace the noise heavy areas to lower populated areas. [5][6]. These new transition routes do not exist yet and therefore have to be designed. These routes do not reflect the new future transition routes, they are merely an assumption on how they could be.

For landing at AAS certain runways are designated as primary preferred runways. Routes to and from these runways pass over less densely populated areas, and thus less people are subjected to noise disturbance. The preference order can be found in table 1.1, where L1 and T1 represent the primary preferred runways for landing and takeoff respectively, and L2 and T2 the secondary. Along with the East-West separation this leads to the problem that potentially more traffic needs to land at a secondary runway, which causes more noise disturbance. With the new to be designed airspace it is intended to always have two runways open for landing as opposed to the current one or two runways.

Three days have been selected that used the preferred runway combinations for a full day in 2019 for the case study. These will be investigated into more detail to see the potential effects of these measures. The selected days are 16 September (Busy day, 762 landings), 26 October (Average day, 677 landings), and 21 March (Quiet day, 504 landings).

Table 1.1: Runway preference order [5].

Preference	Landing		Take-off	
	L1	L2	T1	T2
1	06	36R	36L	36C
2	18R	18C	24	18L
3	06	36R	09	36L
4	27	18R	24	18L
5a	36R	36C	36L	36C
5b	18R	18C	18L	18C
6a	36R	36C	36L	09
6b	18R	18C	18L	24

Traffic distribution is also an important factor for an airport, as aircraft have varying separation distance to other aircraft, and each aircraft has its own performance parameters which influence noise and emissions as well. Therefore 5 aircraft are selected to each represent one of the RECAT-EU Wake Turbulence Categories [8] based on their occurrence at AAS. In table 1.2 an overview of the selected aircraft can be found. Note that category F is neglected as this is general aviation, which is not taken into account.

Table 1.2: Distribution of arriving aircraft at Amsterdam Schiphol Airport over RECAT-EU Categories in 2019.

RECAT-EU Category	Amount	Most common type	
Cat A	808	Airbus A380-800	(100%)
Cat B	39500	Airbus A330-300	(18.8%)
Cat C	5564	Boeing B767-300	(73.3%)
Cat D	134530	Boeing B737-800	(41.4%)
Cat E	71674	Embraer EMB190	(51.9%)
Cat F/General Aviation	10599	Not Used	
Total	**265351**		

More detailed information on AAS can be found in appendix A.

Scenarios

Multiple scenarios are designed to be able to validate the tool. These scenarios are based on the current and future situation of the operations around AAS, and will be run for each of the selected days from 2019.

These scenarios are built from three binary variables that are based on the differences between the new and old airspace:

$EastWestSeparation$

If true strict East-West separation is mandatory, no aircraft is allowed to fly from a Western IAF towards an Eastern runway and vice versa. If this variable is false aircraft may arrive from any available IAF on any available runway.

$FixedRunway$

If this variable is true, then in this scenario all aircraft must land on the runway they were assigned on the day from 2019 that is being simulated. This is so that it is possible to compare with current practice. If this variable is false all aircraft have free choice of available runways.

$IAF4$

If this variable is true, then the new 4th IAF is available for arriving aircraft. If it is false the 4th IAF is not available, and thus only the three original IAF are available.

From the variables four combinations are selected as these represent the current and future practices the current and future practice of handling arriving aircraft at AAS best:

Old scenario

This scenario is based on the current practice at AAS, with no 4th IAF, fixed runway selection as it was in 2019, and no East-West separation. It is used to be able to compare the influences of the potential changes to the Dutch airspace with the current practice.

Base scenario

This scenario is the same as the old scenario, except that it does include the 4th IAF. This is so that the effect of the 4th IAF can be clearly seen, and the base scenario is used as a baseline for the effect of the other measures.

New and Separation scenario (NAS)

This scenario is meant to resemble the new airspace, with East-West separation, the 4th IAF being available, and aircraft not being held to their originally assigned runways.

New without Separation scenario (NWS)

Similar to the NAS scenario, but withour East-West separation to see the effect of this measure.

An overview of the scenarios is given in table 1.3.

Table 1.3: Variable Settings for Each Scenario

	Old	Base	NAS	NWS
$EastWestSeparation$	False	False	True	False
$FixedRunway$	True	True	False	False
$IAF4$	False	True	True	True

Also for each scenario separately, a different setting of the tool for the importance of noise disturbance compared to CO_2 emissions is available to research the effects of these settings. This is done by setting the variables $NOISE$ and $EMISSION$ to a value between 0-100% respectively. Together these variables must add up to 100%. The notation for a base scenario with equal importance of noise and emissions would therefore become $BASE_{E50\%,N50\%}$.

RECAT-EU

In order to come up with a tool that is able to approach a proper representation of the true situa-

tion around Amsterdam Airport Schiphol the separation minima are a key factor to prevent aircraft being scheduled too close to each other. For this the RECAT-EU separation criteria are used [9]. RECAT-EU is a new categorisation of aircraft, with the aim to increase runway capacity for arriving and departing flights by redefining the wake turbulence categories and their separation minima [9]. Using these minima results in a minimum amount of separation time between aircraft. The calculation of the minimal separation and more detailed information on RECAT-EU can be found in appendix B.

2. Methodology

2.1. Method Selection

Three methods are considered to be used in creating the IAF selection tool. A short description of each method and the workings will be given, more detailed information on each method can be found in appendix F.

Genetic Algorithms

Genetic Algorithms are based on the theory of evolution and mimic the workings of natural selection. The principle is that first a population is created by creating a set of possible solutions to the problem at hand. Each member of the set exists out of randomly generated values (genes) for each decision value in the tool, called the chromosome of that member. A score is then assigned to each member of the population based on its performance. In this case how well it distributes aircraft over the IAF at AAS. Based on these scores a the best scoring members of the population are selected to create the second generation of population. The selected members then procreate and produce children which inherit part of their parents genes to create a new population. It is also possible that mutations occur in the genes of the children to allow for new possible better solutions to the problem. This process is then repeated until the algorithm converges to a solution.

The benefit of GA is that it is able to solve difficult problems that other algorithms fail to solve. This is because GA is able to simultaneously test many points from all over the solution space and work with many types of data [10]. This does however result in the drawback that the tool is likely to settle for a local optimum instead of the global optimum.

Reinforcement Learning Algorithms/Q Learning

The principle of a reinforcement algorithm is an algorithm that tries to maximize its reward. The characteristics of trial and error and delayed reward are the most important distinguishing features of reinforcement learning [11]. The reinforcement algorithm that was selected is the Q-learning algorithm. The Q stands for Quality, which in this case represents the usefulness of a certain action in gaining future reward [12]. In figure 2.1 the formula on which Q-learning is based is given. Q represents the Q-table or matrix with variables [state, action], depicted by s_t and a_t respectively in the formula. The learning rate is the rate at which the tool accepts new knowledge, and the discount factor determines how important possible future gains are for the algorithm. By continuously running the algorithm ultimately an optimal path can be found.

Reinforcement learning is useful for systems that are easy to judge, but hard to specify. This is because no full mathematical model is needed, it just needs the results of actions taken. The problem with this is that it therefore needs a lot of data which must be obtained in the learning phase [13]. Another problem is that during the learning phase, it is not always clear what connections the tool makes within the data, which may lead the algorithm to do something it was not intended to do.

Mixed Integer Programming

Mixed Integer Programming is a mathematical technique where functions are minimized or maximized when subjected to various constraints. Therefore a full understanding of the problem and the influence on the outcome of each variable is required. The principle is to find an optimal feasible solution to a set of equations of which some of the variables are strictly integer or binary, while others can be any real number. The equation the tool is trying to optimize is the objective function. By changing the value of the decision variables using the branch and bound technique a global optimum can be found that also adheres to all the constraints, if a feasible solution is available. The branch and bound technique works by first removing all the integrality restrictions to find a solution to the problem, if this solution is not optimal then one or multiple decision variables are branched. Branching means creating two or more new MIP problems which exclude the infeasible solution, but do not exclude any other feasible solution [14]. In other words, extra constraints are added to limit the search area of certain variables. Continuously doing so finally results in the optimal solution to the problem.

$$Q^{new}(s_t,a_t) \leftarrow \underbrace{Q(s_t,a_t)}_{\text{old value}} + \underbrace{\alpha}_{\text{learning rate}} \cdot \overbrace{\Big(\underbrace{r_t}_{\text{reward}} + \underbrace{\gamma}_{\text{discount factor}} \cdot \underbrace{\max_a Q(s_{t+1},a)}_{\text{estimate of optimal future value}} - \underbrace{Q(s_t,a_t)}_{\text{old value}}\Big)}^{\text{temporal difference}}$$

$$\underbrace{\qquad\qquad\qquad\qquad\qquad\qquad\qquad\qquad\qquad\qquad}_{\text{new value (temporal difference target)}}$$

Figure 2.1: Q-learning formula [15].

Since a full mathematical model is required for this algorithm a full understanding of the problem is required, which is not always possible. MIP does guarantee a global optimum solution to the problem if one is available.

Method Choice
Each method was scored on their performance in the categories data availability, accuracy of solution, execution speed, and feasibility of solution. An overview of the scores can be seen in table 2.1.

Table 2.1: Score Overview of Selected Algorithms.

	GA	MIP	RL
Data Availability	+	+	--
Accuracy of Solution	-	+	0
Execution Speed	+	-	0
Feasibility of Solution	+	++	+

Reinforcement learning was discarded as an option since the data required is not available, or would take a long time and a great investment to obtain. The research was continued with both mixed integer programming, and genetic algorithms. The IAF selection tool presented was implemented using both algorithms. After implementation of the tool it was found that MIP produced such considerable better solutions, while not having a considerably higher execution time compared to GA, that GA was discarded. The GA algorithm was instead used to check solutions found in the MIP implementation of the tool, and to find mistakes in the tool itself. All results presented in this research are therefore from the MIP implementation of the tool.

2.2. IAF Selection Tool

To optimize for IAF selection while taking into account the noise produced over populated areas and the emissions as well as keeping an eye on delay, a mathematical model is created. The mathematical model used in this research is largely based upon the method proposed by Pinol and Beasley [16], which was in turn based on earlier research of Beasley [17][18][19].

2.2.1. Model

In order to be able to properly define the mathematical model it is important to state the variables used and what they entail. These variables can be considered the input of the model. They are set and are used to define the constraints and objective function later on. The input variables are as follows:

- P The amount of aircraft taken into account for this optimization
- Q The amount of initial approach fixes available
- R The amount of runways available for landing
- E_i The earliest landing time for aircraft i, with $i \in \{1 \cdots P\}$
- T_i The target landing time for aircraft i, with $i \in \{1 \cdots P\}$
- L_i The latest landing time for aircraft i, with $i \in \{1 \cdots P\}$
- S_{ij} The separation time required between aircraft i and aircraft j where i lands before j on the same runway, with $(i, j) \in \{1 \cdots P\}^2, i \neq j$
- s_{ij} The separation time required between aircraft i and aircraft j where i lands before j on a different runway, with $(i, j) \in \{1 \cdots P\}^2, i \neq j$

Using the notation provided above, separation variables S_{ij} and s_{ij} are not specifically bound to one aircraft type, but are aircraft dependent. This leaves room to account for special flight characteristics that would require a different separation time. It could for instance be used to simulate a mayday call from an aircraft resulting in a temporarily closed airspace for other aircraft. In this model however, the separation times are pre-processed using the RECAT-EU separation criteria as explained in appendix B. Currently, s_{ij} assumes a fixed separation between aircraft using different runways disregarding the runways. This works fine for the use-case of Amsterdam Airport Schiphol as a maximum of 2 runways for landings is used simultaneously, but if an airport uses more runways for landings simultaneously it can be that it is preferred to change this variable to also be runway dependent.

2.2.2. Decision Variables

The decision variables are the variables that are allowed to take on different values within set boundaries in order to find the optimal solution. For this model they are defined as follows:

$$z_{irq} = \begin{cases} 1 & \text{if aircraft } i \text{ lands on runway } r \text{ via} \\ & \text{IAF } q, i \in \{1 \cdots P\}, r \in \{1 \cdots R\}, q \in \{1 \cdots Q\} \\ 0 & \text{otherwise} \end{cases}$$

$$\gamma_{ij} = \begin{cases} 1 & \text{if aircraft } i \text{ and } j \text{ lands land on the} \\ & \text{same runway, } (i, j) \in \{1 \cdots P\}^2, i \neq j \\ 0 & \text{otherwise} \end{cases}$$

$$\delta_{ij} = \begin{cases} 1 & \text{if aircraft } i \text{ lands before aircraft } j, \\ & (i, j) \in \{1 \cdots P\}^2, i \neq j \\ 0 & \text{otherwise} \end{cases}$$

$x_i \geq 0$ The scheduled landing time for aircraft i, $i \in \{1 \cdots P\}$

2.2.3. Constraints

In order to obtain viable results, constraints need to be added to the model. These constraints prevent the

algorithm of finding optimal solutions that would not be possible in the application they are meant for.

Time window constraints
Each aircraft must land between its earliest and latest possible landing times. To guarantee this, the following constraint needs to be added:

$$E_i \leq x_i \leq L_i, \qquad \forall i \in \{1 \cdots P\} \tag{2.1}$$

This approach is used for the genetic algorithm, a more algorithmically convenient constraint is used for the mixed integer linear programming model. An extra decision variable y_i is defined which will be the proportion of the time window that has elapsed before aircraft i has landed. This is defined as follows:

$$0 \leq y_i \leq 1, \qquad \forall i \in \{1 \cdots P\} \tag{2.2}$$

$$x_i = E_i + y_i(L_i - E_i) \tag{2.3}$$

Separation time constraints
To prevent aircraft from being scheduled too close to each other and therefore possibly creating dangerous situations it is important that sufficient separation between aircraft is guaranteed. In order to know which aircraft need to have sufficient separation between them it is important to know the order of the aircraft coming to land. This can be done by a strict first come first serve principle, however this usually does not really provide an optimal solution. Therefore the order is part of the optimization. To ensure this order the following constraint is used:

$$\delta_{ij} + \delta_{ji} = 1, \qquad \forall (i,j) \in \{1 \cdots P\}^2, i \neq j \tag{2.4}$$

If aircraft i lands on the same runway as aircraft j, aircraft j land on the same runway as aircraft i.

$$\gamma_{ij} = \gamma_{ji}, \qquad \forall (i,j) \in \{1 \cdots P\}^2, i \neq j \tag{2.5}$$

Then the separation constraint must ensure that if aircraft i lands before aircraft j on the same runway, then aircraft j needs to land at least S_{ij} time after aircraft i. If they land on different runways the separation time needs to be at least s_{ij}. M is a large number that is used to ensure the constraint is met if aircraft j lands before aircraft i ($\delta_{ji} = 1$).

$$x_j \geq x_i + S_{ij}\gamma_{ij} + s_{ij}(1 - \gamma_{ij}) - M\delta_{ji}, \qquad \forall (i,j) \in \{1 \cdots P\}^2, i \neq j, M \gg 0 \tag{2.6}$$

Runway constraints
To ensure each aircraft is only assigned to one runway and IAF combination, the summation of all available combinations of IAF and runway is taken and set equal to 1 per aircraft. This ensures that each aircraft can only follow one transition route, resulting in the following constraint:

$$\sum_{q=1}^{Q} \sum_{r=1}^{R} z_{irq} = 1, \qquad \forall i \in \{1 \cdots P\} \tag{2.7}$$

If aircraft i and j land on the same runway, $\gamma_{ij} = \gamma_{ji} = 1$, then the assigned transition route for both aircraft must end at the same runway as well. Since there are multiple transition routes between the various IAFs and the selected runway the sum is taken over all the IAFs available for the given runway. Similarly, if aircraft i and j are not assigned to the same runway transition routes to the different runways must be selected. This is guaranteed by the following constraint:

$$\gamma_{ij} \geq \sum_{q=1}^{Q} z_{irq} + \sum_{q=1}^{Q} z_{jrq} - 1, \qquad \forall (i,j) \in \{1 \cdots P\}^2, i < j, r \in \{1 \cdots R\} \tag{2.8}$$

Here it can be seen that if $\gamma_{ij} = 1$, thus the aircraft land at the same runway, $\sum_{q=1}^{Q} z_{irq}$ and $\sum_{q=1}^{Q} z_{jrq}$ must be equal to 1 as well. Guaranteeing that both aircraft i and j got assigned a transition route between one of the available IAFs and selected runway r. If they are assigned different runways, $\gamma_{ij} = 0$, then $\sum_{q=1}^{Q} z_{irq}$ and $\sum_{q=1}^{Q} z_{jrq}$ may not both be 1, but one of them can be one, or they can both be 0, to guarantee that the aircraft are assigned different runways.

Scenario specific constraints
For some scenarios not all runway and IAF combinations are available for all aircraft. Therefore conditional constraints that limit the availability of these combinations must be put in place. All scenarios are explained in appendix G.
The first limitation is the availability of the 4th IAF. The 4th IAF is available in the Base, NAS, and NWS scenarios, but not for the Old scenario. Therefore the following constraint is put in place:

$$\text{If } IAF4 = True: \quad z_{irq} = 0, \qquad \forall i \in \{1 \cdots P\}, r \in \{1 \cdots R\}, q = IAF4 \tag{2.9}$$

The second limitation is that for the Old and Base scenario, all aircraft are forced to take the shortest path available to them to the runway that was assigned to aircraft i on the original landing date. This is to mimic the current practice of handling aircraft around AAS. Given that for each aircraft i there is a shortest route to the originally assigned runway $m \in \{1 \cdots R\}$ via IAF $n \in \{1 \cdots Q\}$, this leads to the following constraint:

$$\text{If } FixedRunway = True: \quad z_{irq} = 0, \qquad \forall i \in \{1 \cdots P\}, r = m, q = n \tag{2.10}$$

Finally, for the NAS scenario there is the East-West separation of transition routes, meaning no aircraft

can approach from a Western IAF towards an Eastern runway and vice-versa. Resulting in the following constraints:

$$EastRunway = [36R, 18C, 27] \tag{2.11}$$
$$WestRunway = [06, 18R, 36C]$$
$$EastIAF = [ARTIP, IAF4]$$
$$WestIAF = [SUGOL, RIVER]$$

$$\text{If } r \in EastRunway \text{ and } q \in WestIAF: \quad z_{irq} = 0, \quad \forall i \in \{1 \cdots P\} \tag{2.12}$$

$$\text{If } r \in WestRunway \text{ and } q \in EastIAF: \quad z_{irq} = 0, \quad \forall i \in \{1 \cdots P\} \tag{2.13}$$

2.2.4. Objective

The objective function is split in three different parts: The delay, CO_2 emission, and noise.

Delay

For airliners it is important that aircraft land close to their scheduled arrival time. This is to prevent passengers from missing connections, or the aircraft being delayed for the return flight. Therefore it is important to try to minimise the delay as much as possible, however arriving too early also means a higher cost for standing at the gate and probably more emitted CO_2 since the aircraft had to fly faster than expected. Thus it is preferred to land exactly at the target time T_i, or if this is not possible as close to it as possible. In order to be able to model this, 4 new variables are defined:

- $\alpha_i = \max(0, T_i - x_i)$ The time that aircraft i lands before target time T_i, $i \in \{1 \cdots P\}$
- $\beta_i = \max(0, x_i - T_i)$ The time that aircraft i lands after target time T_i, $i \in \{1 \cdots P\}$
- g_i The penalty given for every time step aircraft i lands early, $i \in \{1 \cdots P\}$
- h_i The penalty given for every time step aircraft i lands late, $i \in \{1 \cdots P\}$

Now it is possible to set the objective function for delay as follows:

$$\text{minimize} \sum_{i=1}^{P} (\alpha_i g_i + \beta_i h_i) \tag{2.14}$$

Additional constraints need to be introduced in order to link α_i and β_i to decision variable x_i:

$$x_i = T_i - \alpha_i + \beta_i, \quad \forall i \in \{1 \cdots P\} \tag{2.15}$$
$$0 \le \alpha_i \le T_i - E_i, \quad \forall i \in \{1 \cdots P\} \tag{2.16}$$
$$\alpha_i \ge T_i - x_i, \quad \forall i \in \{1 \cdots P\} \tag{2.17}$$
$$0 \le \beta_i \le L_i - T_i, \quad \forall i \in \{1 \cdots P\} \tag{2.18}$$
$$\beta_i \ge x_i - T_i, \quad \forall i \in \{1 \cdots P\} \tag{2.19}$$

Emissions

Since the goal of this research is to try and make a quantitative trade-off between CO_2 emissions and noise disturbance, it is clear that one of the key factors that must be minimized is emissions. As described in appendix C, the calculation of fuel usage is done according to equation (C.1). For each second aircraft i arrives early, α_i, the fuel used is corrected for the fuel use for flying at maximum operating speed MMO. Since only the total early arrival time is known, it first must be calculated what time the aircraft has to fly at MMO to achieve the amount of seconds arriving earlier compared to flying on cruise speed $Mcruise$, as well as the time it would have flown on $Mcruise$ given the same distance, d. This is done in equation (2.21) to equation (2.24).

$$\alpha_i = T_{Mcruise_i} - T_{MMO_i} \tag{2.20}$$

$$\begin{aligned} d &= V_{TAS_{cruise-Mcruise}} \cdot T_{Mcruise_i} \\ &= V_{TAS_{cruise-MMO}} \cdot T_{MMO_i} \end{aligned} \tag{2.21}$$

Combining these equations then gives,

$$V_{TAS_{cruise-Mcruise}} \left(\alpha_i + T_{MMO_i}\right) = V_{TAS_{cruise-MMO}} \cdot T_{MMO_i} \tag{2.22}$$

Resulting in:

$$T_{MMO_i} = \alpha_i \cdot \frac{V_{TAS_{cruise-Mcruise}}}{V_{TAS_{cruise-MMO}} - V_{TAS_{cruise-Mcruise}}} \tag{2.23}$$

And similarly:

$$T_{Mcruise_i} = \alpha_i \cdot \frac{V_{TAS_{cruise-MMO}}}{V_{TAS_{cruise-MMO}} - V_{TAS_{cruise-Mcruise}}} \tag{2.24}$$

First, it is then necessary to subtract the fuel that would have been used if the aircraft would have flown at $Mcruise$ for $T_{Mcruise_i}$ amount of time. This is done by multiplying with a fuel flow, which is assumed to be constant and is based on $W_{APPROACH}$, $V_{TAS_{cruise-Mcruise}}$, and the cruise altitude. Then the fuel used for this section of flight at MMO needs to be added. Similarly, this is done by multiplying the time it took to fly this section by the fuel flow, which is again assumed to be constant and is based on $W_{APPROACH}$, $V_{TAS_{cruise-MMO}}$, and the cruise altitude. For aircraft arriving late an estimation is made on the extra fuel used for every second of delay, β_i. A constant fuel flow is assumed, which is based on W_{LOITER}, $V_{TAS_{cruise-Mcruise}}$, and the cruise altitude. This is all performed in equation (2.25). All weight

and fuel estimation calculations are performed in appendix C.

$$
\begin{aligned}
F_i = & \qquad (2.25)\\
&\sum_{r=1}^{R}\sum_{q=1}^{Q}\left(FUEL_{APPROACH_{irq}} + \sum^{t} FUEL_{CRUISE_{t_{irq}}}\right)\cdot z_{irq}\\
&- T_{Mcruise_i}\cdot \dot{m}_{fuel_{early,Mcruise}}\\
&+ T_{MMO_i}\cdot \dot{m}_{fuel_{early,MMO}}\\
&+ \beta_i \cdot \dot{m}_{fuel_{late}}, \qquad \forall i \in \{1\cdots P\}
\end{aligned}
$$

The Emission objective[1] is then given by equation (2.26).

$$\text{minimize} \sum_{i=1}^{P} F_i \qquad (2.26)$$

Noise

In appendix D it is discussed how the amount of noise produced by a certain set of aircraft flying a certain route is calculated. This results in a $OBJ_{L_{DEN}}$ for each location on the grid. The goal is to minimise the noise disturbance for residents in the neighborhood of the airport. Therefore it should be prevented that highly populated areas are also areas with a lot of aircraft noise. If a large amount of noise would be created over scarcely populated areas, fewer people have hinder of it, thus this is more preferable than a large amount of noise over densely populated areas. Of course, the goal remains to minimise the total amount of people who are severely hindered by aircraft noise. This results in equation (2.28), with X and Y being the size of the grid and $POP(x,y)$ the population grid.

$$OBJ_{L_{DEN}} = \sum_{i=1}^{F} 10^{\frac{SEL_i + w_i}{10}} \qquad (2.27)$$

$$\text{minimize} \sum_{x=1}^{X}\sum_{y=1}^{Y} OBJ_{L_{DEN}}(x,y)\cdot POP(x,y) \qquad (2.28)$$

Full objective

Now that the various parts have been discussed they can be added together to form the full objective function. To prevent certain elements of the objective function dominating the outcome of the model they can all be normalized. To be able to do so an extra constant has been added before each part of the objective function. Furthermore a constant Ψ is introduced to be able to vary the importance of the noise and emission part of the objective. The full objective function then becomes:

$$
\begin{aligned}
&\text{minimize:} \qquad (2.29)\\
&C_{DELAY}\sum_{i=1}^{P}(\alpha_i g_i + \beta_i h_i) + C_{EMISSION}\cdot\Psi\sum_{i=1}^{P} F_i\\
&+ C_{NOISE}\cdot(2-\Psi)\sum_{x=1}^{X}\sum_{y=1}^{Y} OBJ_{L_{DEN}}(x,y)\cdot POP(x,y)
\end{aligned}
$$

where Ψ can take any number between and including 0 and 2. ($\Psi = [0,2]$)

For clarity Ψ has been replaced by $EMISSION$ and $NOISE$. These variables have values ranging between 0% and 100%, based on the value of Ψ. If $\Psi = 0$, then the noise and emission part of the objective function exist for 0% of the emission objective, and therefore the variable $EMISSION = 0\%$. Similarly this shows that the noise and emission part of the objective function exists for 100% out of the noise objective, and thus $NOISE$ would take the value of 100%. If $\Psi = 1$, the noise and emission part of the objective function exists out of equal parts for the noise and emission objectives, and thus $EMISSION = NOISE = 50\%$. The calculation for all values for Ψ can be found below.

$$EMISSION = \frac{\Psi}{2}\cdot 100\% \qquad (2.30)$$

$$NOISE = \frac{2-\Psi}{2}\cdot 100\% \qquad (2.31)$$

2.3. Route Optimization

To be able to perform the weight and fuel calculations it is required to know the flown path of the aircraft. The originally flown paths of the aircraft are not known. Also an optimal route to all the available IAFs is required to be able to optimally distribute aircraft over the IAF. Therefore the flown routes have to be approximated. This is done by creating a moving front route optimization algorithm based on the research of Girardet [21]. The exact working of the moving front algorithm is explained in appendix E.

The algorithm was set to only optimize the route within the optimization area, since otherwise the computational time would become too large. After consideration with members from the industry a distance of 1000km from AAS is assumed to be the maximum distance the Dutch air traffic control has influence on the route and speed of the aircraft. The optimization area is therefore set to be a square around AAS with a minimal distance of 1000km towards the borders. Within the borders of the optimization area Special Use Airspaces are defined, these SUA are prohibited areas for commercial aircraft and thus the algorithm takes this into account and let the aircraft fly

[1] In the IAF selection model the fuel use is directly used, to get to the CO_2 emitted this value needs to be multiplied by 3.16 [20]. This has no effect of the working or the outcome of the model.

around these areas. Outside the optimization area it is assumed that aircraft fly the shortest path towards AAS at a constant airspeed.

2.4. Verification & Validation

The verification and validation of the IAF Optimization Model is found in appendix H. Only one discrepancy was found during this process, where one of the runs failed to produce a solution. It could be proven that the overlapping previous and following runs produce a viable solution, and therefore the failed run was not found to be an issue to the working of the full model.

3. Results

The results of the performance of each of the scenarios for the noise and emission objective cost can be found in figure 3.1, figure 3.2, and figure 3.3 for each of the selected days respectively. For these figures it is important to note that a decrease in noise and emission results in a more favorable solution, as the aim is to minimize both. The delay objective cost is not shown in these figures as for none of the scenarios this was found to be more than an average deviation of 2 minutes per aircraft, which is the time window currently used by AAS for arriving aircraft. Therefore it is assumed that this does not have significant influence on the selection of the scenarios. For the objective function however the delay objective cost remains important as it assures the tool tries to keep aircraft at their originally assigned landing times. In figure 3.1, figure 3.2, and figure 3.3 the red line indicates the Pareto optimal front. The Pareto front shows all Pareto optimal scenarios, this means that for these scenarios it is not possible to select another scenario which is better for all stakeholders [22]. The effects of the various scenarios combined with the prioritization between noise and emission on the solutions produced by the tool are discussed in detail in appendix G for the Pareto optimal scenarios as well as the $BASE_{E50\%,N50\%}$ and $OLD_{E50\%,N50\%}$ scenarios. In appendix G.6.1 the Pareto optimal optimizations for a busy day can be found, in appendix G.6.2 for an average day, and in appendix G.6.3 for a quiet day. In this section the general performance of the tool will be discussed.

Scenario Objective Costs for a Busy Day

For the busy day in figure 3.1 it can be seen that the base scenario scores better than the old scenario on both the noise objective cost and the emission objective cost. The NAS scenarios also all perform better than the old scenario on both emission and noise. Compared to the base scenario all NAS scenarios still perform better on the noise objective cost, but only 3 out of the 5 scenarios also perform better on the emission objective cost. For the NWS scenarios only the scenario fully optimized for the emission objective cost has a lower emission objective cost than the base scenario, but at the cost of a slightly higher noise objective cost. All other NWS scenarios have a considerably lower noise objective cost compared to the base scenario, but also all have a higher emission objective cost.

Scenario Objective Costs for an Average Day

For the average day in figure 3.2 it can be seen that the base scenario performs better than the old scenario on both the noise objective cost and the emission objective cost as well. Compared to both the base and old scenario all NAS and NWS scenarios provide a significant decrease in the noise objective cost, but only the scenarios fully optimized for the emission objective cost also provides a decrease in emission objective cost for both the NAS and NWS scenarios.

Scenario Objective Costs for a Quiet Day

For the quiet day in figure 3.3 it can be seen that the base and old scenario score almost identical, with the base performing slightly better on both the noise, and emission objective cost. All NAS scenarios provide a solution with a lower emission objective cost compared to the base and old scenario, but at the cost of a much higher noise objective cost. For the NWS scenarios it is seen that the scenario fully optimized on the emission objective cost indeed has the best score for the emission objective cost, but at the cost of a much higher noise objective cost compared to the base and old scenario. The other NWS scenarios provide a significant decrease in noise objective cost while being almost equal on the emission objective cost compared to the base and old scenario.

In general it can be seen for all scenarios, that when the importance of noise goes up, the noise objective cost goes down. Similarly this also holds for the emission objective cost.

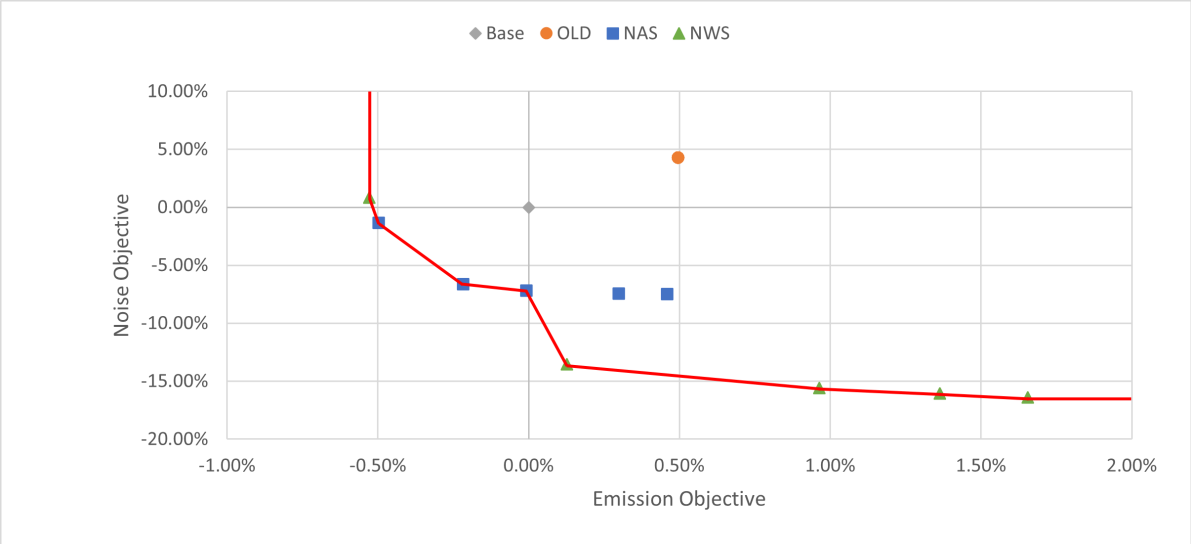

Figure 3.1: Pareto Optimal Solutions for 16 September 2019.

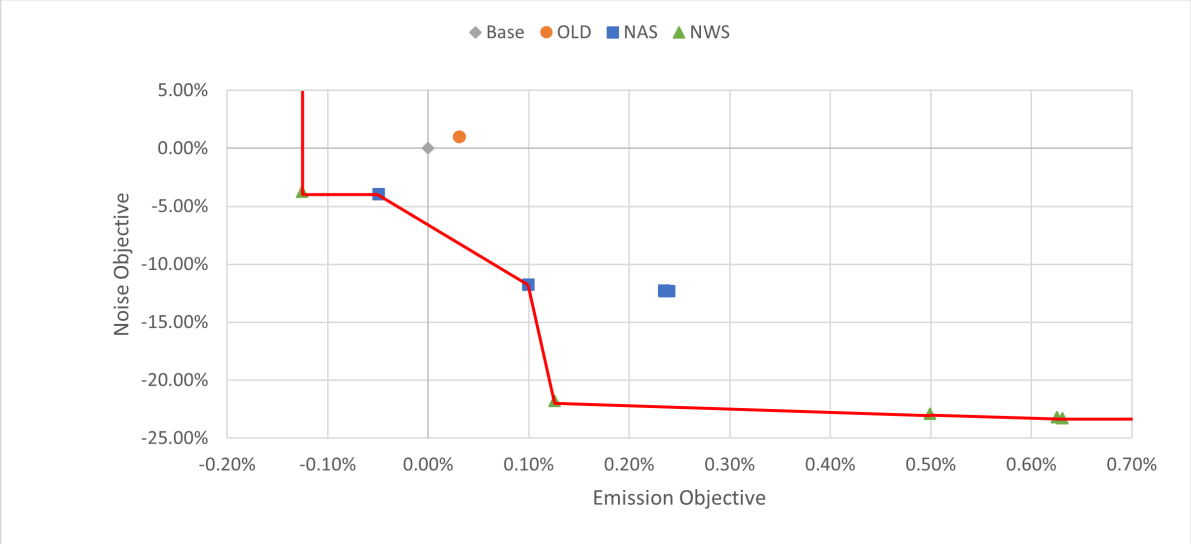

Figure 3.2: Pareto Optimal Solutions for 26 October 2019.

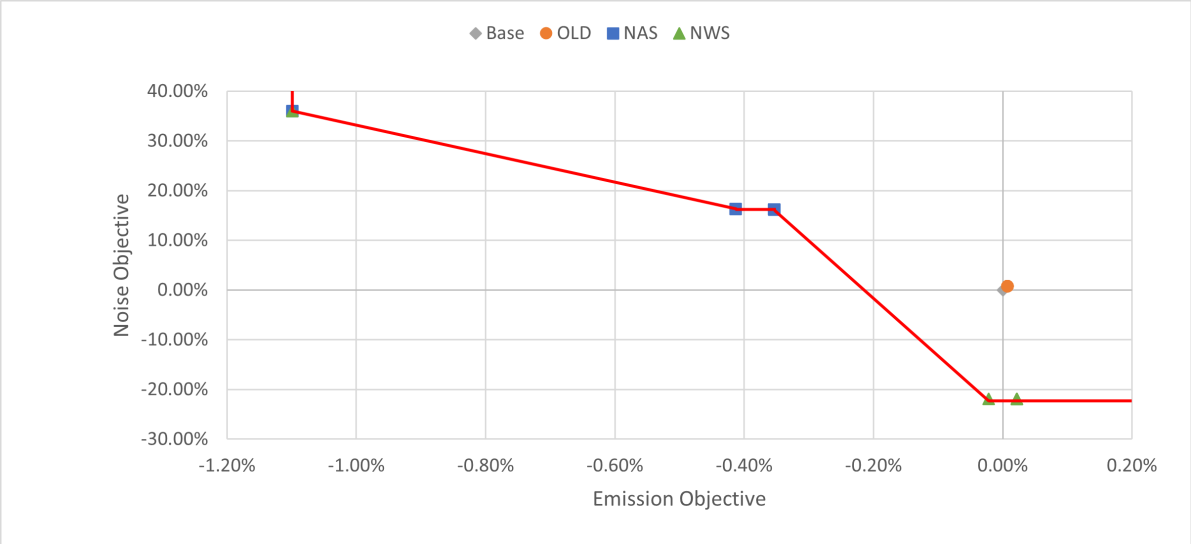

Figure 3.3: Pareto Optimal Solutions for 21 March 2019.

In the next section the effects of the various scenarios on the busy day will be presented. The other scenarios are discussed in appendix G.

3.1. Busy Day, 16 September 2019

Noise

From the Noise Objective costs as seen in figure 3.1 it is very clear that when the Noise Objective becomes more important the costs go down, which is exactly as expected. However, when looking at figure 3.4 this does not hold for the amount of people experiencing a certain threshold value. This is because the Noise Objective does not optimise for only these groups, but for all people affected by noise emitted around AAS. This could therefore mean that for the tool it is more beneficial to reduce noise for a large group that was already below the 48+dB(A) threshold at the cost of slightly more people inside the 48+dB(A) threshold area. One of the reasons for this is to prevent the tool of allowing large amounts of people just below these threshold values.

An example of what this looks like can be seen in figure 3.5. Here the $BASE_{E50\%,N50\%}$ scenario is shown with the scenario with the lowest noise cost ($NWS_{E0\%,N100\%}$) and how they compare to the $BASE_{E50\%,N50\%}$ scenario. From the noise contour it can be seen that especially over higher populated areas $NWS_{E0\%,N100\%}$ performs considerably better as it aims to stay away from these areas, which are indicated by the grey areas in the comparison figure. All noise contours for each scenario can be found in appendix I.1.

In general it can be stated that all scenarios perform better than the $OLD_{E50\%,N50\%}$ Scenario. The addition of the 4th IAF alone can result in a decrease of 4.3% point as seen when comparing the $OLD_{E50\%,N50\%}$ Scenario with the $BASE_{E50\%,N50\%}$ Scenario. This does however comes at the cost of an increased amount of people that experience the average threshold levels of 48+dB(A) and 58+dB(A).

Combining the extra IAF with NAS ($NAS_{E50\%,N50\%}$, $NAS_{E75\%,N25\%}$, $NAS_{E100\%,N0\%}$) has the potential to further decrease the Noise Objective cost with 7.17% point, while also decreasing the amount of people experiencing the threshold levels compared to the $OLD_{E50\%,N50\%}$ scenario, especially in the 58+dB(A) region.

Looking at the NWS scenarios it is seen that an even bigger potential decrease can be achieved of 16.38% point when compared to the $BASE_{E50\%,N50\%}$ scenario, while scoring even better in the 48+dB(A) threshold area than the NAS scenarios. The 58+dB(A) NWS scenarios perform approximately equal to the NAS scenarios. An important note to make here is that it is unlikely that the NWS scenarios are feasible for a busy day as explained in appendix G.4.

Emissions and Flighttime

The Emission Objective costs can also be found in figure 3.1. Similar to the Noise Objective the costs go down when the objective becomes more important. From the indexed values it shows that the total difference in emitted CO_2 differs from 0.53% point ($NWS_{E100\%,N0\%}$) below the $BASE_{E50\%,N50\%}$ scenario to 1.66% point above it, as can also be seen in figure 3.6. What also stands out from this graph is that the flighttime follows almost the same trend as the emissions, which of course is not very strange since if an aircraft flies longer it also uses more fuel, and thus emits more CO_2 since the Emission Objective is directly related to the fuel use of an aircraft.

The reason that the difference in Emission Objective cost between the various scenarios is limited compared to the Noise objective is that where the full noise cost is calculated within the section between the IAF and the Runway, the emitted CO_2 is calculated for the whole flight, thus resulting in smaller deviations in the final number. But since the total amount of CO_2 emitted during a day is a high number this still has a considerable impact as a 1% point difference could mean an increase or decrease of the CO_2 emitted of approximately 255,000 kg on a busy day.

In general it can be stated that adding the 4th IAF results in a CO_2 reduction of 0.49% point, as seen by looking at the $BASE_{E50\%,N50\%}$ and $OLD_{E50\%,N50\%}$ scenario. When looking at the NAS scenarios it is seen that all have a lower or comparable amount of emissions compared to the $BASE_{E50\%,N50\%}$ scenario. The NWS scenarios clearly show more variation, with espacially $NWS_{E0\%,N100\%}$, $NWS_{E25\%,N75\%}$, and $NWS_{E50\%,N50\%}$ having a higher emission cost compared to both the $BASE_{E50\%,N50\%}$ and $OLD_{E50\%,N50\%}$ scenarios. The reason for this is simple since with adding more options comes the availability of choosing less noise costly routes, but at the cost of a longer flighttime and emission cost.

For the flighttime similar trends are found.

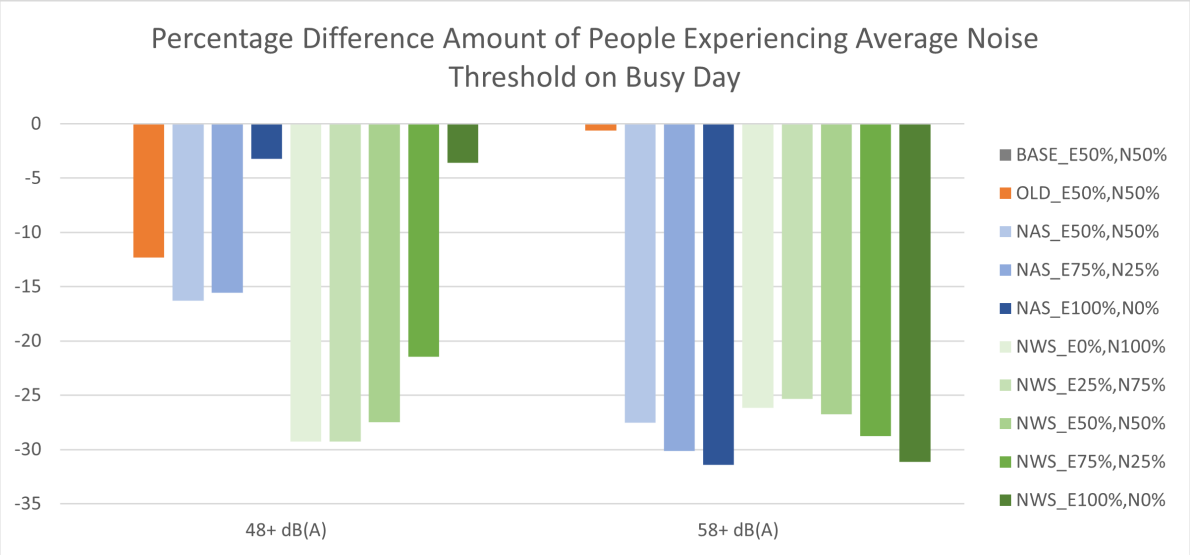

Figure 3.4: Percentage Difference Amount of People Experiencing Average Noise Threshold Compared to $BASE_{E50\%,N50\%}$ Scenario on a Busy Day (16 September 2019).

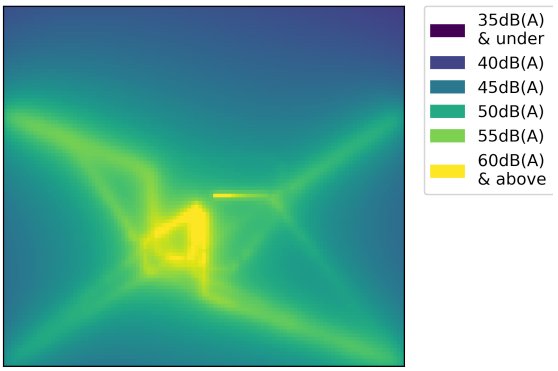

(a) L_{DEN} Average for $BASE_{E50\%,N50\%}$.

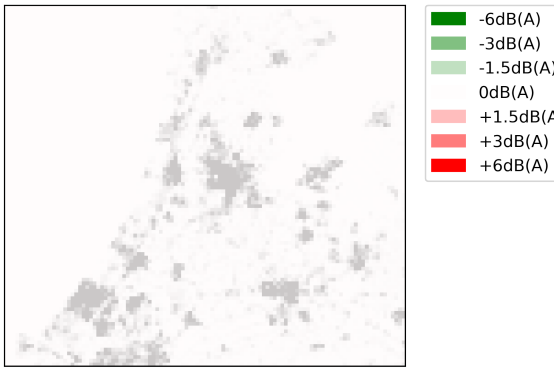

(b) Change in L_{DEN} Average Compared to $BASE_{E50\%,N50\%}$ for $BASE_{E50\%,N50\%}$.

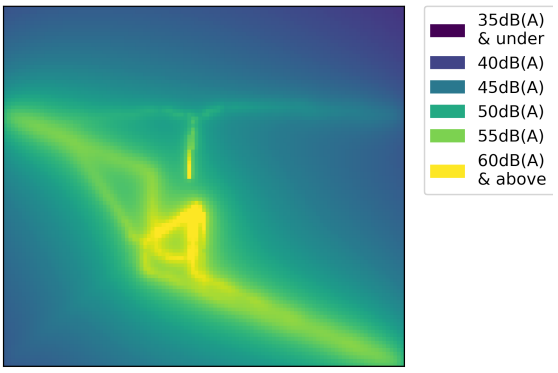

(c) L_{DEN} Average for $NWS_{E0\%,N100\%}$.

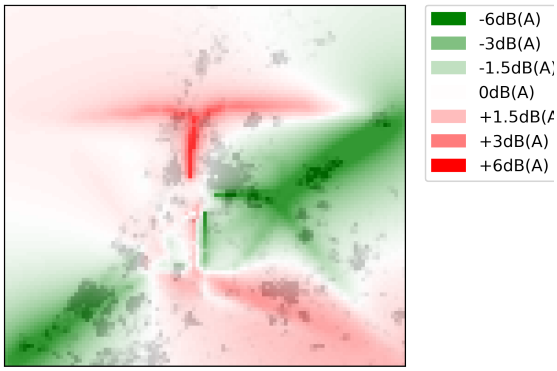

(d) Change in L_{DEN} Average Compared to $BASE_{E50\%,N50\%}$ for $NWS_{E0\%,N100\%}$.

Figure 3.5: Example L_{DEN} Noise Contours for a Busy Day, 16 September 2019.

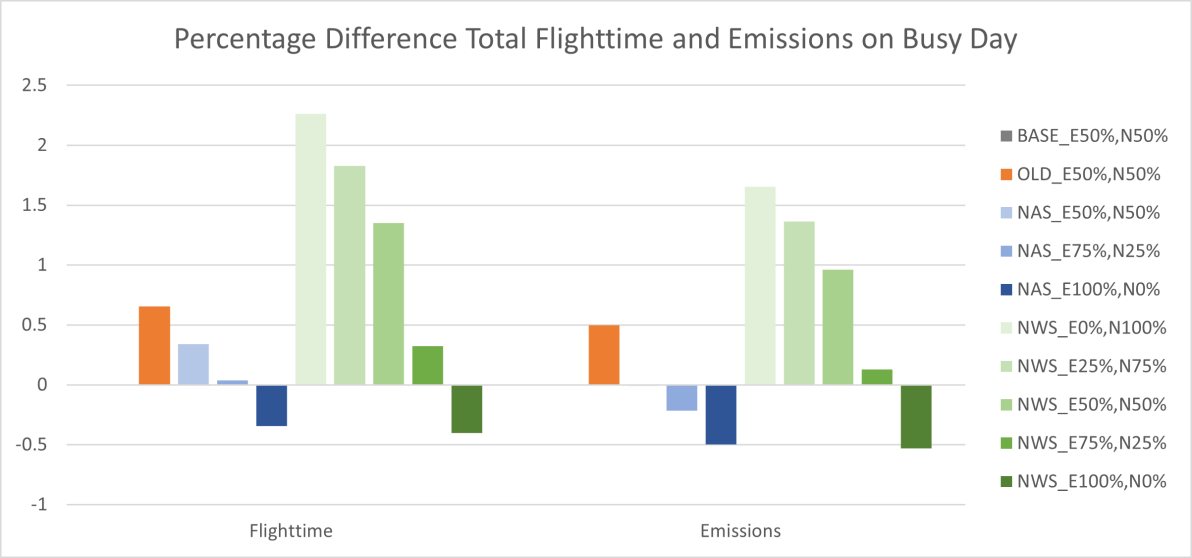

Figure 3.6: Percentage Difference Total Flighttime and Emissions Compared to $BASE_{E50\%,N50\%}$ Scenario on a Busy Day (16 September 2019).

4. Discussion

The goal of this research can be split into two questions. The first question would be:
Is it feasible to create an IAF selection tool that optimally distributes the aircraft over the IAFs based on a quantitative trade-off between noise disturbance and CO2 emissions?

The outcome of this research is an improved version of the solution to the aircraft landing problem as proposed by Pinol and Beasley [16]. Their method only provided the basic concept to a solution of the aircraft landing problem, such as guaranteed separation and runway assignment. This research proves that it is possible to expand this method by taking into account the flight path the aircraft needs to take to arrive at the most optimal runway, the IAF and transition routes, noise disturbance from these routes, the emissions from aircraft flying these routes, all while adhering to the minimal safety margins required.
It can thus be concluded that the Mixed Integer Programming tool as proposed in section 2.2 is able to provide this parameterized tool capable of optimally distributing aircraft over the IAFs based on a quantitative trade-off between noise and CO_2 emissions. The tool however does prove to be close to its current computational capabilities as small changes to the original tool were required to be able to obtain feasible and optimal results. The main example for this being the reduction of the time of each increment run, limiting the time an aircraft can deviate from it's originally assigned landing time to 15 minutes plus or minus. This was found to be of no problem for this research, but increased complexity and therefore computational requirements could prove this to become a problem. Future research should therefore look to further optimize the running of the tool to minimize the required computational power.

The second question can then be formulated as:
Is the IAF selection tool effective to reduce noise disturbance around airports while keeping the increase in environmental impact at a minimum?

To answer this question it is important to know that quite a broad array of assumptions had to be made, which might influence the outcome of the tool and therefore the findings of this research. One very big factor in this is the unknown planned fixed transition routes for AAS, and the effect of the planned so called curved approaches [6]. This lead to the assumption to keep as close as possible to the current approaches for AAS, but since AAS currently does not use fixed approaches this is still only an approximation of the current practice. This also lead to the problem that there is no data on fixed approaches as they are not used, meaning the results from the Old scenario, as proposed in appendix G to be as close to the current practice, could in fact still be off by quite a margin. Another big uncertainty is the location, and therefore the routes to and from, the 4th IAF. Currently its final position is not fixed and thus for this research an assumption for this needed to be made. Other restrictions of the tool that could possibly influence the feasibility or the outcome of the tool are discussed in section 4.1. In general it is assumed that this tool and the findings thereof are close to what these would be

if the changes in the Dutch airspace were in place for the investigated days.

As seen in appendix G, for each of the days investigated there the Base scenario always performs better than the Old scenario, which is assumed to be close to current practice, for the used objective functions in the tool. This implies that adding the extra IAF results in a better solution. What stands out is the significant difference in delay objective cost for all the scenarios, but since for all scenarios and days this stays well below the current planning window of 2 minutes this is not expected to be a significant problem. Also, there is a large variation is the noise objective cost as seen in figure 3.1, figure 3.3, and figure 3.2. This implies that the various scenarios presented provide large gains or losses compared to the Base scenario depending on the scenario selected. For the emission cost it stands out that the differences are relatively small, but this is mainly because the whole flight is taken into account and only a part of the flight path is altered to provide the various options. For the NWS scenarios it is however not known if they are feasible on every day, as they inflict more workload on the ATC, and it is unlikely that they are able to be implemented for the busy and average days. This is because in this research the curved approach is not taken into account, nor the departing traffic. It is expected that implementing the NWS scenario with these would lead to too many conflict areas. For the Quiet day however it is expected that this should be possible as there is plenty of capacity on the runways, as is illustrated by the very low cost for delay. For this day it is also important that NWS is available, otherwise it is expected that with the new Dutch airspace the results will be worse compared to the current practice. Further investigation is required to when NWS would be viable and when NAS would be the only option. Interesting would then also be to see if it is possible to combine the two on a single day, resulting in using NWS in quiet hours and NAS during the busy hours of a day and if this would be desirable for all stakeholders.
In general, it can be concluded that the tool is able to provide a solution that reduces the noise disturbance around airports while keeping the environmental impact at a minimum, since for all days there is a scenario available that performs better than the Base and Old scenario for both the noise and emission objective costs. If all stakeholders were to accept a small increase in CO_2 even larger gains in reducing the noise objective cost can be achieved. However, the final choice on which scenario would fit which day the best is one that cannot be made solely on these scores, as the decision of the valuation of either the noise and emission objective cost is a political one. They in no way compare to each other and thus makes it impossible to make a decision based on these numbers. These are merely to give an indication of the various options at hand, and to possibly assist in making the final decisions.

4.1. Restrictions and Assumptions

IAF Capacity

For this research the capacity availability for each IAF was not taken into account. The reason for this is that capacity for IAFs is capped at a certain amount of flights per IAF per hour, which is quite hard to quantify for individual aircraft. Therefore it was assumed that with at most 2 runways open for landing at any time and 3 or 4 available IAFs this would not lead to significant problems. On a rare occasion however not taking into account the IAF capacity might render a solution infeasible. It is assumed that this would be able to be avoided by allowing one or more aircraft to divert from the fixed transition route to fit in between the other aircraft, as it is known that for the actual landing on the runway the capacity constraint is met.

Noise Disturbance from Delay

The noise disturbance around the airport is only taken into account for aircraft flying the transition route between the IAF and the runway. However, since aircraft that are assigned a delay are assumed to take this delay either by holding at the IAF or by given a vector close to the IAF, this will have an impact on the perceived noise and thus disturbance directly below and around the IAF. It is not expected that this difference is very large, but since it is not investigated the exact difference is unknown.

Maximum 15 Minutes Diversion from Original Landing Time

Due to limitations in the computational power available the tool is currently not able to allow for aircraft landing more than 15 minutes early or late. This is no problem for this research or tool since it works with actual landing data on the investigated days, but if the tool were to be used to assign aircraft to a time slot for the future it is not possible for the tool to cope with aircraft that have significant delay, or that arrive much earlier than expected.

Departing Traffic

Departing traffic is not taken into account, thus possible found solutions might not be viable due to conflicting departures. This means that the current tool is not accurate enough to fully state that the solution presented would also be fully feasible. As stated before it is assumed that for the Busy and Average day the NWS scenario would create too much workload

for ATC to be used in combination with departing aircraft. This would need to be implemented into the tool to see if this would actually be feasible.

Wind and Weather
It was found that including wind for the current tool would require way too much computational power. Therefore the decision was made that for this research the wind and weather would not be included in the tool. For future research this would be an important aspect of further research as it could significantly improve the the accuracy of aircraft arriving times.

5. Conclusion

For years the market for commercial air travel was only increasing, especially before the COVID-19 global pandemic. Even though the pandemic put a temporarily halt to the growth of air traffic, the markets are growing back to their size before the pandemic quickly [1]. This brings back all the problems of an increasingly more busy airport for its surroundings, especially now a lot of people experienced how it would be if there was less traffic and therefore less disturbance around the airport. This ignites the discussion between an airport that wants to expand and the surrounding residents that do not want an increase in noise. To accommodate both less noise costly approach and departure routes are investigated, but often these routes result in higher emissions due to longer flighttimes. However with the growing knowledge of the effect of CO_2 emissions on the Earth this is also not desirable.
The goal of this research is therefore stated as follows: *The goal of this study is to research the feasibility and effectiveness of an IAF selection tool that is able to optimally distribute aircraft over the IAF based on a quantitative trade-off between noise disturbance and CO2 emissions.*

This research shows that it is feasible to create an IAF selection tool by presenting a mathematical formulation for the IAF selection tool. In combination with a mixed integer programming algorithm this research shows that the IAF selection tool is able to optimally distribute aircraft over the IAF based on a quantitative trade-off between noise disturbance and CO2 emissions.
It is also proven that this approach is effective, as depending on the selected scenario and day possible noise reductions up to 24% compared to the current practice are found, whereas for emissions reductions up to 1% are found. Also solutions that show a significant decrease in both noise and emissions were found by the IAF selection tool, therefore proving that using such a tool could provide benefits for all stakeholders.

6. Recommendations

Implementation of Departing Aircraft
To see if the results of the tool are actually viable the departing traffic must also be implemented. Until then it is impossible to fully guarantee that the outcome and findings of the tool are actually viable and feasible for real world application. In future research this must therefore be taken into account.

Decrease Computational Weight of Tool
As stated in section 4.1 the reason that aircraft are currently only available to divert 15 minutes from their originally assigned landing time is because the tool is close to its current computational limits. Implementing departing traffic will only increase the computational weight of the tool, and therefore it is very important that during future research extra resources are spent to minimize the computational weight of the tool to guarantee the tool keeps working properly. If this is not possible or the achieved decrease is not enough other optimization algorithms must be considered again.

Machine Learning Tool
At the beginning of this research the use of a machine learning tool during this research was deemed infeasible due to the lack of data. With the tool presented in this research it would become possible to create the required data. This could then be used to base a machine learning algorithm tool upon. The benefit of this is that the machine learning tool is expected to be much faster than the mixed integer programming method as it does not have to calculate every variable for each flight, but instead makes an estimation based on historic data. This allows for quick reruns of the tool to allow for last minute changes to the plan, therefore making the tool viable to be used as a real time planning aid for ATC.

Effect Fixed Transition Routes
This research uses fixed transitional routes as they are planned on being used for AAS in the future redesign of the Dutch airspace. Currently however AAS does not use fixed transition routes, and therefore it would be interesting to investigate what the sole effect of implementing these transition routes would be. It is at least expected to increase noise disturbance for people living under the fixed transition routes, as they will have more aircraft flying directly above their heads. However, if these routes are able to be lead in such a way that they hardly fly over anyone, then a large group of people will potentially benefit from the decreased noise disturbance as fewer aircraft fly close to their homes.

Implementation of Noise Disturbance on Other Factors, Such as Nature Preserves

Currently the tool only takes into account the noise disturbance for people living in the surroundings of AAS. There are however more areas that are vulnerable to noise disturbance, such as nature preserves. In future research limitation could be set on the amount of noise a certain area is allowed to perceive on average during a day.

Bibliography

[1] Allianz Global Corporate & Specialty, "Aviation trends post Covid-19: Nine issues to watch as the industry prepares for take-off," 2021.

[2] Amsterdam Airport Schiphol, "Traffic and transport figures," https://www.schiphol.nl/en/schiphol-group/page/transport-and-traffic-statistics/, Accessed: 2021-06-21.

[3] Luchtverkeersleiding Nederland, "Integrated Aeronautical Information Package," https://www.lvnl.nl/eaip/2021-06-03-AIRAC/html/index-en-GB.html, Accessed: 2021-06-21.

[4] "Amsterdam Airport Schiphol," http://www.vliegtuigenspotter.nl/spotters-info/amsterdam-airport-schiphol-ehamams/, Accessed: 2021-06-23.

[5] Schiphol Group, *Nieuw Normen en Handhavingstelsel Schiphol*, 2016.

[6] Luchtverkeersleiding Nederland, "Programma Luchtruimherziening, discussion paper v3, Buizenconcept en baangebruik," 2020.

[7] Luchtverkeersleiding Nederland, "IAF and STAR Amsterdam Airport Schiphol," www.lvnl.nl/eaip/2019-08-01-AIRAC/graphics/eAIP/EH-AD-2.EHAM-STAR.pdf, Accessed: 2021-06-23.

[8] EASA, "Assignment Of Aircraft Types To RECAT-EU Wake Turbulence Categories," https://www.easa.europa.eu/sites/default/files/dfu/datasheet_-_assignment_of_icao_aircraft_types_to_recat-eu_wake_turbulenc.pdf, Accessed: 2021-06-24.

[9] Rooseleer, F. and Treve, V., ""RECAT-EU" European Wake Turbulence Categorisation and Separation Minima on Approach and Departure," 02 2018.

[10] Haupt, R. and Haupt, S., "Practical Genetic Algorithms," 1998.

[11] Sutton, R. and Barto, A., *Reinforcement Learning, second edition: An Introduction*, The MIT Press, 2018.

[12] Violante, A., "Simple Reinforcement Learning: Q-learning," https://towardsdatascience.com/simple-reinforcement-learning-q-learning-fcddc4b6fe56, Accessed: 2021-02-25.

[13] Aggarwal, C., *Neural Networks and Deep Learning*, Springer, 2018.

[14] Hoffman, K. and Padberg, M., "Combinatorial and Integer Optimization," http://www.esi2.us.es/~mbilbao/combiopt.htm, Accessed: 2021-03-09.

[15] Zitter, L., "What Is Reinforcement Learning?" https://www.springboard.com/blog/reinforcement-learning/, Accessed: 2021-02-25.

[16] Pinol, H. and Beasley, J., "Scatter Search and Bionomic Alghorithms for the aircraft landing problem," *European Journal of Operational Research*, , No. 171, 2006, pp. 439–462.

[17] Beasley, J., Krishnamoorthy, M., Sharaiha, Y., and Abrahamson, D., "Scheduling aircraft landings - The static case," *Transportation Science*, , No. 34, 2000, pp. 180–197.

[18] Beasley, J., Krishnamoorthy, M., Sharaiha, Y., and Abrahamson, D., "Displacement problem and dynamically scheduling aircraft landings," *Journal of the Operational Research Society*, , No. 55, 2004, pp. 54–64.

[19] Beasley, J., Sonander, J., and Havelock, P., "Scheduling aircraft landings at London Heathrow using a population heuristic," *Journal of the Operational Research Society*, , No. 52, 2001, pp. 483–493.

[20] Environmental and Energy Study Institute, "Fact Sheet | The Growth in Greenhouse Gas Emissions from Commercial Aviation (2019)," https://www.eesi.org/papers/view/fact-sheet-the-growth-in-greenhouse-gas-emissions-from-commercial-aviation, Accessed: 2022-02-14.

[21] Girardet, B., Lapasset, L., Delahaye, D., Rabut, C., and Bernier, Y., "Generating Aircraft Trajectories with respect to Weather Conditions," *ISIATM*, July 2013, 2nd International Conference on Interdisciplinary Science for Innovative Air Traffic Management, hal-00867818.

[22] Pardalos, P. M. and Du, D.-Z., "PARETO OPTIMALITY, GAME THEORY AND EQUILIBRIA," *Springer*, Vol. 17, 2007.

[23] Meteoblue, "Climate Amsterdam Airport Schiphol," https://www.meteoblue.com/en/weather/historyclimate/climatemodelled/amsterdam-airport-schiphol_netherlands_6296680, Accessed: 2021-06-23.

[24] KDC Mainport, "Speed And Route Advisor (SARA)," https://kdc-mainport.nl/wp-content/uploads/2009/09/CONOPS-SARA-v-1.0.pdf, Accessed: 2021-06-23.

[25] Bouwels, B., *Off-Idle Continuous Descent Operations at Schiphol Airport*, Master's thesis, Delft University of Technology, 2021.

[26] Eurocontrol, "COVID-19 impact on the European air traffic network," https://www.eurocontrol.int/covid19, Accessed: 2021-08-05.

[27] van der Meijden, S., *Improved Flexible Runway Use Modeling*, Master's thesis, Delft University of Technology, 2017.

[28] Luchtverkeersleiding Nederland, *Minimum Vectoring Altitudes*, 2021.

[29] Lamers, M., *Enhanced Runway Capacity at Airports with Complex Runway Layouts*, Master's thesis, Delft University of Technology, 2016.

[30] Eurocontrol Experimental Centre, "User Manual for the Base of Aircraft Data (BADA) REVISION 3.8," EEC Technical/Scientific Report No. 2010-003, 2010, Accessed: 2022-02-16.

[31] Facebook Connectivity Lab and Center for International Earth Science Information Network - CIESIN - Columbia University, "High Resolution Settlement Layer (HRSL)," https://towardsdatascience.com/simple-reinforcement-learning-q-learning-fcddc4b6fe56, 2016, Source imagery for HRSL © 2016 DigitalGlobe, Accessed: 2021-02-25.

[32] Eurocontrol Experimental Centre, "The Aircraft Noise and Performance (ANP) Database : An international data resource for aircraft noise modellers," https://www.aircraftnoisemodel.org/, Accessed: 2021-08-09.

[33] Ruijgrok, G., *Elements of aviation acoustics*, Delft University Press, 1993.

[34] Sethian, J. and Vladimirsky, A., "Ordered upwind methods for static Hamilton-Jacobi equations," *Proceedings of the National Academy of Sciences*, 2001.

[35] Sethian, J. and Vladimirsky, A., "Ordered upwind methods for static Hamilton-Jacobi equations: Theory and algorithms," *SIAM Journal on Numerical Analysis*, 2003.

[36] Darwin, C., *The origin of the species by means of natural selection*, 1859.

[37] "Introduction to Genetic Algorithms," https://towardsdatascience.com/introduction-to-genetic-algorithms-including-example-code-e396e98d8bf3#:~:text=A%20genetic%20algorithm%20is%20a,offspring%20of%20the%20next%20generation., Accessed: 2021-02-19.

[38] Rocha, M. and Neves, J., "Preventing premature convergence to local optima in genetic algorithms via random offspring generation," *Lecture Notes in Computer Science (including subseries Lecture Notes in Artificial Intelligence and Lecture Notes in Bioinformatics)*, Vol. 1611, 1999, pp. 127–136.

[39] Russell, S. and Norvig, P., *Artificial Intelligence: A Modern Approach*, Prentice Hall, 2010.

[40] Françoise, V., Fonteneau, R., and Ernst, D., *How to Discount Deep Reinforcement Learning: Towards New Dynamic Strategies*, 2015.

[41] The Pennsylvania State University, "A Brief Introduction to Linear Programming," `https://www.courses.psu.edu/for/for466w_mem14/Ch11/HTML/Sec1/ch11sec1.htm`, Accessed: 2021-03-08.

[42] Land, A. and Doig, A., *An automatic method for solving discrete programming problems*, Econometria, 1960.

[43] Vielma, J., *MIXED INTEGER LINEAR PROGRAMMING FORMULATION TECHNIQUES*, 2014.

[44] Gurobi, "Mixed Integer Programming Basics," `https://www.gurobi.com/resource/mip-basics/`, Accessed: 2021-03-09.

[45] Sen, S. and Sherali, H., *A BRANCH AND BOUND ALGORITHM FOR EXTREME POINT MATHEMATICAL PROGRAMMING PROBLEMS*, 1985.

[46] Ministerie voor Infrastructuur & Waterstaat, *Ontwerp-Voorkeursbeslissing Luchtruimherziening*, 2021.

[47] Kuendee, P. and Janjarassuk, U., *A Comparative Study of Mixed-Integer Linear Programming and Genetic Algorithms for Solving Binary Problems*, IEEE, 2018.

[48] Rieser, V., Robinson, D., Murray-Rust, D., and Rounsevell, M., *A Comparison of Genetic Algorithms and Reinforcement Learning for Optimising Sustainable Forest Management*, 2011.

[49] Xiang, Z., *A comparison of genetic algorithm and reinforcement learning for autonomous driving*, 2019.

II

Appendices

A

Case Study Amsterdam Airport Schiphol

Amsterdam Airport Schiphol (AAS) is the biggest airport of The Netherlands and the 3rd largest airport of Europe in terms of passengers with 71.7 million passengers in 2019 [2].

A.1. Airport Layout

AAS has 6 runways, of which 5 are mainly used for commercial aviation and 1, the Oostbaan, mainly for general aviation [3]. In table A.1 an overview of all the runways is given.

Table A.1: Runways Amsterdam Airport Schiphol.

Name	Runway direction/code	Length	Width	Surface
Polderbaan	18R/36L	3,800 m	60 m	Asphalt
Kaagbaan[1]	06/24	3,439 m	45 m	Asphalt
Buitenveldertbaan[1]	09/27	3,453 m	45 m	Asphalt
Aalsmeerbaan[1]	18L/36R	3,400 m	45 m	Asphalt
Zwanenburgbaan	18C/36C	3,300 m	45 m	Asphalt
Oostbaan[1, 2]	04/22	2,020 m	45 m	Asphalt

[1] Prohibited (landing and take-off) for aircraft with a MTOM exceeding 600,000 kg
[2] Prohibited for ICAO/EASA code letter F aircraft

The reason that AAS has so many runways (and also with various headings) is twofold. For one, you need a certain amount of capacity to process a certain amount of flights, but also due to the relatively strong winds and the changing heading of these winds. Especially when compared to other airports with all parallel runways like Atlanta Heartsfield Jackson it is clear from figure A.1 that AAS does not only have more variation in wind heading, but that the winds are also much more powerful. The layout of the runways can be seen in figure A.2.

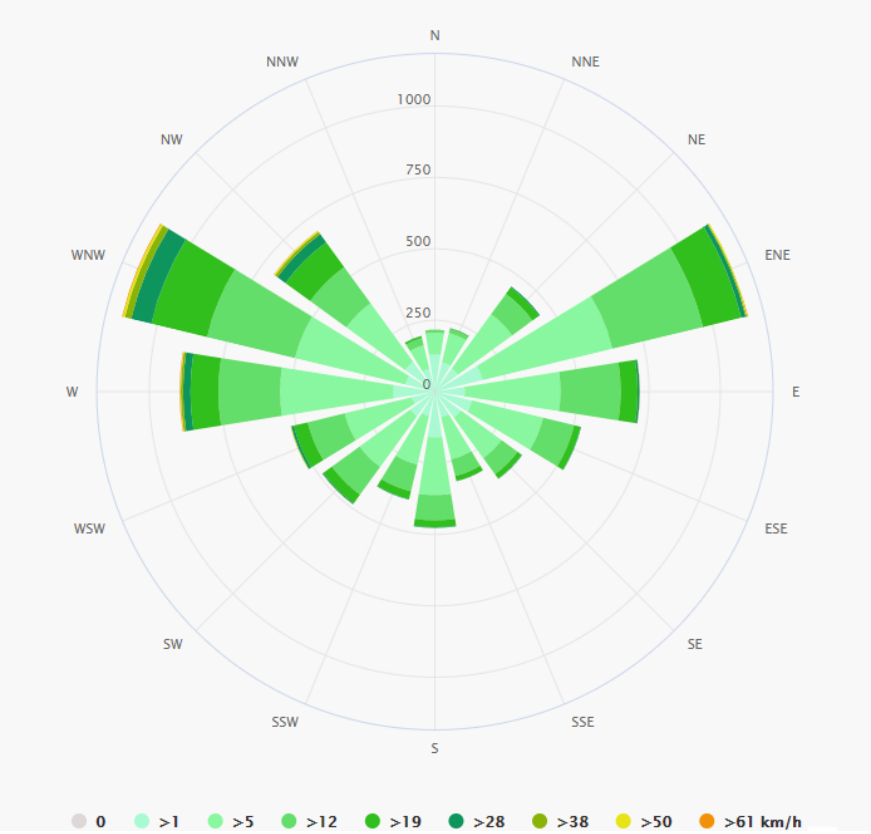

(a) Windrose Hartsfield–Jackson Atlanta International Airport.

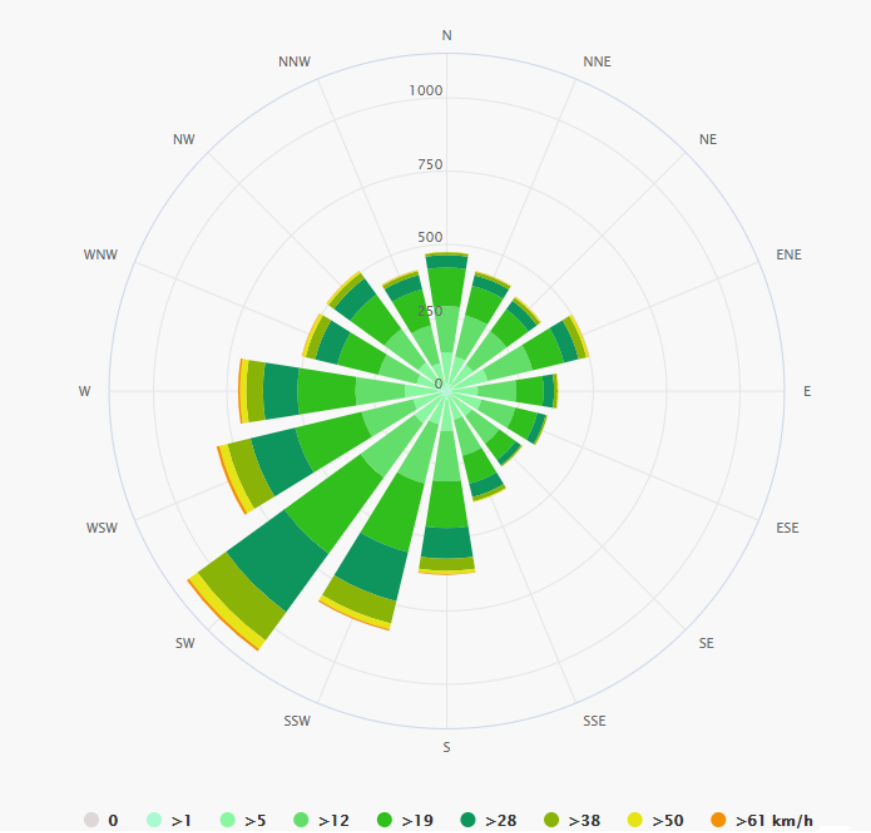

(b) Windrose Amsterdam Airport Schiphol.

Figure A.1: Wind speed, direction and duration for Atlanta and Amsterdam [23].

Figure A.2: Runway layout Amsterdam Airport Schiphol [4].

A.2. Initial Approach Fix

Currently AAS has 3 IAFs, namely RIVER above the harbor of Rotterdam, SUGOL out of the coast of IJmuiden and ARTIP close to Lelystad, as can also be seen in figure A.3. For this research also a fourth IAF will be considered as this new IAF will be added with the new layout of the Dutch airspace [5]. No information on the exact location of this IAF is currently known, but looking at the layout of the other IAFs it is likely that it will be placed somewhere above a low populated area in the province of Noord-Brabant. To be able to come up with a viable solution to the problem the future location of this fourth IAF has been estimated for this study. It is important to note that this is in no way based on official resolutions regarding the redesign of the Dutch airspace. An overview of the current IAFs and their coordinates is given in table A.2. In the new to be designed airspace it is likely that the position of the current IAFs will shift somewhat. Therefore and for practical reasons, the assumption was made that the 4 IAFs would make a perfect rectangle. This results in the used locations of the IAFs in this research as can be seen in table A.3

Table A.2: Current Initial Approach Fixes for Amsterdam Airport Schiphol.

IAF	Coordinates	Restrictions
RIVER	51.91278, 4.13250	FL070 - FL100 MAX 250KIAS
SUGOL	52.52556, 3.96722	FL070 - FL100 MAX 250KIAS
ARTIP	52.51121, 5.56908	FL070 - FL100 MAX 250KIAS

Table A.3: Assumed New Initial Approach Fixes for Amsterdam Airport Schiphol, Not Based on True Data.

IAF	Coordinates	Restrictions
RIVER	51.910, 3.970	FL100 MAX 250KIAS
SUGOL	52.520, 3.970	FL100 MAX 250KIAS
ARTIP	52.520, 5.570	FL100 MAX 250KIAS
IAF4	51.910, 5.570	FL100 MAX 250KIAS

A.3. Standard Arrival Route

To get to the IAF aircraft first need to enter the Dutch airspace. This is done by flying over one of the Entry Co-Ordination Points (Entry COP) and to follow one of the Standard Terminal Arrival Routes (STAR) to the IAF. Each IAF has a designated set of Entry COP from which the IAF can be reached [7]. An Entry COP thus only serves one IAF. Since the fourth IAF does not exist yet the position of the Entry COPs needed to be estimated. An overview of the Entry COPs, the IAF they serve and their coordinates can be found in table A.4. For Entry COP Eelde/EEL it is important to note that it is not on the border of the airspace and actually has multiple ways from the border to get to EEL [7]. These are taken into account in the model. An overview of the current EntryCOPs, STARs and IAFs can be seen in figure A.3. Note that STAR PESER is not in table A.4 as this STAR would be in the way for the 4th IAF and already has an infrequent availability due to the presence of interfering traffic from Eindhoven Airport.

Table A.4: Entry COP Coordinates for Amsterdam Airport Schiphol.

IAF	Entry COP	Coordinates
RIVER	DENUT	51.23612, 3.65760
	HELEN	51.23531, 3.86971
	PUTTY	51.36585, 4.33761
SUGOL	LAMSO	52.73290, 2.99436
	MOLIX	52.80000, 3.06867
	REDFA	51.84806, 1.93556
	TOPPA	53.40250, 3.56139
ARTIP	Eelde/EEL	53.12500, 6.58333
	NORKU	52.21556, 6.97639
	Rekken/RKN	52.09413, 6.72328
4th IAF	All aircraft crossing the Dutch border between 51.29688, 5.21331, and 52.14626, 6.8789 are allowed to use IAF4.	

A.4. Transition Routes

Currently all runways have a transition route from (almost) all IAFs. With the restructuring of the Dutch airspace it is planned to make a strict East-West separation [6]. This would mean that, with a runway configuration of 18C and 18R for landing, aircraft entering the Dutch airspace from the East would always land on runway 18C and aircraft entering from the West on runway 18R. The reason this is done is to accommodate for so called tubes that aircraft must fly in to go from the IAF to the runway. The benefit of these tubes is a lower workload for the Air Traffic Controller by limiting the amount of routes and conflict areas, and a higher airspace capacity. It also provides the possibility to use curved approaches which could decrease the noise disturbance around the airport, as it would be better possible to fly around some densely populated areas [5][6]. These new transition routes do not exist yet and therefore have to be designed. These routes do not reflect the new future transition routes, they are merely an assumption on how they could be.

Besides the curved approach, the Continuous Descent Approach will also be an important factor in the new system [6]. CDA is already a common approach for AAS, as it has the benefit of aircraft flying at a higher altitude for a longer time and then start a continuous near idle glide towards the runway. Compared to the classic stepped approach this helps in reducing the noise disturbance as well as the aircraft not only fly higher on average, but also with a lower thrust setting at lower altitudes, thus also reducing noise and emissions. A clear visualization of this can be found in figure A.4.

For landing at Schiphol certain runways are designated as primary preferred runways. This is because they have little population in their final approach path and therefore create less noise disturbance compared to other runways. This preference for landing and take-off can be seen in table A.5, where L1 and T1 represent the primary preferred runways for landing and takeoff respectively, and L2 and T2 the secondary. In table A.5 it can be seen that for preference 1, 2, 3, 5b, and 6b the Western runways 06 and 18R are the most preferred runways. This results along with the strict East-West separation into the problem that all traffic coming from the East needs to land at a secondary preferred runway, potentially resulting in more noise disturbance [6]. Similarly this holds for preference 4, 5a, and 6a where the preferred runway is in the East of the airport, and with the East-West separation cannot be reached from a Western IAF.

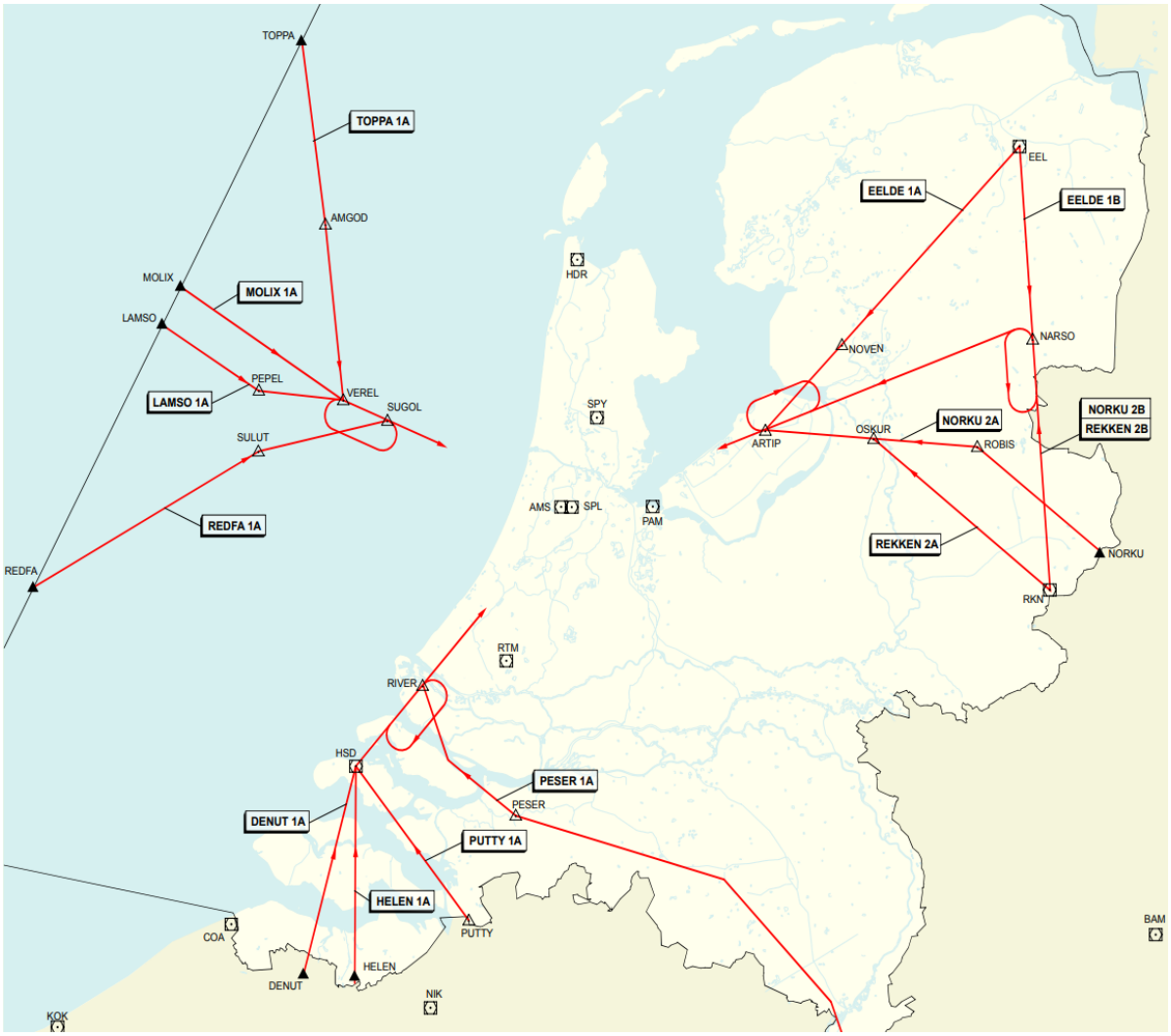

Figure A.3: Initial Approach Fixes and Standard Terminal Arrival Routes Amsterdam Schiphol Airport [24].

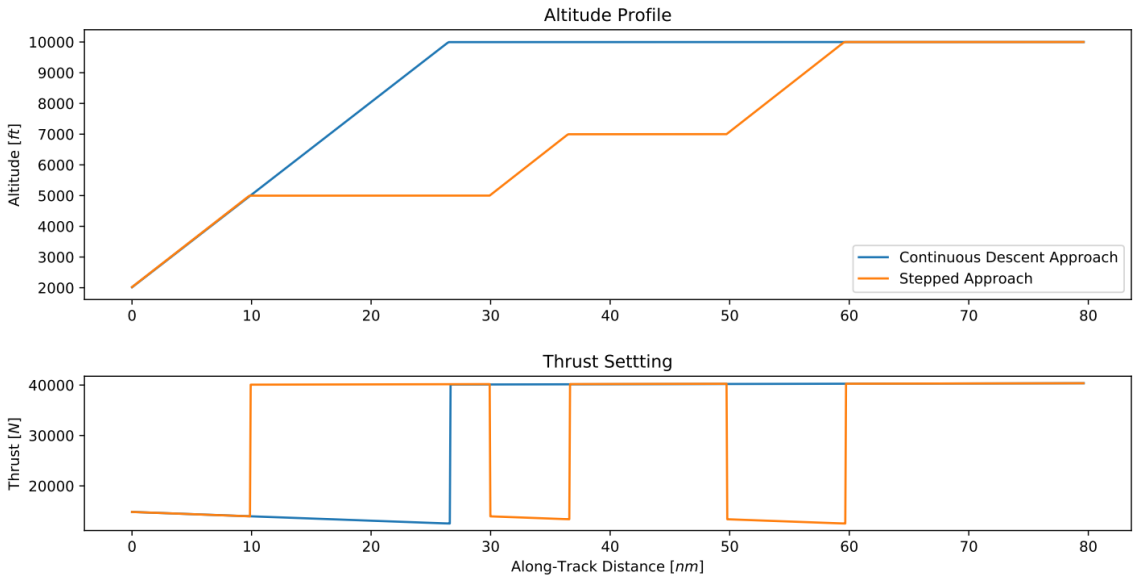

Figure A.4: Comparison between Continuous Descent and Stepped Approach [25].

Table A.5: Runway preference order [5].

Preference	Landing		Take-off	
	L1	L2	T1	T2
1	06	36R	36L	36C
2	18R	18C	24	18L
3	06	36R	09	36L
4	27	18R	24	18L
5a	36R	36C	36L	36C
5b	18R	18C	18L	18C
6a	36R	36C	36L	09
6b	18R	18C	18L	24

A.5. Traffic

Traffic distribution is also an important factor for an airport as aircraft have a certain minimal separation based on their weight classification. This also determines airport capacity, which will be discussed in greater detail in appendix B. Larger aircraft also create more noise and therefore it could be beneficial to send those to a primary preferred runway. For the year 2019 all landings are categorized in the RECAT-EU Wake Turbulence Categories [8]. In table A.6 an overview of this distribution can be seen. Note that category F is neglected as this is all general aviation and this is not handled in the same way as commercial traffic (separate runway) at AAS. Also a most common type with a corresponding percentage of the share it has within it's RECAT-EU category is given as an indication of the type of aircraft within a category. As simplification the most common type of a category will represent all aircraft within a category. In the model category A will not be considered as in the entirety of 2019 only 0.3% of all flights were of this type.

Scenarios

For the model it is important to have representative data to validate the potential findings. Therefore three different scenario files are selected. Because of the international pandemic caused by COVID-19 years 2020 and 2021 are not representative due to the drop in flights during these years [26]. Therefore the final year before the pandemic reached Europe 2019 was used to obtain scenarios for the model. The most busy, average, and least busy day in case of aircraft landing movements are selected from days that solely used the preferred runway combinations from table A.5. The most busy day in case of aircraft landings was found to be the 16th of September with 762 movements, the average day was found to be the 26th of October with 677 movements and the least busy day was found to be the 21st of March with 504 movements. The distribution per hour over

Table A.6: Distribution of arriving aircraft at Amsterdam Schiphol Airport over RECAT-EU Categories in 2019.

RECAT-EU Category	Amount		Most common type	
Cat A	808	(0.3%)	Airbus A380-800	(100%)
Cat B	39500	(15.0%)	Airbus A330-300	(18.8%)
Cat C	5564	(2.1%)	Boeing B767-300	(73.3%)
Cat D	134530	(51.2%)	Boeing B737-800	(41.4%)
Cat E	71674	(27.3%)	Embraer EMB190	(51.9%)
Cat F/General Aviation	10599	(4.0%)		
Total	**265351**			

the days can be found in table A.7, table A.8 and table A.9 respectively.
With the new to be designed airspace it is intended to always have two runways open for landing (table A.5), as opposed to the current one or two runways. Based on the actual runway use of the 3 scenarios a runway availability is made with the runway preferences taken into account. An overview of this can be found in table A.10

Table A.7: Amount of aircraft arriving at Amsterdam Airport Schiphol per hour on 16 September 2019.

Time	**Arrivals**	**Time**	**Arrivals**	**Time**	**Arrivals**	**Time**	**Arrivals**
00:00-01:00	1	06:00-07:00	67	12:00-13:00	36	18:00-19:00	40
01:00-02:00	0	07:00-08:00	42	13:00-14:00	64	19:00-20:00	31
02:00-03:00	4	08:00-09:00	34	14:00-15:00	27	20:00-21:00	24
03:00-04:00	11	09:00-10:00	53	15:00-16:00	30	21:00-22:00	17
04:00-05:00	12	10:00-11:00	33	16:00-17:00	43	22:00-23:00	11
05:00-06:00	52	11:00-12:00	54	17:00-18:00	69	23:00-00:00	7

Total amount of arriving aircraft on 16 September 2019 was 762 (Excl landings on 04-22)

Table A.8: Amount of aircraft arriving at Amsterdam Airport Schiphol per hour on 26 October 2019.

Time	**Arrivals**	**Time**	**Arrivals**	**Time**	**Arrivals**	**Time**	**Arrivals**
00:00-01:00	1	06:00-07:00	65	12:00-13:00	31	18:00-19:00	27
01:00-02:00	0	07:00-08:00	41	13:00-14:00	57	19:00-20:00	16
02:00-03:00	3	08:00-09:00	36	14:00-15:00	20	20:00-21:00	22
03:00-04:00	9	09:00-10:00	54	15:00-16:00	22	21:00-22:00	3
04:00-05:00	15	10:00-11:00	35	16:00-17:00	33	22:00-23:00	17
05:00-06:00	44	11:00-12:00	53	17:00-18:00	62	23:00-00:00	11

Total amount of arriving aircraft on 26 October 2019 was 677 (Excl landings on 04-22)

Table A.9: Amount of aircraft arriving at Amsterdam Airport Schiphol per hour on 21 March 2019.

Time	**Arrivals**	**Time**	**Arrivals**	**Time**	**Arrivals**	**Time**	**Arrivals**
00:00-01:00	2	06:00-07:00	31	12:00-13:00	28	18:00-19:00	34
01:00-02:00	0	07:00-08:00	34	13:00-14:00	22	19:00-20:00	28
02:00-03:00	1	08:00-09:00	29	14:00-15:00	32	20:00-21:00	19
03:00-04:00	6	09:00-10:00	34	15:00-16:00	30	21:00-22:00	21
04:00-05:00	10	10:00-11:00	33	16:00-17:00	21	22:00-23:00	10
05:00-06:00	20	11:00-12:00	33	17:00-18:00	21	23:00-00:00	5

Total amount of arriving aircraft on 21 March 2019 was 504 (Excl landings on 04-22)

Table A.10: Overview of runway use for all 3 scenarios.

21 March		**16 September**		**26 October**	
Time	**Runway**	**Time**	**Runway**	**Time**	**Runway**
00:00-23:59	27 + 18R	00:00-05:00	06 + 36R	00:00-21:50	18R + 18C
		05:00-11:50	36R + 36C	21:50-23:59	27 + 18R
		11:50-20:20	06 + 36R		
		20:20-23:59	27 + 18R		

A.6. Performance Specifications Selected Aircraft

In this section the performance parameters for the aircraft selected in appendix A.5 are given.

	Airbus A380-800	Airbus A330-300	Boeing 767-300	Boeing 737-800	Embrear E190
ICAO designation	A388	A333	A763	B738	E190
RECAT-EU	A	B	C	D	E
MMO [-]	0.89	0.86	0.86	0.82	0.82
M_{cruise} [-]	0.85	0.81	0.8	0.79	0.78
Cruise altitude [ft]	43100	41000	43100	41000	41000
$V_{TAS_{cruise-MMO}}$ [kts]	510	493	493	470	470
$V_{TAS_{cruise-Mcruise}}$ [kts]	488	465	459	453	447
$V_{TAS_{approach}}$ [kts]	131	147	140	140	140
Weight					
OEW [kg]	271000	118189	87135	41480	27900
$MTOW$ [kg]	540000	217000	156489	78220	50460
$MZFW$ [kg]	356000	169000	126099	61680	50460
Design Fuel [kg]	216275	70786	44559	21540	13000
Design Payload [kg]	52725	28025	27795	15200	9560
W_{nofuel} [kg]	323725	146214	111930	56680	37460
Aerodynamics					
$C_{d0_{cruise}}$ [-]	1.8130E-02	1.9805E-02	2.4934E-02 [1]	2.5452E-02	2.4800E-02
$C_{d2_{cruise}}$ [-]	4.3198E-02	3.1875E-02	3.9630E-02 [1]	3.5815E-02	4.2903E-02
$C_{d0_{approach}}$ [-]	3.2800E-02	5.5500E-02	5.1890E-02 [1]	4.9200E-02	4.6748E-02 [2]
$C_{d2_{approach}}$ [-]	5.2800E-02	3.2500E-02	4.0100E-02 [1]	4.2400E-02	4.8738E-02 [3]
S [m2]	845.00	361.60	283.35	124.65	92.53
Fuel					
C_{f1}	5.4336E-01	6.1503E-01	6.3947E-01 [1]	7.0057E-01	6.8190E-01
C_{f2}	8.6622E+02	9.1903E+02	1.1403E+03 [1]	1.0681E+03	8.2377E+02
C_{f3}	6.4145E+01	2.1033E+01	1.5664E+01 [1]	1.4190E+01	1.1196E+01
C_{f4}	7.4435E+04	1.1223E+05	-3.328E+05 [1]	6.5932E+04	8.9804E+04
$C_{f_{cruise}}$	9.3051E-01	9.3655E-01	9.5439E+01 [1]	9.2958E-01	9.7996E-01
Noise					
Idle Thrust [lb]	10915	4572	4200	649	1080
Noise Level Idle Thrust at 1000ft [dB]	87.9 [4]	86.9 [4]	86.7 [4]	82.7 [4]	82.0 [4]

[1] Due to probable wrong coefficients, as explained in appendix C, coefficients of a similar aircraft are used; the Airbus A310

[2] No data for approach on E190, taken factor 1.885 times $C_{d0_{cruise}}$, based on other AC

[3] No data for approach on E190, taken factor 1.136 times $C_{d2_{cruise}}$, based on other AC

[4] Obtained by interpolating various thrust settings

B

RECAT-EU Separation

In order to come up with a model that is able to approach a proper representation of the true situation around Amsterdam Airport Schiphol the separation minima are a key factor to prevent aircraft being scheduled too close to each other. For this the RECAT-EU separation criteria are used [9].

B.1. How RECAT-EU works

RECAT-EU is a new categorisation of aircraft, with the aim to increase runway capacity for arriving and departing flights by redefining the wake turbulence categories and their separation minima [9]. RECAT-EU is based on the ICAO categories for separation which uses the Maximum Take Off Mass to classify aircraft in 3 categories: Light, Medium and Heavy (4 if the A380-800 is considered as separate category). The Light category is designated for aircraft below 7 tons MTOM, Medium for all aircraft between 136 tons and 7 tons, and the Heavy for aircraft over 136 tons. Since especially the Medium and Heavy classification have a large span of MTOM lots of aircraft have to keep a higher separation than would strictly be required to be safe. A reclassification thus can contribute to a higher runway capacity. Taking the example of a B767-300 with a trailing A340-600, a separation of 4 nautical miles is required since they are both in the ICAO categorisation Heavy. With the RECAT-EU approach this would be reduced to 2.5NM since the B767-300 is much smaller and lighter than the A340-600, therefore making it safe to trail closer. RECAT-EU has 6 categories named A to F which are not only based on the Maximum Take Off Weight, but also on the wingspan of an aircraft, as this for a great deal also influences the wake vortex an aircraft creates. In figure B.1 the categorisation process for assigning aircraft can be found.

B.2. RECAT-EU Separation Minima

With the new categories come new separation minima as discussed in the previous section. There are two different ways to approach separation. One is Distance-Based Separation (DBS) and the other is Time-Based Separation (TBS). For approaching aircraft TBS is based on DBS by calculating the minimal time aircraft should be apart from each other based on the speed of the two aircraft and the minimal distance between the two during landing. A trailing aircraft that is slower than the leading aircraft can thus leave the IAF on a shorter distance than prescribed (still 1000ft vertically separated) since the leading aircraft will gain ground and at touchdown the perfect separation is achieved. This way, a higher capacity can be reached than when the minimal distance is already enforced when departing from the IAF. Similarly, a faster trailing aircraft must leave more space when departing from the IAF to not come too close to the leading aircraft. The minimum distance between approaching aircraft can be found in table B.1. The bracketed values indicate the minimum radar separation as is applicable per current ICAO doc 4444 provisions [9]. In order to go from DBS to TBS equation (B.1) can be used.

$$\mu_1 = \frac{n + s_{ij}}{V_j} - \frac{n}{V_i} \tag{B.1}$$

Another important factor in separation for approaching aircraft is the runway occupancy time. The runway occupancy time is dependent on several factors. Many of these have to do with aircraft characteristics, how-

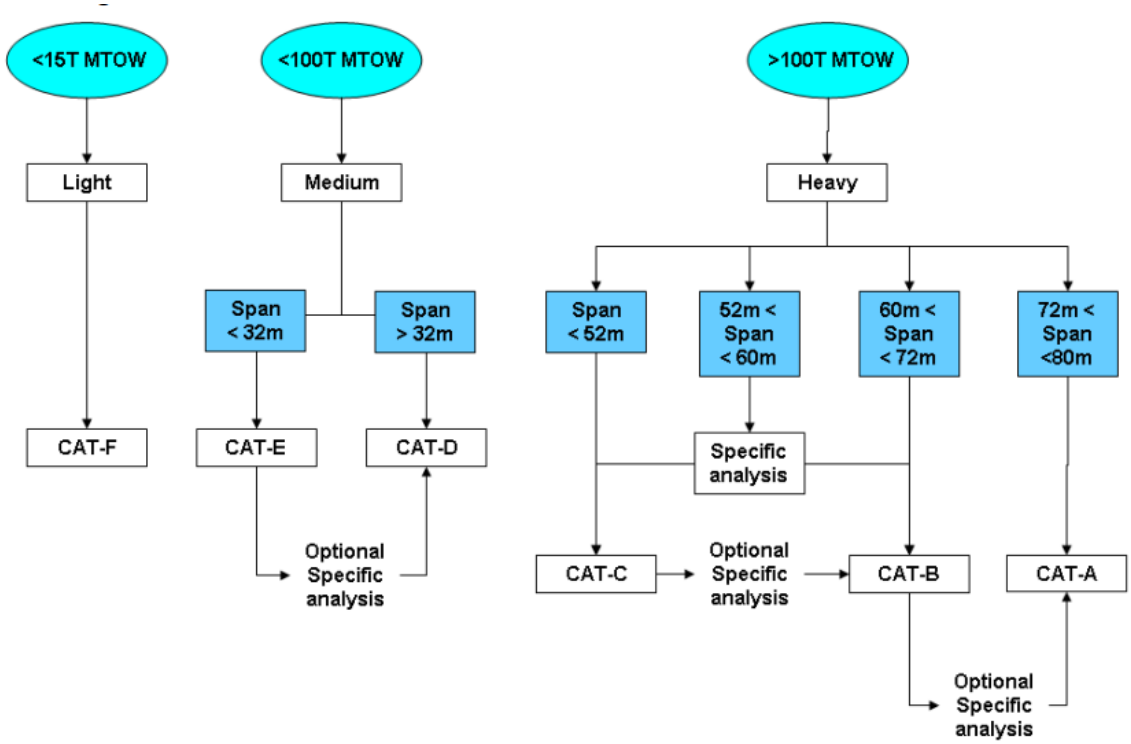

Figure B.1: Categorisation process and criteria for assigning an existing aircraft type into RECAT-EU scheme [9].

ever a correction for the human factor is also included [27]. The runway occupancy times for arriving aircraft are given in table B.2.

$$\mu_2 = AROT_i \tag{B.2}$$

In order to find the minimum TBS between two aircraft landing on the same runway, the maximum of the two separation times has to be taken.

$$T_{ij} = max(\mu_1, \mu_2) \tag{B.3}$$

Besides needing a separation when aircraft land on the same runway, it can also be that a certain separation is required between aircraft when they land on different runways. In the example of AAS, this is for instance the case for parallel runway pairs 36R & 36C and 18R & 18C since they are too close to each other to guarantee the required 3NM horizontal or 1000ft vertical separation within the terminal area airspace. Since a continuous descent approach is assumed, it is not possible for these pairs of parallel runways to achieve 1000ft vertical separation, meaning that 3NM horizontal separation needs to be achieved. The amount of time between the leading and trailing aircraft on the different runways then becomes:

$$T_{ij_{parallel}} = \frac{3NM - \text{Minimal Distance Between Approach Paths}}{min(V_i, V_j)} \tag{B.4}$$

There are also intersecting runways at Amsterdam Airport Schiphol, such as 06 & 36R and 27 & 18R. To keep sufficient time between aircraft using these runways it is important that the previous aircraft cleared the runway before the next one can land on the other intersecting runway. However, it can be that the beginning of the runway still lies closer than 3NM to the beginning of the other runway, thus this needs to be taken into account as well. Resulting in the following calculation:

$$T_{ij_{intersect}} = max\left(\frac{3NM - \text{Minimal Distance Between Approach Paths}}{min(V_i, V_j)}, AROT_i\right) \tag{B.5}$$

Finally, there is one more case that needs to be considered. If runway usage would switch from 36R+36C to 18R+18C then the Zwanenburgbaan (36C/18C) would be used from two sides in a small amount of time.

Thus, it is important to guarantee enough separation should this scenario occur. This separation is based on the minimal requirements an aircraft needs to perform a go-around while another aircraft is approaching head-on. Equation (B.6) gives the equation for this case. Where MVA is the Minimum Vectoring Altitude, which is the minimum height aircraft need to have to clear nearby obstacles, ROD being the Rate of Descent, and c the communication buffer. For AAS the MVA is set to 1700ft in CTR1 [28], the ROD is assumed to be 740 ft/min and the communication buffer 20 seconds [27].

$$T_{ij_{opposite}} = \frac{MVA}{ROD} + c \tag{B.6}$$

Only the separation between two arriving aircraft is considered in this section, since AAS in general does not use mixed runway operations (arrival following departure, and departure following arrival) it is not taken into account in this research, and since departing traffic is not considered neither is the separation between departure following departure.

Table B.1: RECAT-EU WT distance-based separation minima on approach and departure [9].

RECAT-EU scheme Leading \ Trailing		Super Heavy A	Upper Heavy B	Lower Heavy C	Upper Medium D	Lower Medium E
Super Heavy	A	3 NM	4NM	5 NM	5 NM	6 NM
Upper Heavy	B	(2.5NM)	3 NM	4 NM	4 NM	5 NM
Lower Heavy	C	(2.5NM)	(2.5NM)	3 NM	3 NM	4 NM
Upper Medium	D	(2.5NM)	(2.5NM)	(2.5NM)	(2.5NM)	(2.5NM)
Lower Medium	E	(2.5NM)	(2.5NM)	(2.5NM)	(2.5NM)	(2.5NM)

Table B.2: Arrival Runway Occupancy Time (AROT) for RECAT-EU categories [29].

RECAT-EU Category	AROT (s)
Cat A / Super Heavy	47
Cat B / Upper Heavy	47
Cat C / Lower Heavy	45
Cat D / Upper Medium	45
Cat E / Lower Medium	45

C

Emission

To be able to estimate the amount of emissions emitted by an aircraft during a leg of flight it is necessary to create a reasonably accurate model. It was decided to do so based on the total amount of fuel used, this is because most emissions are proportional to the amount of fuel used. A kilogram of Jet A1 fuel produces approximately 3.16kg of CO_2 [20]. In this chapter, the workings of the CO2 emission approximation model will be discussed in more detail.

C.1. Fuel Usage

In order to be able to model the emitted CO_2 of an aircraft it is necessary to model its fuel use. The total amount of fuel use is defined by equation (C.1).

$$F = \int_0^t \dot{m}_{fuel_t} dt \tag{C.1}$$

During different phases of the flight different fuel flows are needed to get the right performance of an aircraft. Also due to changes in weight due to fuel usage, the fuel flow required changes continuously. During take-off a lot of power is needed to get to cruise level, during cruise an ideal engine setting can be used at which the engines operate optimally, and during landing the engine setting can for large parts be idle resulting in a low fuel flow.
Thus, to create a very accurate approach of the total amount of fuel used, one must calculate the fuel flow for every moment in time during the flight. Since this would take a large amount of time, some approximations are made.
The take-off phase is largely dependent on the airport the aircraft departs from and since this research does not focus on this phase it is therefore neglected. Aircraft are therefore assumed to depart at cruise altitude and speed from a location directly above the airport they departed from. For the cruise part of the flight increments of 30 minutes are used for which a constant fuel flow is assumed. This fuel flow is then calculated for the weight of the aircraft at the end that increment, and adjusted to closely represent the true fuel used. For the final phase of flight, the approach, a constant altitude, speed and weight is assumed to calculate the fuel flow.

C.1.1. Fuel Flow Calculation

The fuel flow for the various configurations and weights for the aircraft types selected in table A.6 is calculated using Base of Aircraft Data (BADA) from Eurocontrol [30]. All values for the coefficients used can be found in appendix A.6.
The fuel flow is then calculated as follows for cruise:

$$\dot{m}_{fuel_t} = f_{cr} = \eta \cdot T_{HR} \cdot C_{fcruise} \tag{C.2}$$

And for approach the fuel flow is equal to:

$$\dot{m}_{fuel_t} = f_{ap} = max(f_{nom}, f_{min}) \tag{C.3}$$

With the thrust specific fuel consumption η:

$$\eta = C_{f1} \cdot \left(1 + \frac{V_{TAS_{kts}}}{C_{f2}}\right) \tag{C.4}$$

$$V_{TAS_{kts}} = \frac{V_{TAS}}{0.51444444} \tag{C.5}$$

The minimum fuel flow f_{min} corresponding to idle thrust descent conditions, which is dependent on the geopotential pressure altitude H_p:

$$f_{min} = C_{f3} \cdot \left(1 - \frac{H_p}{C_{f4}}\right) \tag{C.6}$$

And the nominal fuel flow f_{nom}:

$$f_{nom} = \eta \cdot T_{HR} \tag{C.7}$$

For both it is assumed that the thrust required equals the amount of drag the aircraft experiences.

$$T_{HR} = D \tag{C.8}$$

$$D = C_d \cdot \frac{1}{2} \cdot \rho \cdot V_{TAS}^2 \cdot S \tag{C.9}$$

C_d then follows from the drag polar for the appropriate configuration of the aircraft.

$$C_d = C_{d0} + C_{d2} \cdot C_l^2 \tag{C.10}$$

$$C_l = \frac{2 \cdot m \cdot g_0}{\rho \cdot V_{TAS}^2 \cdot S} \tag{C.11}$$

C.1.2. Assumptions per Flight Segment

An important factor in the fuel use calculation is the mass of the aircraft. If the mass decreases, so does the required fuel flow to the engines to keep a constant speed. For each aircraft type a fixed no fuel weight is defined and can be found in appendix A.6. This is the starting point from the calculation, in other words, the calculation is made backwards to calculate the amount of fuel the aircraft would have left, and the fuel it used along the way. All these assumptions are made to prevent needing to calculate the fuel flow for every time step of each flight, as this would take too long to compute for the intended use of the model.

Loiter

To be able to divert to another airport or loiter around the airport in case of unforeseen circumstances, aircraft take on extra fuel. The total amount of fuel required for such a loiter procedure is assumed to be equal to the amount of fuel required to fly for 1 hour on the no fuel weight. This amount is then increased by 5% since this was found to be the margin of error by not calculating the fuel flow for every second, but assuming a constant fuel flow for the entire hour. This then results in a loiter mass for each aircraft type as seen in equation (C.12)

$$W_{LOITER} = W_{nofuel} + FUEL_{LOITER} \tag{C.12}$$

Approach

For approach it is assumed that aircraft fly at a constant speed that is equal to the average of the speed they are supposed to arrive with at the IAF of 250kts and the approach speed for each aircraft type. Also, it is assumed that aircraft fly at a constant altitude of 7000ft, which was found to be the approximate average of all the transitional routes. The average weight is assumed to be equal to W_{LOITER} since the total time spent during approach is limited. Along with the time each aircraft type is estimated to take for each transition route, this then results in the amount of fuel used during the approach phase and the weight before this phase.

$$W_{APPROACH} = W_{LOITER} + FUEL_{APPROACH} \tag{C.13}$$

Cruise
The calculation of the fuel used during the cruise phase of the flight is cut into increments of each 30 minutes of flight. For each increment a fixed speed and altitude are used. This is done to significantly reduce the required computational time. For the first increment the $W_{APPROACH}$ is used as weight, for the second increment the weight found in the first increment etc. Until the total flight time is covered. The weight at the beginning of the cruise phase then becomes:

$$W_{CRUISE} = W_{APPROACH} + \sum^{t} FUEL_{CRUISE_t} \tag{C.14}$$

Departure
The departure phase is not taken into account for any flight. This is because each airport has it's own procedures and it is infeasible to create an assumption for each airport. Therefore aircraft are assumed to start their flight at cruise height and speed directly above their origination airport.

C.2. CO_2 Emission

Following from the Fuel usage the total amount of CO_2 emitted can be calculated. As stated before each kilogram of Jet A1 fuel produces approximately 3.16kg of CO_2 [20]. This results in the following formula for CO_2 emission.

$$CO_2 = \left(m_{fuel}(t_1) - m_{fuel}(t_0)\right) \cdot 3.16 \tag{C.15}$$

D

Noise

Amsterdam Airport Schiphol lies close to very densely populated areas, with the city center of Amsterdam only 11 kilometers away from the airport. Transportation wise this is very convenient due to the fast and many connections this location provides, but in terms of noise disturbance, the high amount of people nearby is not ideal. Therefore it is important to try and minimise the noise disturbance for the surrounding areas. To be able to do so a noise model needs to be created, which aims to capture the locations where the noise disturbance is the highest and whether there are ways to avoid highly populated areas. The noise model used in this research includes all arriving traffic for AAS below a level of 10,000ft. The model only takes population density into account, other factors such as nature preserves are currently not considered, but could be implemented in the future.

D.1. Population model

In order to know where the high density population areas are with respect to AAS and it's transition routes a population model must be used which clearly shows where these areas are. This is done according to the method proposed by [27], which results in a population density grid map with a grid size of 1x1km. The map encloses the area between the various IAFs of AAS and a section North of it, as some of the transition routes are further North than the IAFs are. This then includes the full area where aircraft approaching AAS fly below 10,000ft to be able to fully map the noise levels from transition routes. A visual representation of this is given in figure D.1, where AAS is shown in black and the population density is put on a three color green-yellow-red scale going from little to no residents (green) to highly populated areas (red). The contour of The Netherlands is clearly visible, as well as Dutch cities like Amsterdam, Haarlem and The Hague.

The data used to create this map is obtained from CIESIN's High Resolution Settlement Layer (HRSL) [31]. The HRSL uses machine learning techniques to identify buildings from satellite images and combine this with general population estimates based on pubicly available census data.

D.2. Aircraft sound emission data

To be able to create a model that is an accurate representation of true events, the aircraft selected to represent their categories as seen in appendix A.5 each need to have their own noise profile. This profile is based on the transition route and data of the Aircraft Noise Model from Eurocontrol Experimental Centre [32]. In this database a large collection of information about aircraft performance can be found, as well as a detailed description on standard approach procedures for a certain aircraft type and sound emissions at a certain thrust setting and altitude. This leads to a reasonable approximation of the actual noise profile for that type of aircraft. Since one aircraft represents an entire category of aircraft and the effects of wind and banking on noise emissions are not taken into account, it is clear that a perfect representation will not be achieved, but it is assumed that this method will result in a close representation of the real world events. Validating the model against the original current approach procedure of Amsterdam Airport Schiphol will also result in a good comparison for the findings in the outcome of the model.

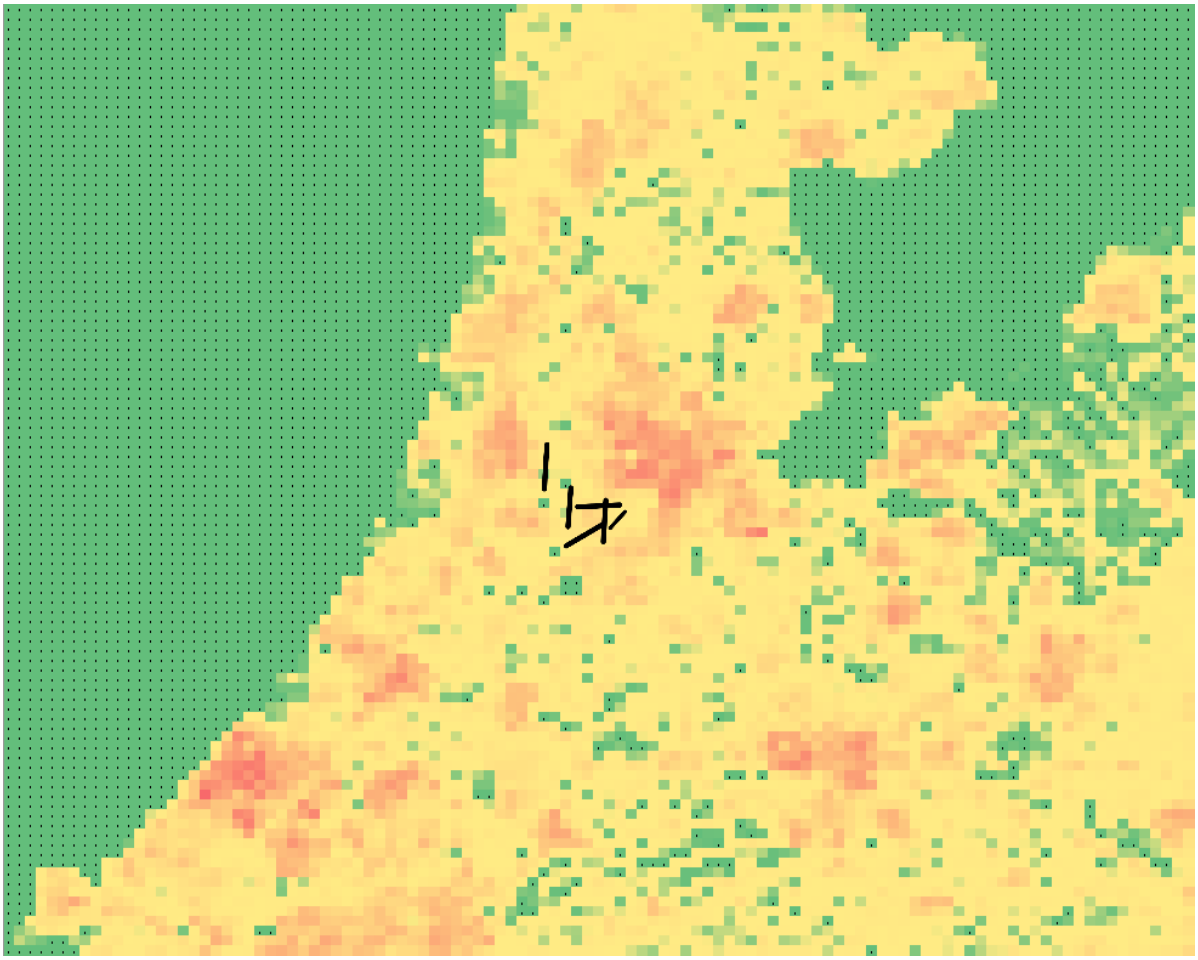

Figure D.1: Generated population grid around AAS.

Table D.1: Day, Evening and Night penalties for Day-Evening-Night Average Level [33].

	Day	**Evening**	**Night**
Time Period	07:00 - 19:00	19:00 - 22:00	22:00 - 07:00
Penalty (dB)	0	$\sqrt{10}$	10

D.3. Noise Calculation

The human perception of sound is defined by the Sound Pressure Level (SPL). The SPL gives a relation between the pressure of a certain sound wave in comparison to a reference sound pressure p_{e_0}. This reference sound pressure in air is defined as $2 \cdot 10^{-5} Pa$, also referred to as the threshold of hearing. In comparison a jet engine at 50m distance may produce $200Pa$ of pressure, equivalent to a SPL of 140 dB. The logarithmic relation between two sound pressures is given in equation (D.1). The SPL is given in dB, which is a logarithmic scale.

$$SPL = 10log\left(\frac{p_e^2}{p_{e_0}^2}\right) \tag{D.1}$$

Besides pressure there are also other factors that influence the perception of noise. These factors include duration, frequency, regularity and time of day [33]. To account for frequency the frequency weighting filters are used. The most common used filter is the A-weighted filter, which was found to be a good approximation of perception for all sound levels [33]. To achieve this, a correction ΔL_A is applied to the SPL, resulting in the A-weighting corrected band level L_A. This is negative for frequencies that are perceived as less annoying and positive for frequencies that are perceived annoying.

$$L_A(i) = SPL(i) + \Delta L_A(i) \tag{D.2}$$

The A-weighting sound level can than be found by adding the $L_A(i)$ for all frequencies with respect to the logarithmic scale as seen in equation (D.3). Here (i) represents the various frequencies.

$$L_A = 10log\sum_i 10^{\frac{L_A(i)}{10}} \tag{D.3}$$

To account for the effect of duration of a certain noise event, equation (D.4) can be used to calculate the Sound Exposure Level. The SEL integrates the sound level of an event over the time it occurred. This way it is also possible to calculate the effect of multiple sound levels for certain periods of time. It is thus an indication of the total amount of sound someone is exposed to within a certain time frame, with T_0 defining the time step size, which is usually set to 1 second. The SEL for a certain type of aircraft at a set height and configuration can be obtained from the Aircraft Noise Model [32].

$$SEL = 10log\left[\frac{1}{T_0}\int_0^T 10^{\frac{L_A(t)}{10}}\,dt\right] \tag{D.4}$$

Finally to adjust for the perception of sound during different parts of the day the Day-Evening-Night Average Level L_{DEN} is used. The model allows for penalties for events that occur at different times during the day. During the night sound is usually experienced as more annoying and therefore has the highest penalty, whereas during the day sound is usually perceived less annoying and thus no extra penalty will be applied. The penalties w_i for each part of the day can be found in table D.1. In comparison an addition of 3 dB represents approximately a doubling in observed noise. The time span that is evaluated is given by T_{ref}, usually set to 1 day ($24 \cdot 3600s$). The formula for L_{DEN}, which is used to calculate the noise contours in appendix I, can be found in equation (D.5).
For the IAF selection model used in this research, as described in section 2.2, equation (D.5) is changed slightly since the effect of noise on the objective function was too marginal when using a logarithmic scale. Therefore this was changed to equation (D.6).

$$L_{DEN} = 10log\left[\frac{1}{T_{ref}}\sum_{i=1}^{F} 10^{\frac{SEL_i + w_i}{10}}\right] \tag{D.5}$$

$$OBJ_{L_{DEN}} = \sum_{i=1}^{F} 10^{\frac{SEL_i + w_i}{10}} \tag{D.6}$$

E

Route optimization

Route optimization is a key factor for airlines. The shorter the to be flown routes, the shorter the flight-time. Shorter flight-times decrease costs for airlines since more flights can be made with a smaller amount of aircraft, but more important for this research, the shorter the to be flown route is, the less fuel needs to be consumed by the aircraft to get to its destination. This results in lower CO2 emissions per flight.

In order to be able to make a quantitative trade-off between noise and CO2 emissions, and make decisions to assign which aircraft to which IAF, it is important to know the most optimal route from the origin of the aircraft to each of the IAFs. This is not just equal to the shortest route from origin to destination as Special Use Airspace (SUA) and weather scenarios may alter the most optimal route from the origin to the various IAFs.

In appendix E.1 the optimization area will be discussed and how aircraft are handled if they originate from outside this area. Appendix E.2 discusses the way weather scenarios are incorporated into the model to achieve a realistic model. In appendix E.3 the special use airspace are covered. Finally, the route optimization algorithm used is discussed in appendix E.4.

E.1. Optimization Area

A specific area in which the route will be optimized is defined to limit the run time of each optimization and to limit the required data. After consulting members from the industry, the minimum range that needs to be taken into account was set to be 1000 kilometer around Amsterdam Schiphol Airport. The reason for this is that it is then possible to divert aircraft to other routes that better fit the approach of one of the IAFs. Making the area smaller would result in either infeasible solutions, or long detours, as first the standard route would be followed. For convenience, the area was chosen to be a rectangular box with distances to the borders of at least 1000km. This resulted in an area that runs from latitudes 43.3°North to 61.3°North and longitudes 10°West till 19.6°East.

A substantial number of aircraft come to Amsterdam Airport Schiphol from airports that are not within the optimization area. To accommodate for these flights it is assumed that these flights directly fly the shortest route from their origin to AAS up to the point where they enter the optimization area. From the point they enter the optimization area, the aircraft are treated the same to aircraft that originated from within the optimization area. From the edge of the optimization area weather, restricted area's etc. are also taken into account. An example of this for a route between New York and Amsterdam is given in figure E.1.

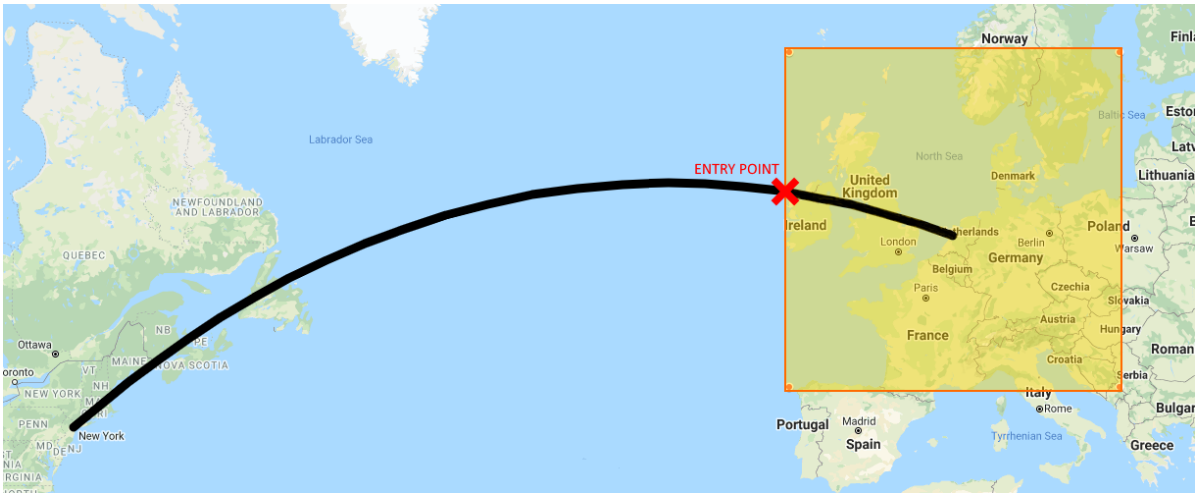

Figure E.1: Example of route from New York to Amsterdam Schiphol Airport.

E.2. Weather Data

Outside of the optimization area, no weather data is taken into account. This is because it would slow the model down too much and it would require too many data points. Within the optimization area the possibility to generate a wind field to create more accurate and feasible solutions to the optimization problem is provided.
Ultimately it was decided not to use this since including wind fields outside of the optimization area resulted in a too high computational time, as this would result in aircraft being influenced by wind only a part of the flight. It was assumed that it would be better to not use the wind data then have it partly, as both are close to the truth, but not close enough to be a true approximation and incorporating the wind takes up a lot of computational power and therefore time.
However, since the option is built into the model, this section describes the data and where it originated from. The wind data is obtained from Copernicus[1]. ERA5 data in a netCDF format is used for the specific cruise height, date and hour the aircraft was estimated to land on Amsterdam Airport Schiphol. The wind field remains constant over the duration of the optimization since the data is only available on an hourly basis and the execution speed of the model would become too low if an active wind field would be used. Due to similar reasons of execution speed it was also decided that each of the data points for which the u and v component of wind are available would only be used on whole coordinate degrees, while the data is available for a quarter of a degree. Between data points interpolation is used to create a full wind field for every position of the aircraft inside the optimisation area.

No other types of weather are considered in the standard model. However, it is possible to simulate the closure of a certain part of airspace due to, for instance a severe snowstorm, by creating a restricted airspace. This would mean aircraft are not allowed to enter that section of airspace and the model will then find a route around it. The working of this is explained in the next section.

E.3. Special Use Airspace/Restricted Airspace

Certain parts of airspace are not available for civil aviation. These Special Use Airspace (SUA) are areas designated for operations of such nature that they limit the availability of free routing for civil aviation. It can be that only designated corridors can be used in these areas or that the airspace is completely closed for all civil aviation. Often these areas are military airspace where air forces can train or execute missile launches, rendering the area unsafe for regular traffic. Areas that prohibit civil aviation are added in the model to prevent aircraft flying over them and keep a feasible solution. In a similar way, corridors can be made through which aircraft have to fly if they want to cross a certain area. The model obtains these areas from a .txt file where the SUA are given as polygons based on coordinates.

[1] https://cds.climate.copernicus.eu/cdsapp#!/home

E.4. Route Optimization Algorithm

The route optimization algorithm used in this research is based upon the research done by Girardet on "Generating Aircraft Trajectories with respect to Weather Conditions" [21]. This research is based on the Free-Flight concept as introduced by SESAR in Europe and NextGen in the United States. The Free-Flight concept is based on the idea that aircraft may fly whenever and wherever they want to accommodate for direct routing, optimal altitudes, favourable winds, and avoiding hazards. This results in shorter flight times and less environmental impact due to the ideal flight conditions [21]. In contrary of Girardet [21] other aircraft are not taken into account in the route optimization. As the research focuses on the arrivals of Amsterdam Airport Schiphol, the aircraft landing there are the only ones taken into account. To include collision avoidance in the optimization would require information of the whereabouts of all aircraft within the European airspace at that specific point in time, which is not within the scope of this research.
Since this model only optimizes the en-route part of the trajectory of the aircraft, the target of this algorithm is to minimise the time it takes from a certain airport on an optimal cruise speed and height to all of the IAFs of Amsterdam Airport Schiphol. This thus results in four different routes per aircraft, which can then be used in the next part of the optimization as described in section 2.2. This way it is possible to decide which IAF would be the most optimal to fly to for this specific aircraft. For the most part of the journey of the aircraft it will be at a constant True Air Speed V_{cruise} and altitude, but for the final part towards the IAF the aircraft descends to FL100 or 10.000ft and slows down to 250 kts TAS. This is taken into account by reducing the TAS linearly from 120 NM before the IAF and by adjusting the fuel flow for this section of the flight. This results in the equations of motion as seen in equation (E.1). Where θ is the heading angle, $W_x(x,y)$ the East component of the wind, and $W_y(x,y)$ the North component of the wind.

$$\begin{aligned} \dot{x}(t) &= V_{TAS} cos(\theta(t)) + W_x(x,y) \\ \dot{y}(t) &= V_{TAS} sin(\theta(t)) + W_y(x,y) \end{aligned} \tag{E.1}$$

The goal is to generate a trajectory by optimizing the heading such that a trajectory with the minimal travel time between origin and destination is found. Assuming a (near) constant TAS and flight level this trajectory is also fuel optimal [21]. The proof of how this can be written into a Hamilton-Jacobi equation can be found in [21].
The Ordered Upwind algorithm was designed to approximate the solution of Hamilton-Jacobi equations. Sethian and Vladirminsky introduced their ideas first in [34]. In further research it was proven that the algorithm converges to the viscosity solution of the Hamilton-Jacobi equations, a weak solution of a partial differential solution (PDE) [35]. The principle of Ordered Upwind is to avoid iterations by using information on the characteristics of the PDE, exploiting the fact that the value function u is strictly increasing along the characteristics. The strength of the Ordered Upwind method is the ability to compute information about the characteristic as the solution is constructed. In contradiction to the Fast Marching Method for isotropic problem, the characteristics and gradient of the value function are not in the same direction. In [34] Sethian provides a method to solve this problem, where bounds obtained from the wavefront speed are used to define the maximum angle between the characteristics and the gradient of the value function. In order to compute the value function u an unstructured triangulated mesh is used.
There are three different classifications for the mesh points, as can also be seen in figure E.2:

- *Accepted*; The set of mesh points where u has been computed and frozen.
- *Considered*; The set of mesh points where an estimate v of u has been computed, but not frozen.
- *Far*; All other mesh points where an estimate v of u is not computed (yet).

Besides the classifications there are also two sets created:

- *AcceptedFront*; A subset of *Accepted* mesh points that are adjacent to *Considered* mesh points.
- *AF*; A set of line segments $[\mathbf{x}_j, \mathbf{x}_k]$ between adjacent *AcceptedFront* mesh points.

For each *Considered* mesh point $\mathbf{x}$ a new set *NearFront* is defined. It is a subset of *AF* segments, which are close to the considered meshpoint $\mathbf{x}$. The full mathematical model behind this algorithm can be found in [21]. At each point in the mesh an estimation on the fastest route is computed using the wavefront propagation as function of the aircraft speed. A geometric representation of this is given in figure E.3.
In figure E.4 an example is given for a certain wind grid and how the optimal routes would then be after optimizing for time.

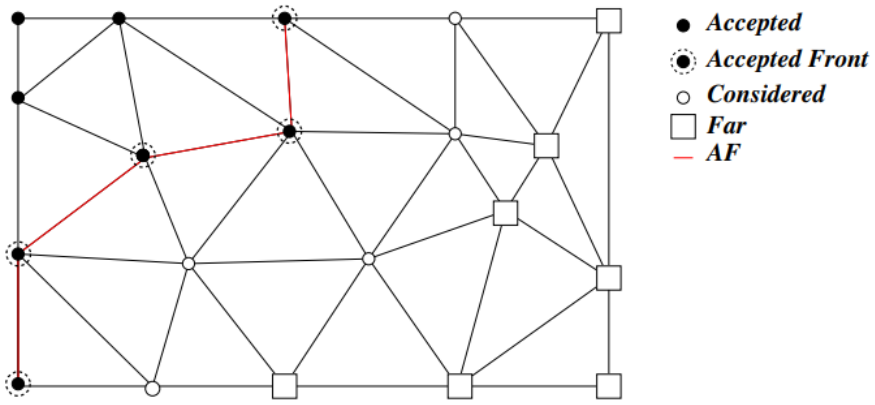

Figure E.2: All the mesh points are assigned to three different sets: Accepted, Considered and Far. Accepted Front is a subset of the Accepted set. The AF set describes the front [21].

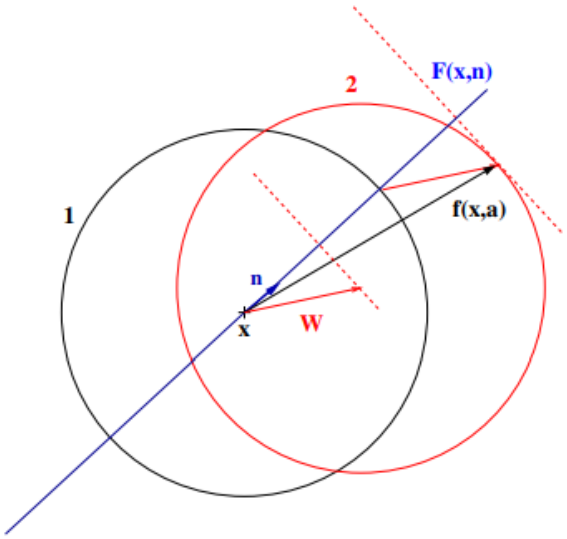

Figure E.3: The figure shows how to compute the speed of the wavefront $F(\mathbf{x},\mathbf{n})$ in the normal direction **n** at the point **x**. Circle 1 represents the true airspeed profile for the aircraft at the point x and circle 2 represents the speed of the aircraft profile f(**x**,**a**) for all **a** at the point **x**. The speed of the wavefront F(**x**,**n**) is equal to the maximum of the projection of the aircraft's speed profile f(**x**,**a**) on the direction normal **n** [21].

E.5. Validation & Verification

For the route optimization model used in this research, use was made of the moving front algorithm as presented by Girardet [21]. This means that the mathematical formulation of the model is already verified and validated in that research. In this section therefore only the implementation of this model will be looked at.

E.5.1. Verification

Verification of the route optimization model means that it must be confirmed that the model behaves as expected, and that there are no mistakes in the model itself. Unit testing was used to check if each section and formula provided the correct and expected output. The complete working of the model is verified by looking at the output of the model, which is indeed as intended. The model outputs a Python file containing a dictionary that contains a list of variables for each aircraft and IAF combination on a single day. The aircraft callsign and the IAF name are used as the keys of this dictionary. The list contains the following variables; The total flighttime from the edge of the optimization area towards the indicated IAF in seconds, the total distance from the edge of the optimization area towards the indicated IAF in meters, the total time from the originating airport towards the edge of the optimization area in seconds, and the total distance from the

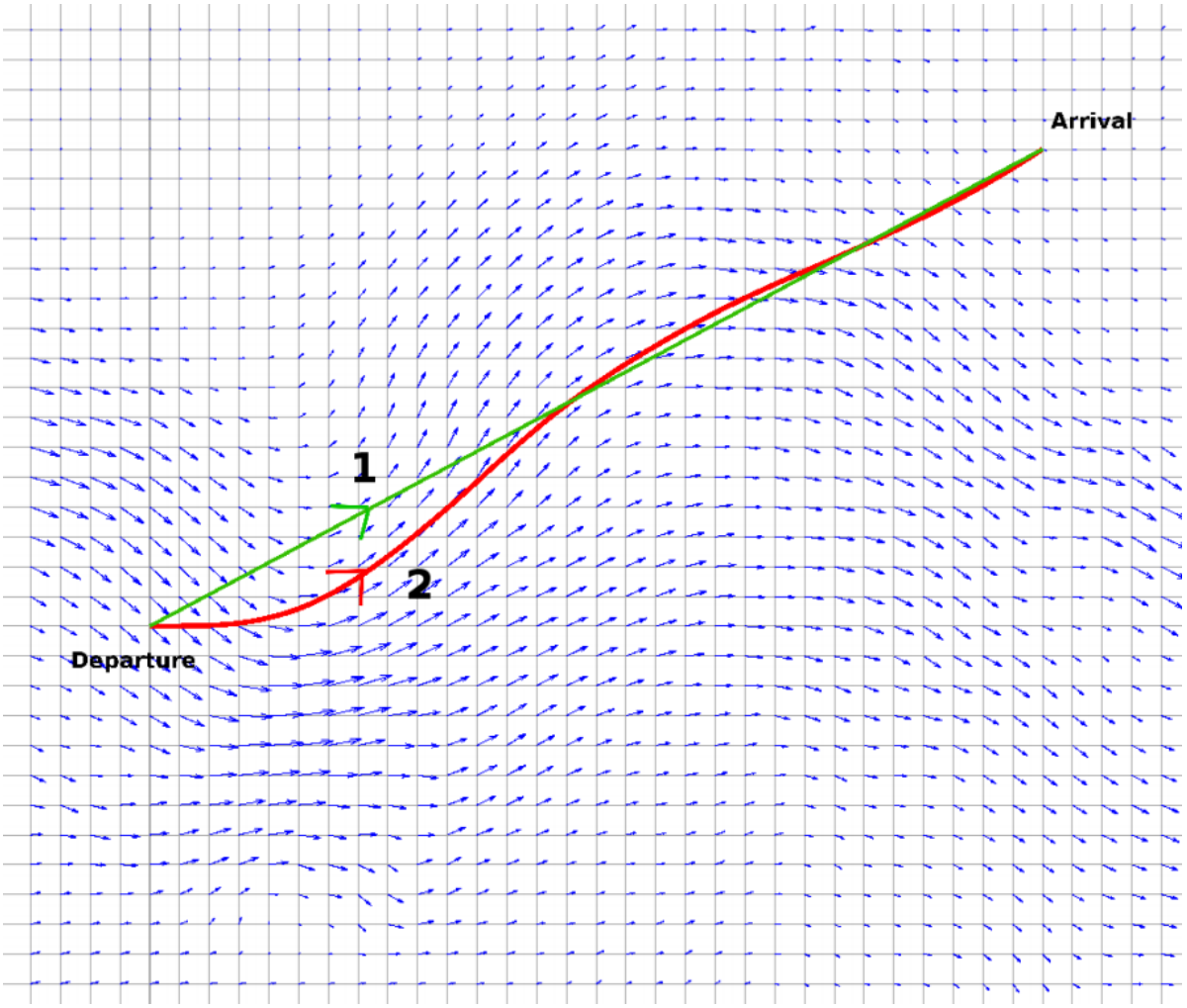

Figure E.4: Trajectories: 1. Direct route/Optimal route without wind (green), 2. Optimal route with wind (red) [21].

originating airport towards the edge of the optimization area in meters. Below an example on how this looks can be seen:
{('CAI792', 'RIVER'): [11919, 2696835, 7119.751288034683, 1578468.5795842935, 4799, 1118366]}

E.5.2. Validation

To validate the route optimization model it is necessary to check the outcome of the model, and if it is what it is expected to be. Two things need to be checked. The first one being the check if the model matches the time and distance between two coordinates as the crow flies, for a given speed. This is done by running a simulation of an aircraft flying from A to B on a set speed for a set distance. To check if the model performs up to standard both inside as outside the optimization area it is required that point A is outside the optimization area, and point B inside of it.
The chosen flight is a flight from New York John F. Kennedy International Airport towards IAF SUGOL. The total distance for this flight is 5,789km as the crow flies. The aircraft was given a constant speed of 459 knots. The expected time for the 5,789km with this speed would then be 24516 seconds. The model provided a calculated distance of 5800.853 km, and a calculated flighttime of 25408 seconds. For the distance flown this results in a 0.2% difference, for the flown time this results in a 3.6% difference. Both are deemed acceptable for the use of the route optimization model in this research.
The second thing that needs to be validated is that the model adheres to its constraints. When a Special Use Airspace (SUA) is in place the model needs to find a way around these SUAs. This is because these SUAs are restricted airspaces that are generally not available to commercial aviation. The easiest way to validate this is by visual inspection of the model. In figure E.5 it can be seen that indeed the model adheres nicely to the

areas where it is not allowed to go through (in black) and still optimizes the route within the areas that are still available.

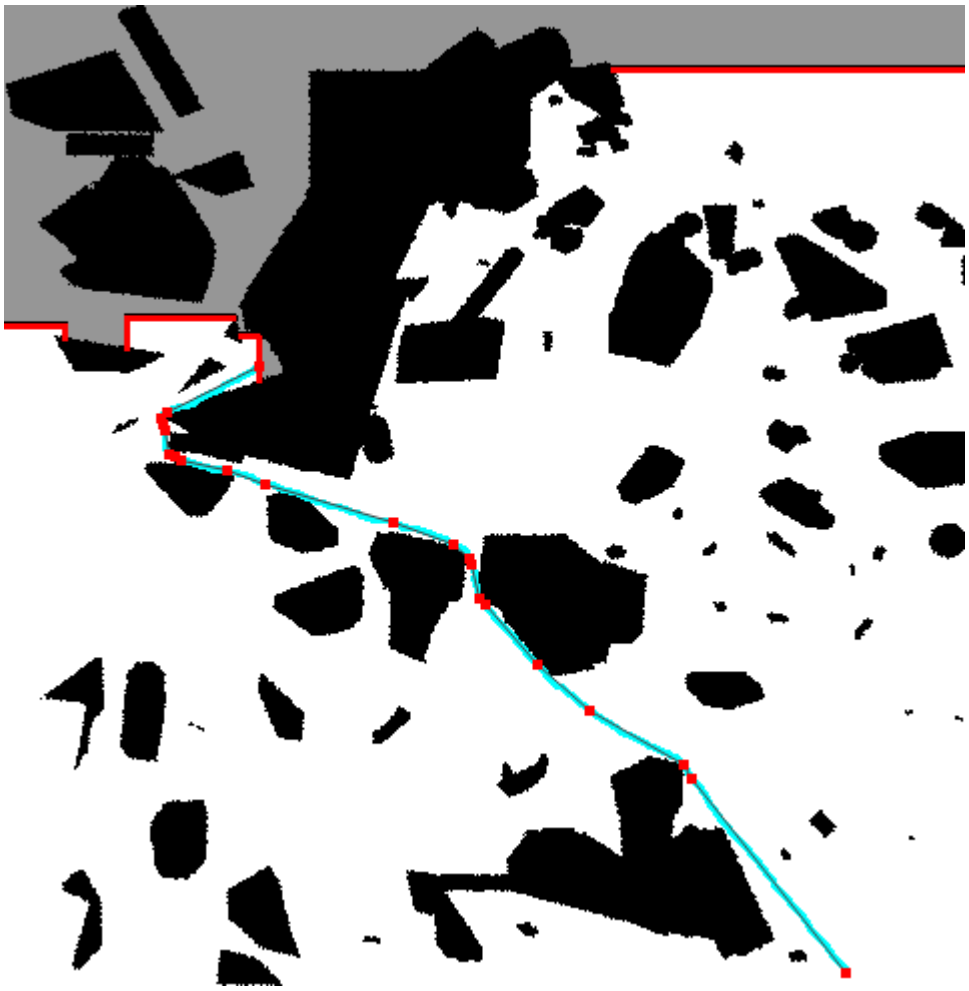

Figure E.5: Visual Validation of Route Optimization Model Adhering to Constraints.

F

Method Selection

In this chapter various methods to address this optimization problem are introduced. First, the workings and idea behind each model will be described and the positive and negative features will be discussed. Afterwards, a comparison between the models is made and it is decided which model would suit this problem the best.

F.1. Genetic Algorithms

A genetic algorithm is an algorithm that is based on Charles Darwin's theory of evolution through natural selection [36]. The process of natural selection starts with the selection of the fittest individuals from a population. These fittest individuals will then create offspring which inherit parts of the genes of their parents. If the parents had a good fitness, their offspring potentially has a better fitness which in term increases their chances of survival. This process will then be repeated until at a certain point in time the population reached a climax of their fitness and no improvements can be made anymore.

F.1.1. Working Principle of Genetic Algorithms

As explained in [37] the genetic algorithm mimics the workings of natural selection. There are five stages in a genetic algorithm, namely the initial population, fitness function, selection, crossover and mutation. These will be discussed and elaborated upon below.

Initial Population

The initial population exists out of a set of random, yet feasible solutions to the problem. Each member of the population exists out of a certain set of genes, together this set of genes makes the chromosome of this member of the population. In figure F.1 an example is shown of how this could look like.

Fitness Function

The fitness function determines the fitness of each member of the population, the fitness score. Based on this fitness score the likelihood of being selected for reproduction is determined. If the fitness score of a certain member of the population is higher than another, its chances of reproduction are higher. For instance if the fitness function would have equalled:

$$Fitness = Gene(1) \cdot 10 - Gene(2) \cdot 3 + Gene(3) \cdot 2 + Gene(4) \cdot 4 - Gene(5) \cdot 9 + Gene(6) \cdot 3 \tag{F.1}$$

Looking at figure F.1 a population of 4 can be seen. If their chromosomes are put into the fitness function from equation (F.1), then A1 would have a fitness score of 0, A2 would equal 7, A3 = 6 and A4 = 2. Thus leading to the conclusion that A2 has the highest fitness score and thus the highest chance to reproduce.

Selection

After the likelihood of reproduction is determined by the fitness function, the selection of the members of the population that will reproduce will be done. The higher the likelihood, the higher the chance that that particular member of the population will be chosen.

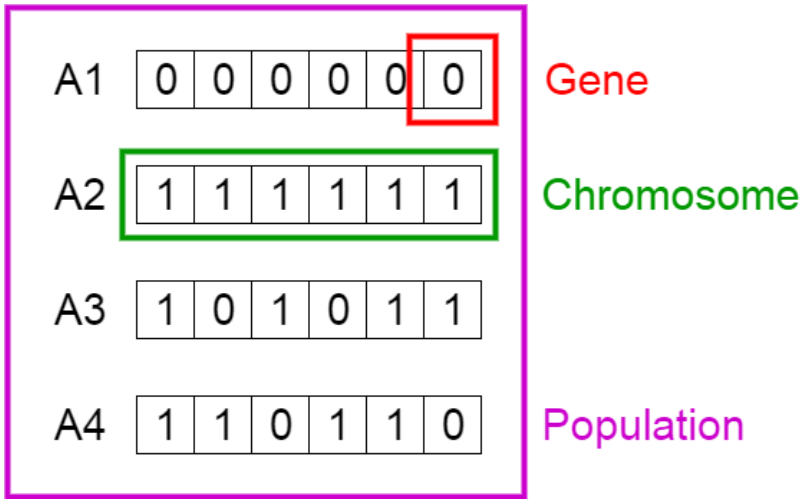

Figure F.1: Example population, chromosome and genes [37].

Crossover

The crossover part is the most significant part in a genetic algorithm. For the pair of parents that are going to reproduce, a crossover point is selected at random. This crossover point decides which genes of the parents are exchanged between the pair and which not. Exchanging of the genes occurs until the crossover point is reached. This process is shown in figure F.2. The resulting offspring following this process is shown in figure F.3.

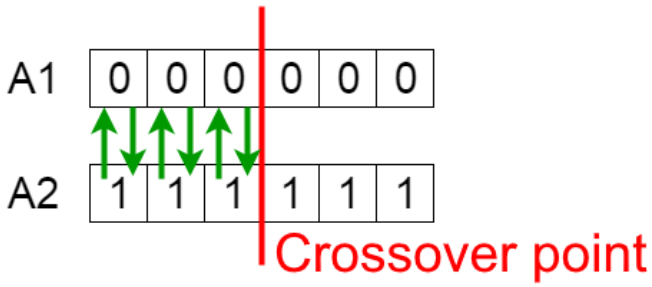

Figure F.2: Crossover point and exchanging genes between parents A1 and A2 [37].

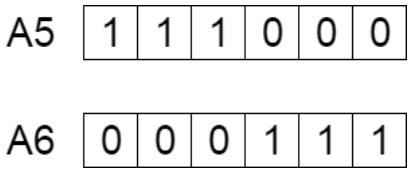

Figure F.3: Offspring of A1 and A2 [37].

Mutation

Within some of the offspring a mutation might occur, meaning that at the offspring there is one or multiple genes that are not inherited from their parents, but the inherited gene takes on a different value. There are various ways a mutation could occur among which a gene shift, where for instance Gene(4) would take the place of Gene(2) and therefore shifting Gene(2) and Gene(3) to the places of Gene(3) and Gene(4) respectively. Another common mutation is inversion, where a certain set of genes in the chromosomes inverts it's value. An example of an inversion is given in figure F.4.

As stated in [38] mutations can be a very useful solution to escape local optima and find the global optimum. The reason for this is that due to the mutation a more diverse gene pool exists in the population. This prevents

less favorable genes that are present between the reproducing pair are not guaranteed to be in the offspring. Therefore giving room for improvement by changing the value for this gene. In the example A2 and A3 were the fittest in the initial population. They both share the same value for Gene(5), which gives them a penalty in the fitness of 9. Without mutation their most fit offspring will never get rid of this penalty as the most optimal offspring of A2 and A3 would be [1 0 1 1 1 1], while it is clear that the most fit possibility would be [1 0 1 1 0 1]. Mutations can open up the possibility of finding this optimum even if A2 and A3 would be the only parents.

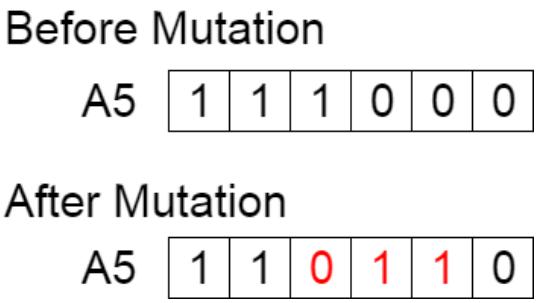

Figure F.4: Mutation through inversion [37].

Repeating steps and terminating model
After having done these steps one generation has passed. The population will remain a fixed size, even after reproducing. Thus meaning that the least fit members die after finishing a generation. In order to get an optimal model, multiple generations will have to pass. This is done by continuously redoing steps fitness function, selection, crossover and mutation. The algorithm terminates if there is no longer a significant difference between the generated offspring and the previous generations.

F.1.2. Positive and negative features
Genetic algorithms have the capability to solve difficult problems that other optimization algorithms fail to solve. This is because GA can simultaneously test many points from all over the solution space with either discrete or continuous parameters or a combination of them, as well as work with many types of data [10]. This can be achieved since the model basically brute forces the optimal solution in an effective way, by keeping the strongest results around and mutating on them. This does however also result in the drawback that it is quite difficult to find the most optimal solution to a problem, as the model is likely to settle for a local optimum instead of continuing to search for the global optimum. Adjusting the coefficients can help in this, but since it is not known what the most optimal solution must be, it is impossible to say whether the model achieved a global or local optimum, except by running all possible variations of variables. This is usually not a possibility.

F.2. Reinforcement Learning Algorithms/Q Learning
When interacting with our environment it is learned that certain behaviour results in certain outcomes and that some behaviour negatively impacts the environment, while other behaviour improves our environment. For instance studying for exams usually results in higher grades, which in turn stimulates to study more for a higher reward. Reinforcement learning is based on this basic principle of learning how to cope with our environment. The algorithm gets positive or negative feedback after performing a certain action and tries to learn from its mistakes, so that next time it will do it right immediately.

F.2.1. Working Principle of Reinforcement Learning Algorithms
The basic working principle of a reinforcement algorithm is an algorithm that tries to maximize its reward. The characteristics of trial and error and delayed reward are the most important distinguishing features of reinforcement learning [11]. A block diagram of the working of reinforcement algorithms can be found in figure F.5.
Q-learning is a type of reinforcement learning which might be useful here. The Q stands for Quality, which in this case represents the usefulness of a certain action in gaining future reward [12]. In figure F.6 the formula on which Q-learning is based is given. Q represents the Q-table or matrix with variables [state, action], depicted by s_t and a_t respectively in the formula. The various parts of the model will be discussed below.

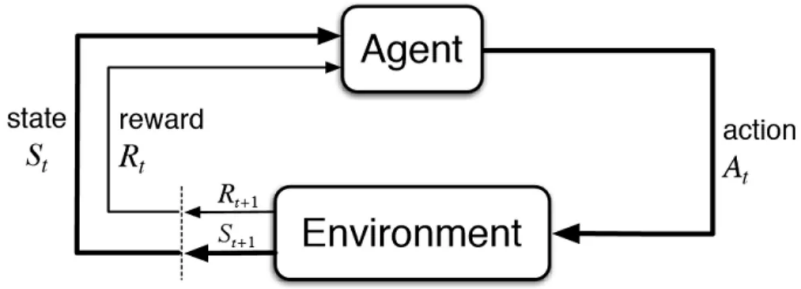

Figure F.5: Reinforcement Model [15].

$$Q^{new}(s_t,a_t) \leftarrow \underbrace{Q(s_t,a_t)}_{\text{old value}} + \underbrace{\alpha}_{\text{learning rate}} \cdot \overbrace{\left(\underbrace{r_t}_{\text{reward}} + \underbrace{\gamma}_{\text{discount factor}} \cdot \underbrace{\max_a Q(s_{t+1},a)}_{\text{estimate of optimal future value}} - \underbrace{Q(s_t,a_t)}_{\text{old value}} \right)}^{\text{temporal difference}}$$
$$\text{new value (temporal difference target)}$$

Figure F.6: Q-learning formula [15].

Q-Table
The Q-table contains the agent's state and possible actions. Given a certain state an action has an reward. So, as an example, if an agent would be in state 0 at time 0 and it's goal is to get cookies. For action 1 he would receive 10 cookies, for action 2 he would receive 4 lollies and action 3 would cost him 2 cookies the Q-table could look as follows:
$Q[0_0, a_0]$ = [0 10 0 -2]
Values for states 1 to 3 are not given, also note that action 0 (remain in the same state) and action 2 do not give cookies and therefore the reward for these actions is 0.

Learning rate
The learning rate is the rate at which the algorithm accepts the new knowledge it acquired. For deterministic environments a learning rate of 1 is optimal, whereas if the problem is stochastic a lower value is required. If the value is too high, the algorithm will forget its previous knowledge and therefore will not converge to a most optimal path. In practice often a value of 0.1 is used [11].

Discount factor
The discount factor determines how important possible future gains are for the algorithm. If it is set to 0, the system will become short sighted and will only go for the direct rewards, whereas if it is set to 1, it will keep track of all steps in the past and what rewards it gave. Even though this would theoretically give the most optimal outcome, setting the discount factor to 1 can result in infinite long histories of all environments, and thus in an insolvable problem, since computation time will become infinite [39]. In some cases, however, starting with a discount value below 1 could lead to instabilities in the algorithm. Therefore, starting with a lower discount factor and building it up as time progresses can accelerate the learning of the algorithm [40].

Repeating steps and terminating model
By continuously running the model according to the formula given in figure F.6, the model will, if all variables are set correctly and an optimum is possible, find an optimal path. This path is found if there is no or little change in the new Q-tables generated. It is also possible to stop the model after a certain amount of iterations, but this then does not guarantee the most optimal solution.

F.2.2. Positive and negative features

Reinforcement learning is useful for systems that are easy to judge, but hard to specify. This is because no full mathematical model is needed, it just needs the results of actions taken. The problem with this is that

it therefore needs a lot of data which must be obtained in the learning phase [13]. Another problem is that during the learning phase, it is not always clear what connections the model makes within the data, which may lead the algorithm to do something it was not intended to do. An example for instance could be that if a robot needs to find the fastest way to cross a bridge of some kind, it concludes that the fastest way is to go around it since in the trial and error phase there was ground around the bridge. But if the robot would not be corrected on time, the next time it encounters a bridge that does have water around it, it will still try and go around and thus fall into the water.

F.3. Mixed Integer Programming

Unlike the previous discussed algorithms, Mixed Integer Programming (MIP) is not based on a biological principle. MIP instead is known as a mathematical technique where functions are minimized or maximized when subjected to various constraints. Therefore, unlike the previous algorithms, a full understanding of the problem and the influence of each variable on the outcome of the problem is required. It is possible to use both linear as quadratic equations, however quadratic equations complicate the model significantly and might make a model unsolvable, thus linear equations are preferred.

F.3.1. Working Principle of Mixed Integer Programming

The principle behind mixed integer programming is to find an optimal feasible solution to a set of equations of which some of the variables can only strictly be integers, while other variables can be any real number. Some of the variables can also strictly be binary. The equation the model is trying to find the optimal solution for is the objective function. The other equations are the requirements that keep a possible solution feasible, therefore they are called the constraints. In equation (F.2) a set of linear equations is given for a mixed integer algorithm in its standard form. Below, the different parts of the algorithm are discussed, namely the objective function, decision variables and the constraints. Finally the branch and bound search strategy is discussed as well as the termination of the model.

$$\begin{aligned} \text{minimize} \quad & c_1 \cdot x + c_2 \cdot y \\ \text{subject to} \quad & Ax + By \geq d \\ & x \geq 0, \qquad x \in \mathbb{R}^n \\ & y \geq 0, \qquad y \in \mathbb{Z}^n\{0,1,2,...\} \end{aligned} \tag{F.2}$$

Decision Variables

The decision variables in an MIP algorithm are the values that need to be determined in order to solve the problem. In other words, the optimization is completed when the best possible values for these variables given the objective function and the constraints are found [41]. Let us say that after obtaining a set of lollies in the previous example we now would like to sell those lollies and have the highest profit margin, but we would also get rid of as many lollies as possible since they are taking up too much space in the garage. The earnings can be denoted by decision variable x as x can take any real value. One of the reasons it is not desired that the decision variable of the earnings is an integer is that than it is only possible to earn round numbers, so €1 or €2 instead of €1.25 per lolly. For the lollies however, it is nearly impossible to split one lolly into parts and then most likely no one would like to buy it, thus it is only possible to sell whole lollies. The decision variable y is ideal since it can only be integers. Therefore y is the amount of lollies sold.

Objective Function

The objective function is the function that decides what the algorithm tries to optimize. The objective function can still be presented as in equation (F.2), but it could also be written to maximize. If instead of minimizing the objective function, the function needs to be maximized it is equal to the minimization of the negative of the function that needs to be maximized. Therefore the two options of the objective function are given as follows in equation (F.3).

$$\begin{aligned} \text{minimize} \quad & c_1 \cdot x + c_2 \cdot y \\ \text{maximize} \quad & -c_1 \cdot x - c_2 \cdot y \end{aligned} \tag{F.3}$$

From various parties you are offered a certain amount of earnings for a certain amount of lollies and the goal is to find the ideal set of transactions that will optimize the objective of this problem. c_1 and c_2 are simple

constants and indicate the contribution of the decision variables to the objective [41]. Since the objective is to maximize the earnings while also getting rid of as many lollies as possible, it is clear that the constant c_1 needs to be negative since the earnings are denoted by x and similar c_2 also needs to be negative. Depending on the priority to have high earnings and the priority to empty the garage, the magnitude of the values for c_1 and c_2 could be determined.

Constraints

Constraints are in place to guarantee that the model comes up with a valid solution. Thus they define the values the different decision variables may take [41]. The constraints are thus important for the model as some solutions may find a better value for the objective function, but then become impossible. The constraints of equation (F.2) are given in equation (F.4).

$$\begin{aligned} \text{subject to} \quad & Ax + By \geq d \\ & x \geq 0, \qquad x \in \mathbb{R}^n \\ & y \geq 0, \qquad y \in \mathbb{Z}^n\{0,1,2,...\} \end{aligned} \tag{F.4}$$

The first constraint could for instance entail that the earnings of a certain transaction minus the cost of losing some lollies must be greater or equal to a certain threshold, maybe because costs are inflicted when performing a transaction and you do not want to lose money on a transaction. In other words, it could be that you could gain €0,50 by selling the lollies separate and €0,40 per lolly if you sell them by the dozen, but if the transaction cost d would be €0,60 you will not sell singular lollies for €0,50. The second and third constraint limit the search area to only positive numbers for the decision variables x and y. Note that with these constraints there is no limit on the amount of lollies sold and therefore one must have an infinite amount of lollies to get a sensible outcome of this example model. Another constraint thus must be added to limit the amount of lollies sold.

Branch and Bound and terminating model

All state of the art mixed integer programming solvers use the branch-and-bound algorithm [42][43]. Therefore for this research the branch-and-bound algorithm will be discussed. The branch-and-bound algorithm starts with the initial MIP problem, but it is not known how to solve this problem directly. The first step is to remove all integrality restrictions, thus decision variables are no longer strictly integer or binary. This is called the relaxation of the mixed integer programming problem. Now it is possible to find a solution to the problem. If this solution satisfies the integrality restrictions, the solution obtained is optimal and the algorithm can be stopped [14]. If the solution is not feasible then this also holds for the integer program. Else, at least one of the integer variables must be fractional in the solution. To solve this, one or multiple of these fractional variables are selected and 'branched'. Branching means creating two or more new MIP problems which exclude the infeasible solution, but do not exclude any other feasible solution [14]. In other words, extra constraints are added to limit the search area of certain variables. As an example, if y which must be an integer, is found to have the best solution for value $y = 4.7$, then for instance two branches can be made. One including the constraint $y \geq 5$ and the other $y \leq 4$. A visual representation of this process is given in figure F.7.

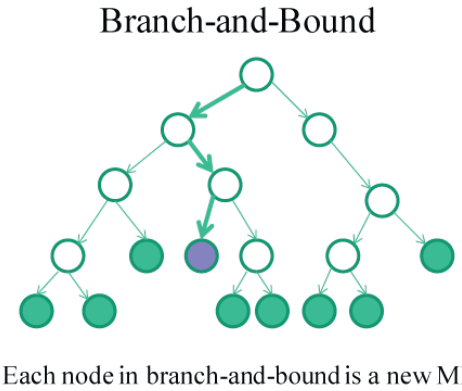

Figure F.7: Branch-and-Bound [44].

If a branch satisfies all integrality restrictions of the original problem it is not necessary to branch further on this branch, this branch can be fathomed and become a permanent leaf on the tree [44]. To be able to find the best branch, and thus the optimal solution to the mixed integer programming problem, it is important to know if the feasible solution just found is also the optimal one. The leaf with the best value for the objective function is known as the incumbent [45]. If thus a new leaf has a better value for the objective function it will become the new incumbent solution. Another option for a branch to be fathomed is if that branch only results in infeasible solutions and thus no further branching is necessary since it will not give any feasible solutions.

To be able to know when the optimal solution is found an upper and lower bound are defined. The upper bound is the current incumbent solution, as no new branch with a worse score for the objective function needs to be considered. The lower bound is defined by taking the minimum of the optimal objective functions of all the nodes. If the gap between the upper and lower bound becomes zero, then the optimal solution has been found and the algorithm can be stopped [44].

F.3.2. Positive and negative features

To be able to use mixed integer programming algorithms to solve optimization problems, it is important that the full scope of the program is known. This is because to be able to use this, first a full mathematical model of the problem needs to be constructed and the objective function needs to be defined. Therefore, the impact of all variables on the model must be known to be able to come up with an algorithm that is capable of finding a feasible optimum for the problem. If this is the case for the problem at hand, then mixed integer programming can be a very good way to obtain that feasible optimum, as the model is not capable of giving an unfeasible solution. For more incomprehensible problems where the effect of all variables is not (completely) known, or the limitation of certain contributions is not fully understood this might likely not be the right approach.

F.4. Method choice

To select the best method for the mathematical model discussed in section 2.2 it is important that the positive and negative features of genetic algorithms, reinforcement learning and mixed integer programming are compared to each other.

There is a difference in the amount of data required for each algorithm. The reinforcement learning algorithm is a data heavy algorithm compared to mixed integer programming and genetic algorithms. This is because it is not based on a mathematical model, but solely on data analysis. This therefore requires a big data set that contains enough data to train the model on. Since Amsterdam Schiphol Airport is a busy hub airport with a considerable noise disturbance problem, there is plenty of data available for this analysis, however all of this data is from the current situation with 3 IAFs and the current distribution over the new IAFs and the standard flying routes towards them. It is therefore unlikely that based on analysis of this data a considerable research can be performed on the redistribution of aircraft over the IAFs and the environmental and noise impacts that come with it. Especially since currently there is no fourth IAF, which will become a big factor in the redesigned Dutch airspace [46], there is thus also no data for the routes to and from this IAF. Creating this data is possible, but would either require redirecting flights from the current standard approaches to fly the new to be designed path, lots of test flights with multiple aircraft types, or a thorough technical analysis on the flight path and emitted noise. All these options require a great amount of resources and are therefore unlikely to be performed in a way that the obtained data is of sufficient quality to base a reinforcement learning algorithm on. For mixed integer programming and genetic algorithms it is much easier to obtain data that is of sufficient quality as they require less data since they are not based on a data analysis.

Other important factors for the to be chosen algorithm are the accuracy, computational time, and feasibility of the proposed solution by the various algorithms. The computational time of genetic algorithms is generally found to be lower than reinforcement learning and mixed integer programming. Mixed integer programming usually has the longest computational time of the three algorithms discussed [47][48][49]. However since the to be designed model will function as an aid to route planning it is expected to run some time before the actual decisions have to be made. Real time decisions will remain in the hands of air traffic controllers and therefore the speed is not the most important factor. Genetic algorithms often have a larger variety on the

solutions found than reinforcement learning [48][49]. Meaning that in less occasions the most optimal solution is found. In general it was found to be that mixed integer programming had the highest accuracy [47]. Finding the optimal solution can be very important since the margins in aviation are slim. Furthermore, every percentage that can be won in either noise or emissions has a positive effect on the environment, whereas optimal routes reduce the costs for airliners. For feasibility, the only algorithm that guarantees a feasible solution is the mixed integer programming algorithm. This is because the constraints inflicted upon the system limit it from finding a solution that is not feasible. In the other algorithms it is however possible to inflict large penalties on infeasible solutions, practically achieving the same, it does however need some extra monitoring since in case of ATM every mistake can be fatal. However, since the final call remains with the air traffic controllers, this is deemed to be enough of a safety net. In table F.1 an overview of the performance of each method can be found.

Table F.1: Score Overview of Selected Algorithms.

	GA	**MIP**	**RL**
Data Availability	+	+	--
Accuracy of Solution	-	+	0
Execution Speed	+	-	0
Feasibility of Solution	+	++	+

In conclusion reinforcement learning is discarded as an option since the data required is not available, or would take a long time and a great investment to obtain. The research was continued with both mixed integer programming, and genetic algorithms. The model presented in section 2.2 was implemented using both algorithms. After implementation of the model it was found that MIP produced such considerable better solutions, while not having a considerably higher execution time compared to GA, that GA was discarded. The GA algorithm was instead used to check solutions found in the MIP implementation of the model, and to find mistakes in the model itself. All results presented in this research are therefore from the MIP implementation of the model.

G

Results

In this chapter the results obtained in this research will be presented. First in appendix G.1, the Base scenario, including all 4 new IAF will be explained, and taken as the basis of the discussion. In appendix G.2, appendix G.3, and appendix G.4 the other scenarios are presented, along with the objective costs found for these scenarios. Not all scenarios are discussed however, to decide which scenarios are interesting a Pareto optimal front is used to select all Pareto optimal scenarios. This is done in appendix G.5. Finally the Pareto optimal scenarios are discussed by day in appendix G.6.

G.1. Base Scenario

To be able to compare the various results with each other, a $BASE_{E50\%,N50\%}$ scenario is created. This $BASE_{E50\%,N50\%}$ scenario is a hybrid scenario where all aircraft are adhered to their originally assigned runways, but with the inclusion of the 4th IAF. The choice for which IAF is selected is based on the amount of time it takes to fly from the origin of the aircraft via an IAF to the assigned runway. In other words, it is based on the shortest route, which is roughly similar to current practice. The optimization is then run with the following settings:

Table G.1: Settings for Base Scenario.

Constant	**Value**	**Description**
C_{NOISE}	1	Normalization constant for Noise Objective
$C_{EMISSION}$	1	Normalization constant for Emission Objective
C_{DELAY}	1	Normalization constant for Delay Objective
$EMISSION$	50%	Importance Emission Objective $EMISSIONS + NOISE = 100\%$
$NOISE$	50%	Importance Noise Objective $EMISSIONS + NOISE = 100\%$
$EastWestSeparation$	$False$	If True: Strict East-West Separation meaning no aircraft can fly from a Western IAF to the Eastern runway and vice versa. If False: No East-West Separation is maintained.
$FixedRunway$	$True$	If True: Aircraft are fixed to the runway they originally landed on on the specific date run. If False: Aircraft have free choice of available runways.
$IAF4$	$True$	If True: Aircraft are allowed to fly via the 4th IAF. if False: The 4th IAF is not available

In table I.1 an overview of all Base scenarios is given.

Table G.2: Base Scenario descriptions.

Scenario	**Description**
$BASE_{E50\%,N50\%}$	Base scenario, with $EMISSION = 50\%$ and $NOISE = 50\%$

Below the cost of these runs can be found:

Table G.3: Objective Costs for $BASE_{E50\%,N50\%}$ Scenario..

	Busy Day 16 September 2019	**Average Day 26 October 2019**	**Quiet Day 21 March 2019**
Delay Objective Cost	5,377	5,899	2
Emission Objective Cost	8,088,974	7,607,592	5,984,908
Noise Objective Cost	106,720	67,754	44,994
Total Objective Cost	8,201,071	7,681,244	6,029,904

In order to be able to compare all the scenarios to the $BASE_{E50\%,N50\%}$ scenario, and to create an equal weight between the objective costs, the costs found in table G.3 are normalized to 10^6. The delay cost however is not normalized, this is done because normalizing the delay objective to the same value as the other objectives limited the model too much in finding optimal solutions for noise and emission cost. Removing the delay objective was also considered, but this resulted in unwanted solutions as aircraft had no incentive anymore to stay close to their originally assigned landing times. Therefore it was decided not to normalize the delay objective cost at all since this number was already much lower than the noise and emission objective costs. This did not produce new problems as for all scenarios the average deviation per aircraft of the originally assigned landing time remained below the currently used time window of 2 minutes. The normalized $BASE_{E50\%,N50\%}$ scenario can be found in table G.4.

Table G.4: Normalized Objective Costs for Base Scenario.

	Busy Day 16 September 2019	**Average Day 26 October 2019**	**Quiet Day 21 March 2019**
Delay Objective Cost	5,377	5,899	2
Emission Objective Cost	1,000,000	1,000,000	1,000,000
Noise Objective Cost	1,000,000	1,000,000	1,000,000
Total Objective Cost	2,005,377	2,005,899	2,000,002

To achieve this normalization, the objective costs are multiplied with normalization factors. These can be found in table G.5.

Table G.5: Normalization Factors for Each Day and Objective.

	Busy Day 16 September 2019	**Average Day 26 October 2019**	**Quiet Day 21 March 2019**
C_{DELAY}	1	1	1
$C_{EMISSION}$	0.12362506744787292	0.13144763973825857	0.16708694822698303
C_{NOISE}	9.370314942239448	14.759355878390776	22.224992479711354

The normalization factors as seen in table G.5 are used in all other runs so that they can be easily compared to the $BASE_{E50\%,N50\%}$ scenario.

G.2. Old Scenario

For the old scenario, an attempt is made to mimic the situation as is current practice if strict approach routes would be followed. This means that the 4th IAF does not exist, so no aircraft will be able to use it to transition towards a runway. The runway is selected based on the original runway the aircraft actually landed on as well and the IAF is selected on the basis of shortest route given the runway, similar to the $BASE_{E50\%,N50\%}$ scenario IAF/runway selection process with the difference that the 4th IAF is not to be selected. This gives the following settings:

Table G.6: Settings for Old Scenario.

Constant	Value	Description
C_{NOISE}	See table G.5	Normalization constant for Noise Objective
$C_{EMISSION}$	See table G.5	Normalization constant for Emission Objective
C_{DELAY}	1	Normalization constant for Delay Objective
$EMISSION$	[0%, 25%, 50%, 75%, 100%]	Importance Emission Objective $EMISSIONS + NOISE = 100\%$
$NOISE$	[100%, 75%, 50%, 25%, 0%]	Importance Noise Objective $EMISSIONS + NOISE = 100\%$
$EastWestSeparation$	$False$	If True: Strict East-West Separation meaning no aircraft can fly from a Western IAF to the Eastern runway and vice versa. If False: No East-West Separation is maintained.
$FixedRunway$	$True$	If True: Aircraft are fixed to the runway they originally landed on on the specific date run. If False: Aircraft have free choice of available runways.
$IAF4$	$False$	If True: Aircraft are allowed to fly via the 4th IAF. if False: The 4th IAF is not available

In table G.7 an overview of all Old scenarios is given.

Table G.7: Old Scenario descriptions.

Scenario	Description
$OLD_{E0\%,N100\%}$	Old scenario, with $EMISSION = 0\%$ and $NOISE = 100\%$
$OLD_{E25\%,N75\%}$	Old scenario, with $EMISSION = 25\%$ and $NOISE = 75\%$
$OLD_{E50\%,N50\%}$	Old scenario, with $EMISSION = 50\%$ and $NOISE = 50\%$
$OLD_{E75\%,N25\%}$	Old scenario, with $EMISSION = 75\%$ and $NOISE = 25\%$
$OLD_{E100\%,N0\%}$	Old scenario, with $EMISSION = 100\%$ and $NOISE = 0\%$

G.2.1. Objective Costs

Table G.8: Difference in Objective Costs Compared to $BASE_{E50\%,N50\%}$ for $OLD_{E0\%,N100\%}$.

Emission = 0% Noise = 100%	Busy Day 16 September 2019	Average Day 26 October 2019	Quiet Day 21 March 2019
Emission Objective Cost	+0.4956%	+0.0314%	+0.0069%
Noise Objective Cost	+4.3011%	+0.9921%	+0.8173%
Total Objective Cost	+2.4811%	+0.5365%	+0.4121%

Table G.9: Difference in Objective Costs Compared to $BASE_{E50\%,N50\%}$ for $OLD_{E25\%,N75\%}$.

Emission = 25% Noise = 75%	Busy Day 16 September 2019	Average Day 26 October 2019	Quiet Day 21 March 2019
Emission Objective Cost	+0.4952%	+0.0309%	+0.0069%
Noise Objective Cost	+4.3011%	+0.9921%	+0.8173%
Total Objective Cost	+2.4810%	+0.5331%	+0.4121%

Table G.10: Difference in Objective Costs Compared to $BASE_{E50\%,N50\%}$ for $OLD_{E50\%,N50\%}$.

Emission = 50% Noise = 50%	Busy Day 16 September 2019	Average Day 26 October 2019	Quiet Day 21 March 2019
Emission Objective Cost	+0.4953%	+0.0309%	+0.0069%
Noise Objective Cost	+4.3011%	+0.9921%	+0.8173%
Total Objective Cost	+2.4806%	+0.5331%	+0.4121%

Table G.11: Difference in Objective Costs Compared to $BASE_{E50\%,N50\%}$ for $OLD_{E75\%,N25\%}$.

Emission = 75% **Noise = 25%**	**Busy Day** **16 September 2019**	**Average Day** **26 October 2019**	**Quiet Day** **21 March 2019**
Emission Objective Cost	+0.4953%	+0.0309%	+0.0069%
Noise Objective Cost	+4.3011%	+0.9921%	+0.8173%
Total Objective Cost	+2.4806%	+0.5331%	+0.4121%

Table G.12: Difference in Objective Costs Compared to $BASE_{E50\%,N50\%}$ for $OLD_{E100\%,N0\%}$.

Emission = 100% **Noise = 0%**	**Busy Day** **16 September 2019**	**Average Day** **26 October 2019**	**Quiet Day** **21 March 2019**
Emission Objective Cost	+0.4953%	+0.0309%	+0.0069%
Noise Objective Cost	+4.3011%	+0.9921%	+0.8173%
Total Objective Cost	+2.4806%	+0.5331%	+0.4121%

G.3. New and Separation Scenario, NAS Scenario

The new scenario is based on plans of redesigning the dutch airspace to incorporate a 2+2 runway use at AAS [5][6]. In this concept the 2+2 means that always 2 runways are available for arriving aircraft and 2 runways are available for departing aircraft. For this, it was stated that it would no longer be possible to allow aircraft to land on a Western runway whilst flying via an Eastern IAF and vice versa. Therefore, the NAS scenario takes into account this East-West separation. Of course for the new scenario also the 4th IAF is included as it is specifically designed for this. This gives the following settings:

Table G.13: Settings for NAS Scenario.

Constant	**Value**	**Description**
C_{NOISE}	See table G.5	Normalization constant for Noise Objective
$C_{EMISSION}$	See table G.5	Normalization constant for Emission Objective
C_{DELAY}	1	Normalization constant for Delay Objective
$EMISSION$	[0%, 25%, 50%, 75%, 100%]	Importance Emission Objective $EMISSIONS + NOISE = 100\%$
$NOISE$	[100%, 75%, 50%, 25%, 0%]	Importance Noise Objective $EMISSIONS + NOISE = 100\%$
$EastWestSeparation$	$True$	If True: Strict East-West Separation meaning no aircraft can fly from a Western IAF to the Eastern runway and vice versa. If False: No East-West Separation is maintained.
$FixedRunway$	$False$	If True: Aircraft are fixed to the runway they originally landed on on the specific date run. If False: Aircraft have free choice of available runways.
$IAF4$	$True$	If True: Aircraft are allowed to fly via the 4th IAF. if False: The 4th IAF is not available

In table G.14 an overview of all NAS scenarios is given.

Table G.14: NAS Scenario descriptions.

Scenario	**Description**
$NAS_{E0\%,N100\%}$	NAS scenario, with $EMISSION = 0\%$ and $NOISE = 100\%$
$NAS_{E25\%,N75\%}$	NAS scenario, with $EMISSION = 25\%$ and $NOISE = 75\%$
$NAS_{E50\%,N50\%}$	NAS scenario, with $EMISSION = 50\%$ and $NOISE = 50\%$
$NAS_{E75\%,N25\%}$	NAS scenario, with $EMISSION = 75\%$ and $NOISE = 25\%$
$NAS_{E100\%,N0\%}$	NAS scenario, with $EMISSION = 100\%$ and $NOISE = 0\%$

G.3.1. Objective Costs

Table G.15: Difference in Objective Costs Compared to $BASE_{E50\%,N50\%}$ for $NAS_{E0\%,N100\%}$.

Emission = 0% **Noise = 100%**	**Busy Day** **16 September 2019**	**Average Day** **26 October 2019**	**Quiet Day** **21 March 2019**
Emission Objective Cost	+0.4590	+0.2395	-0.3535%
Noise Objective Cost	-7.4862%	-12.3173%	+16.1785%
Total Objective Cost	-3.1433%	-5.4733%	+7.9124%

Table G.16: Difference in Objective Costs Compared to $BASE_{E50\%,N50\%}$ for $NAS_{E25\%,N75\%}$.

Emission = 25% **Noise = 75%**	**Busy Day** **16 September 2019**	**Average Day** **26 October 2019**	**Quiet Day** **21 March 2019**
Emission Objective Cost	+0.2996%	+0.2350%	-0.3535%
Noise Objective Cost	-7.4327%	-12.3026%	+16.1785%
Total Objective Cost	-3.2226%	-5.4518%	+7.9124%

Table G.17: Difference in Objective Costs Compared to $BASE_{E50\%,N50\%}$ for $NAS_{E50\%,N50\%}$.

Emission = 50% **Noise = 50%**	**Busy Day** **16 September 2019**	**Average Day** **26 October 2019**	**Quiet Day** **21 March 2019**
Emission Objective Cost	-0.0080%	+0.2345%	-0.3535%
Noise Objective Cost	-7.1670%	-12.2862%	+16.1785%
Total Objective Cost	-3.3847%	-5.4777%	+7.9124%

Table G.18: Difference in Objective Costs Compared to $BASE_{E50\%,N50\%}$ for $NAS_{E75\%,N25\%}$.

Emission = 75% **Noise = 25%**	**Busy Day** **16 September 2019**	**Average Day** **26 October 2019**	**Quiet Day** **21 March 2019**
Emission Objective Cost	-0.2172%	+0.0996%	-0.4133%
Noise Objective Cost	-6.6390%	-11.7760%	+16.3420%
Total Objective Cost	-3.2420%	-5.4777%	+7.9642%

Table G.19: Difference in Objective Costs Compared to $BASE_{E50\%,N50\%}$ for $NAS_{E100\%,N0\%}$.

Emission = 100% **Noise = 0%**	**Busy Day** **16 September 2019**	**Average Day** **26 October 2019**	**Quiet Day** **21 March 2019**
Emission Objective Cost	-0.4979%	-0.0495%	-1.0988%
Noise Objective Cost	-1.3295%	-3.9589%	+36.0132%
Total Objective Cost	-0.8104%	-1.7879%	+17.4571%

G.4. New without Separation Scenario, NWS Scenario

This scenario is similar to the previous one, but incorporated into the research to see the effect of the East-West separation. The only difference is therefore that the East-West separation is not enforced in this scenario. These scenarios are investigated to see what the effect would be of the East-West separation. However, it is unlikely that for all investigated days the NWS scenario would be possible, as the amount of conflict areas in the airspace could increase significantly and therefore the workload for ATC.

The settings for the NWS scenarios are as follows:

Table G.20: Settings for NWS Scenario.

Constant	Value	Description
C_{NOISE}	See table G.5	Normalization constant for Noise Objective
$C_{EMISSION}$	See table G.5	Normalization constant for Emission Objective
C_{DELAY}	1	Normalization constant for Delay Objective
$EMISSION$	[0%, 25%, 50%, 75%, 100%]	Importance Emission Objective $EMISSIONS + NOISE = 100\%$
$NOISE$	[100%, 75%, 50%, 25%, 0%]	Importance Noise Objective $EMISSIONS + NOISE = 100\%$
$EastWestSeparation$	$False$	If True: Strict East-West Separation meaning no aircraft can fly from a Western IAF to the Eastern runway and vice versa. If False: No East-West Separation is maintained.
$FixedRunway$	$False$	If True: Aircraft are fixed to the runway they originally landed on on the specific date run. If False: Aircraft have free choice of available runways.
$IAF4$	$True$	If True: Aircraft are allowed to fly via the 4th IAF. if False: The 4th IAF is not available

In table G.21 an overview of all NWS scenarios is given.

Table G.21: NWS Scenario descriptions.

Scenario	Description
$NWS_{E0\%,N100\%}$	NWS scenario, with $EMISSION = 0\%$ and $NOISE = 100\%$
$NWS_{E25\%,N75\%}$	NWS scenario, with $EMISSION = 25\%$ and $NOISE = 75\%$
$NWS_{E50\%,N50\%}$	NWS scenario, with $EMISSION = 50\%$ and $NOISE = 50\%$
$NWS_{E75\%,N25\%}$	NWS scenario, with $EMISSION = 75\%$ and $NOISE = 25\%$
$NWS_{E100\%,N0\%}$	NWS scenario, with $EMISSION = 100\%$ and $NOISE = 0\%$

G.4.1. Objective Costs

Table G.22: Difference in Objective Costs Compared to $BASE_{E50\%,N50\%}$ for $NWS_{E0\%,N100\%}$.

Emission = 0% Noise = 100%	Busy Day 16 September 2019	Average Day 26 October 2019	Quiet Day 21 March 2019
Emission Objective Cost	+1.6545%	+0.6306%	+0.0218%
Noise Objective Cost	-16.3881%	-23.2785%	-21.9387%
Total Objective Cost	-1.6598%	-7.3004%	-10.9584%

Table G.23: Difference in Objective Costs Compared to $BASE_{E50\%,N50\%}$ for $NWS_{E25\%,N75\%}$.

Emission = 25% Noise = 75%	Busy Day 16 September 2019	Average Day 26 October 2019	Quiet Day 21 March 2019
Emission Objective Cost	+1.3630%	+0.6253%	+0.0218%
Noise Objective Cost	-16.0572%	-23.1783%	-21.9387%
Total Objective Cost	-4.3845%	-7.2803%	-10.9584%

Table G.24: Difference in Objective Costs Compared to $BASE_{E50\%,N50\%}$ for $NWS_{E50\%,N50\%}$.

Emission = 50% **Noise = 50%**	**Busy Day** **16 September 2019**	**Average Day** **26 October 2019**	**Quiet Day** **21 March 2019**
Emission Objective Cost	+0.9633%	+0.4989%	+0.0218%
Noise Objective Cost	-15.5691%	-22.9083%	-21.9387%
Total Objective Cost	-4.9151%	-8.0388%	-10.9584%

Table G.25: Difference in Objective Costs Compared to $BASE_{E50\%,N50\%}$ for $NWS_{E75\%,N25\%}$.

Emission = 75% **Noise = 25%**	**Busy Day** **16 September 2019**	**Average Day** **26 October 2019**	**Quiet Day** **21 March 2019**
Emission Objective Cost	+0.1267%	+0.1259%	-0.0218%
Noise Objective Cost	-13.5561%	-21.7815%	-21.8609%
Total Objective Cost	-5.9868%	-10.1081%	-10.9413%

Table G.26: Difference in Objective Costs Compared to $BASE_{E50\%,N50\%}$ for $NWS_{E100\%,N0\%}$.

Emission = 100% **Noise = 0%**	**Busy Day** **16 September 2019**	**Average Day** **26 October 2019**	**Quiet Day** **21 March 2019**
Emission Objective Cost	-0.5287%	-0.1253%	-1.0988%
Noise Objective Cost	+0.8541%	-3.7334%	+36.0132%
Total Objective Cost	+0.1748%	-1.8227%	+17.4571%

G.5. Pareto Optimal Solutions

Since the objective function is not formed under the agreement of all stakeholders, it can be assumed that they will not all agree on the solution with the lowest objective cost being the best. Therefore it is important to investigate all possible outcomes that are optimal for one stakeholder, or when looking at combined costs is optimal for multiple stakeholders. One way to do so is using Pareto optimality.

G.5.1. Principle of Pareto Optimality

The idea behind Pareto optimality originates from economic equilibrium and welfare policies during the 20th century. The concept is that maximum economic satisfaction is reached when there are no measures to be taken that only benefit a part of the society. No one can be worse off. If there is a measure that benefits some without negatively influencing the others the current situation is not Pareto optimal [22].

A typical example where Pareto optimality is involved is the house purchase problem. In table G.27 three houses A, B, and C are given with costs from 0 to 5 based on their performance in each of 3 categories. All houses are equally expensive so the only decision factors are the categories presented. Looking at table G.27 immediately shows that house B can be eliminated as in no category it is better than house A or C, since it is possible to buy house A or C withour giving in on any of the categories. Looking at the environment category it shows that house A has the highest score of all houses. This means that house A is Pareto optimal, since it is not possible to buy house B or C without giving in on the environment category. Similarly this holds for house C in the appearance category. Making house A and C Pareto optimal and house B not.

Table G.27: Example Pareto Optimality [22].

	A	B	C
Appearance	3	3	5
Comfort	4	4	4
Environment	5	4	3

G.5.2. Pareto Front

To see which solutions are worth investigating into more depth a Pareto front is created. A Pareto front is defined as all combinations of Pareto optimal solutions. So in the case of the example presented in appendix G.5.1 houses A and C would form the Pareto front.

A Pareto front is made for each day in the $BASE_{E50\%,N50\%}$ scenario. The front will consist out of the objective cost for noise and emission. The delay objective is not taken into account for the Pareto front. Variations on the importance of either objective in the objective function are made by changing the values of $EMISSION$ and $NOISE$. They are however, always linked to each other according to the following formula:

$$EMISSION + NOISE = 100\% \tag{G.1}$$

In figure G.1, figure G.2, and figure G.3 the noise and emission objective scores are plotted for all scenarios. In these figures the Pareto front is drawn in red. The Pareto optimal scenarios, which lie at the Pareto front, are selected to be discussed into detail, along with the $BASE_{E50\%,N50\%}$ and Old scenario. The remaining scenarios are not discussed, since these do not present an interesting solution as better ones are available. In appendix G.6.1 the Pareto optimal optimizations for a busy day can be found, in appendix G.6.2 for an average day, and in appendix G.6.3 for a quiet day.

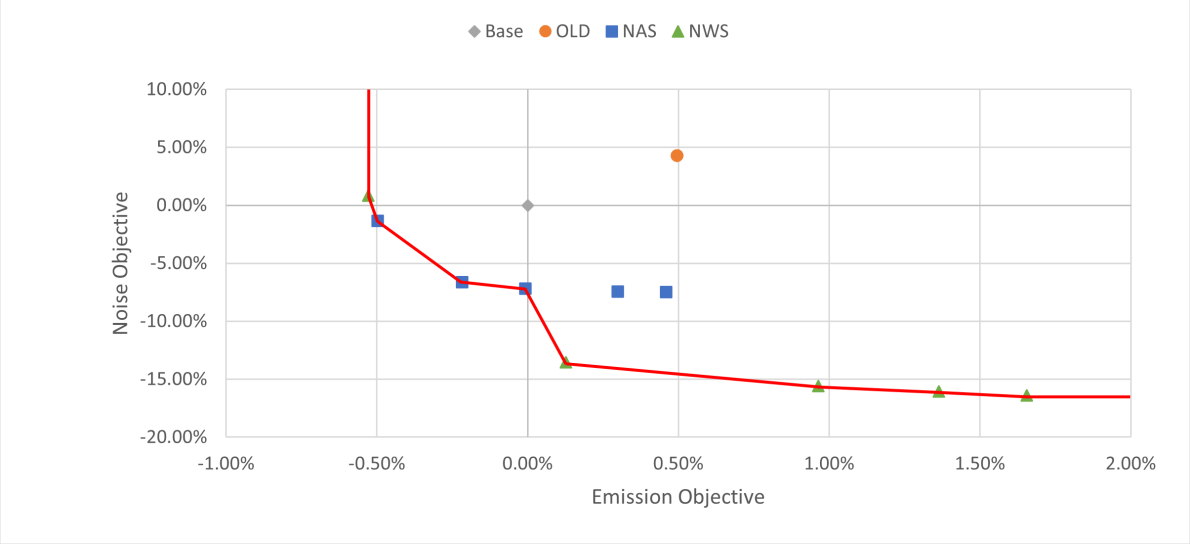

Figure G.1: Pareto Optimal Solutions for 16 September 2019.

For the busy day in figure G.1 it can be seen that the base scenario scores better than the old scenario on both the noise objective cost and the emission objective cost. The NAS scenarios also all perform better than the old scenario on both emission and noise. Compared to the base scenario all NAS scenarios still perform better on the noise objective cost, but only 3 out of the 5 scenarios also perform better on the emission objective cost. For the NWS scenarios only the scenario fully optimized for the emission objective cost has a lower emission objective cost than the base scenario, but at the cost of a slightly higher noise objective cost. All other NWS scenarios have a considerably lower noise objective cost compared to the base scenario, but also all have a higher emission objective cost. The Pareto front is indicated by the red line. This thus means that all scenarios on that line are Pareto optimal.

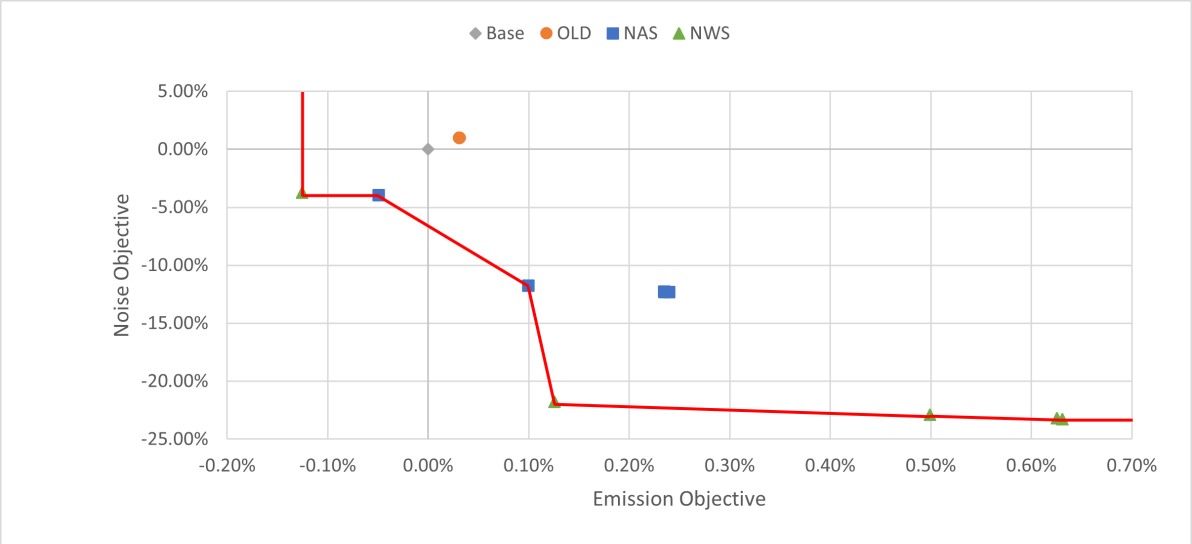

Figure G.2: Pareto Optimal Solutions for 26 October 2019.

For the average day in figure G.2 it can be seen that the base scenario performs better than the old scenario on both the noise objective cost and the emission objective cost as well. Compared to both the base and old scenario all NAS and NWS scenarios provide a significant decrease in the noise objective cost, but only the scenarios fully optimized for the emission objective cost also provides a decrease in emission objective cost for both the NAS and NWS scenarios. The Pareto front is indicated by the red line. This thus means that all scenarios on that line are Pareto optimal.

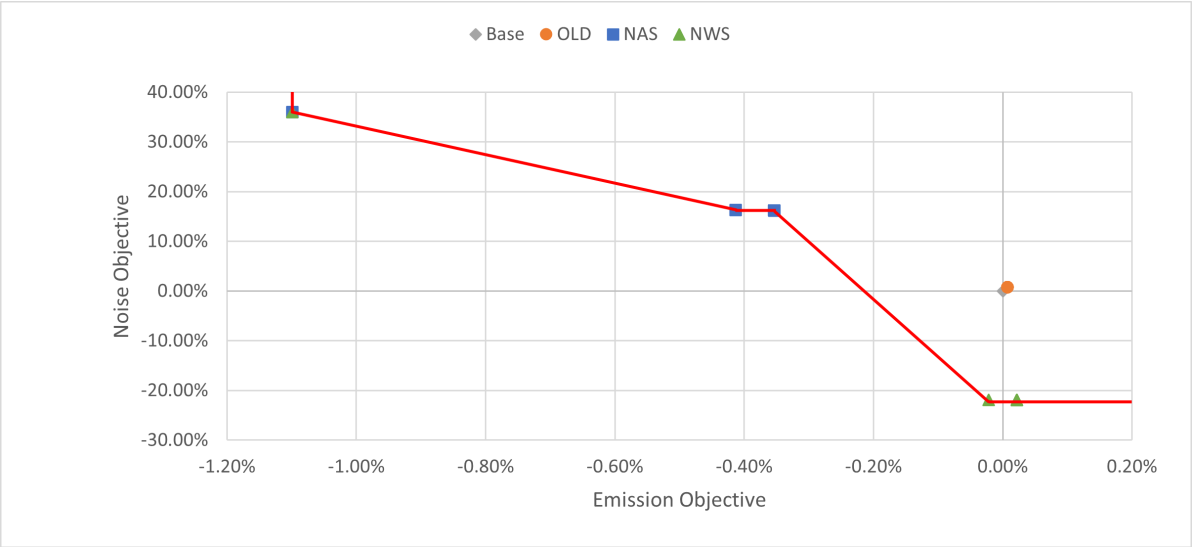

Figure G.3: Pareto Optimal Solutions for 21 March 2019.

For the quiet day in figure G.3 it can be seen that the base and old scenario score almost identical, with the base performing slightly better on both the noise, and emission objective cost. All NAS scenarios provide a solution with a lower emission objective cost compared to the base and old scenario, but at the cost of a much higher noise objective cost. For the NWS scenarios it is seen that the scenario fully optimized on the emission objective cost indeed has the best score for the emission objective cost, but at the cost of a much higher noise objective cost compared to the base and old scenario. The other NWS scenarios provide a significant decrease in noise objective cost while being almost equal on the emission objective cost compared to the base and old scenario. The Pareto front is indicated by the red line. This thus means that all scenarios on that line are Pareto optimal.

G.6. Analysis Pareto Optimal Solutions by Day

The effects and behaviour of the different scenarios on different traffic densities will be analyzed in this section. First the Busy Day will be analyzed in appendix G.6.1, then the Average Day in appendix G.6.2, and finally the Quiet Day in appendix G.6.3.

G.6.1. Busy Day, 16 September 2019

Table G.28: Objective Costs for all Pareto Optimal Scenarios for 16 September 2019 compared to $BASE_{E50\%,N50\%}$ Scenario.

Busy Day, 16 September 2019										
Scenario	Base	OLD	NAS	NAS	NAS	NWS	NWS	NWS	NWS	NWS
Emission	50%	50%	50%	75%	100%	0%	25%	50%	75%	100%
Noise	50%	50%	50%	25%	0%	100%	75%	50%	25%	0%
Emission Objective Cost	0%	+0.49%	-0.01%	-0.22%	-0.50%	+1.66%	+1.36%	+0.96%	0.13%	-0.53%
Noise Objective Cost	0%	+4.30%	-7.17%	-6.64%	-1.33%	-16.38%	-16.06%	-15.57%	-13.56%	+0.85%
Total Objective Cost	0%	+2.48%	-3.38%	-3.24%	-0.81%	-1.66%	-4.38%	-4.92%	-5.99%	+0.17%

Table G.29: Supporting Statistics for all Pareto Optimal Scenarios for 16 September 2019.

Busy Day, 16 September 2019										
Scenario	Base	OLD	NAS	NAS	NAS	NWS	NWS	NWS	NWS	NWS
Emission	50%	50%	50%	75%	100%	0%	25%	50%	75%	100%
Noise	50%	50%	50%	25%	0%	100%	75%	50%	25%	0%
Total Time Early Arrival [s]	4395	3260	4640	4488	4398	4376	4677	4423	3558	3608
Total Time Late Arrival [s]	491	1950	2306	2218	1500	57470	29858	24223	8028	1010
Total People Experiencing 48+ dB(A) [-]	4962293	4351525	4153110	4189549	4803352	3510069	3510423	3597817	3898181	4785488
Total People Experiencing 58+ dB(A) [-]	137764	136923	99814	96247	94486	101712	102847	100902	98133	94889
Total Flighttime [s]	7823589	7874727	7850140	7826431	7796685	8000756	7966541	7929438	7848940	7792256
Total CO_2 Emitted [kg]	25561158	25687751	25559116	25505633	25433895	25984080	25909560	25807388	25593542	25426024

Delay

For the Delay Objective from table G.28 it is important to split the cost in Early Arrival and Late Arrival, as can be seen in table G.29. No aircraft is allowed to deviate more than 15 minutes from their arrival time. Given a total amount of flights for the Busy Day of 762, this shows that the average amount of early arrival time per aircraft for all scenarios is between 4.3 and 6.1 seconds. This is relatively close to each other and a low number when taking the current planning horizon of 2 minutes into account. Similarly, the average late arrival time per aircraft for all scenarios is between 0.6 and 75.4 seconds. This is still well within the 2 minute window, but for some scenarios, especially the ones prioritizing the Noise Objective, the number is considerably higher than the average early arrival time.

Noise

From the Noise Objective costs as seen in table G.28 it is very clear that when the Noise Objective becomes more important the costs go down, which is exactly as expected. However, when looking at table G.29 and figure G.4 this does not hold for the amount of people experiencing a certain threshold value. This is because the Noise Objective does not optimise for only these groups, but for all people affected by noise emitted around AAS. This could therefore mean that for the model it is more beneficial to reduce noise for a large group that was already below the 48+dB(A) threshold at the cost of slightly more people inside the 48+dB(A) threshold area. One of the reasons for this is to prevent the model of allowing large amounts of people just below these threshold values.

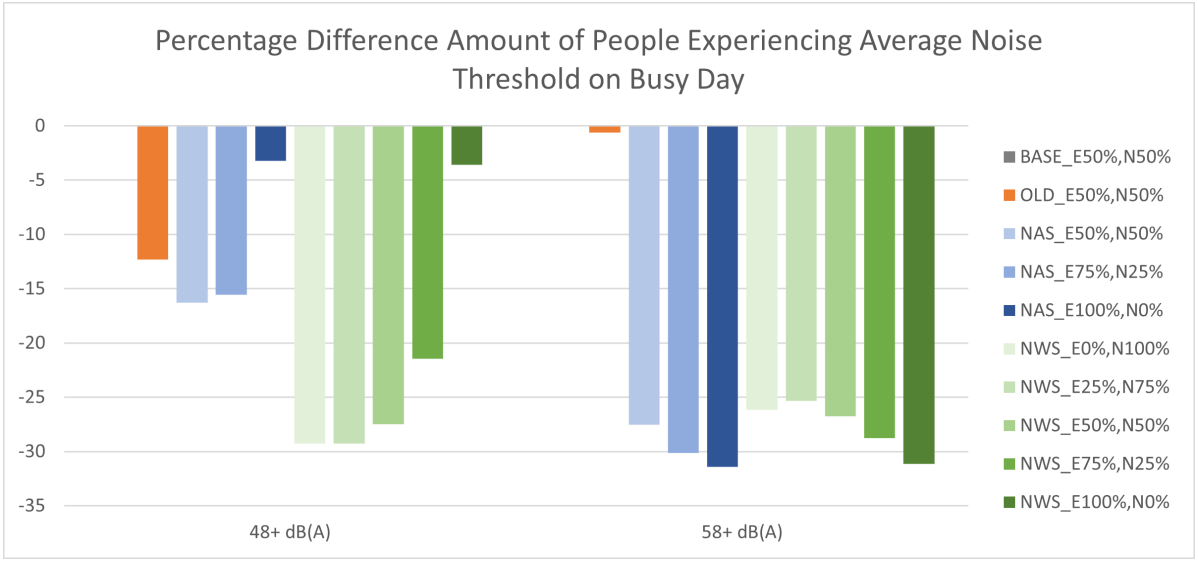

Figure G.4: Percentage Difference Amount of People Experiencing Average Noise Threshold Compared to $BASE_{E50\%,N50\%}$ Scenario on a Busy Day (16 September 2019).

An example of what this looks like can be seen in figure G.5. Here the $BASE_{E50\%,N50\%}$ scenario is shown with the scenario with the lowest noise cost ($NWS_{E0\%,N100\%}$) and how they compare to the $BASE_{E50\%,N50\%}$ scenario. From the noise contour it can be seen that especially over higher populated areas $NWS_{E0\%,N100\%}$ performs considerably better as it aims to stay away from these areas, which are indicated by the grey areas in the comparison figure. All noise contours for each scenario can be found in appendix I.1.

In general it can be stated that all scenarios perform better than the $OLD_{E50\%,N50\%}$ Scenario. The addition of the 4th IAF alone can result in a decrease of 4.3% point as seen when comparing the $OLD_{E50\%,N50\%}$ Scenario with the $BASE_{E50\%,N50\%}$ Scenario. This does however comes at the cost of an increased amount of people that experience the average threshold levels of 48+dB(A) and 58+dB(A).
Combining the extra IAF with NAS ($NAS_{E50\%,N50\%}$, $NAS_{E75\%,N25\%}$, $NAS_{E100\%,N0\%}$) has the potential to further decrease the Noise Objective cost with 7.17% point, while also decreasing the amount of people experiencing the threshold levels compared to the $OLD_{E50\%,N50\%}$ scenario, especially in the 58+dB(A) region.
Looking at the NWS scenarios it is seen that an even bigger potential decrease can be achieved of 16.38% point when compared to the $BASE_{E50\%,N50\%}$ scenario, while scoring even better in the 48+dB(A) threshold area than the NAS scenarios. The 58+dB(A) NWS scenarios perform approximately equal to the NAS scenarios. An important note to make here is that it is unlikely that the NWS scenarios are feasible for a busy day as explained in appendix G.4.

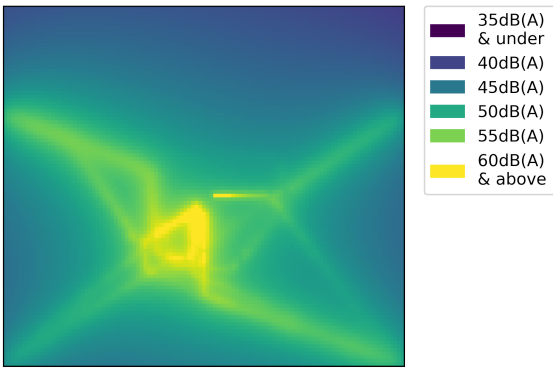

(a) L_{DEN} Average for $BASE_{E50\%,N50\%}$.

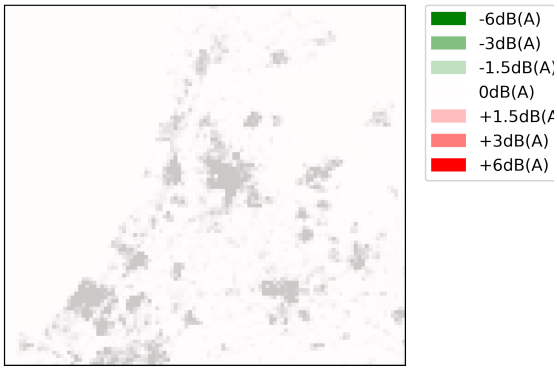

(b) Change in L_{DEN} Average Compared to $BASE_{E50\%,N50\%}$ for $BASE_{E50\%,N50\%}$.

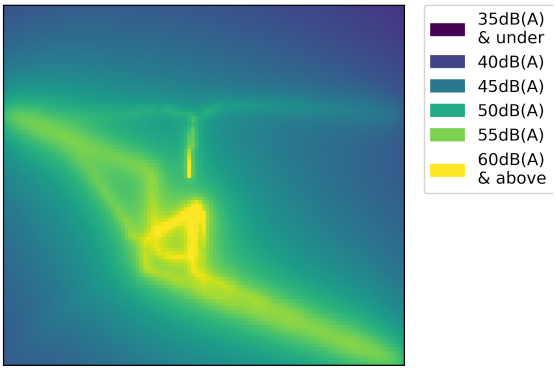

(c) L_{DEN} Average for $NWS_{E0\%,N100\%}$.

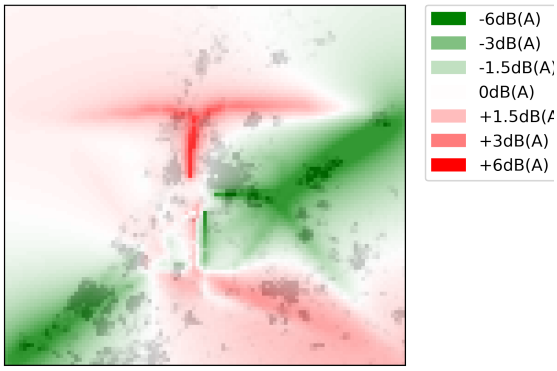

(d) Change in L_{DEN} Average Compared to $BASE_{E50\%,N50\%}$ for $NWS_{E0\%,N100\%}$.

Figure G.5: Example L_{DEN} Noise Contours for a Busy Day, 16 September 2019.

Emissions and Flighttime

The Emission Objective costs can be found in table G.28. Similar to the Noise Objective the costs go down when the objective becomes more important. From the indexed values it shows that the total difference in emitted CO_2 differs from 0.53% point ($NWS_{E100\%,N0\%}$) below the $BASE_{E50\%,N50\%}$ scenario to 1.66% point above it, as can also be seen in figure G.6. What also stands out from this graph is that the flighttime follows almost the same trend as the emissions, which of course is not very strange since if an aircraft flies longer it also uses more fuel, and thus emits more CO_2 since the Emission Objective is directly related to the fuel use of an aircraft.

The reason that the difference in Emission Objective cost between the various scenarios is limited compared to the Noise objective is that where the full noise cost is calculated within the section between the IAF and the Runway, the emitted CO_2 is calculated for the whole flight, thus resulting in smaller deviations in the final number. But since the total amount of CO_2 emitted during a day, as seen in table G.29, is a high number this still has a considerable impact as a 1% point difference could mean an increase or decrease of the CO_2 emitted of approximately 255,000 kg on a busy day.

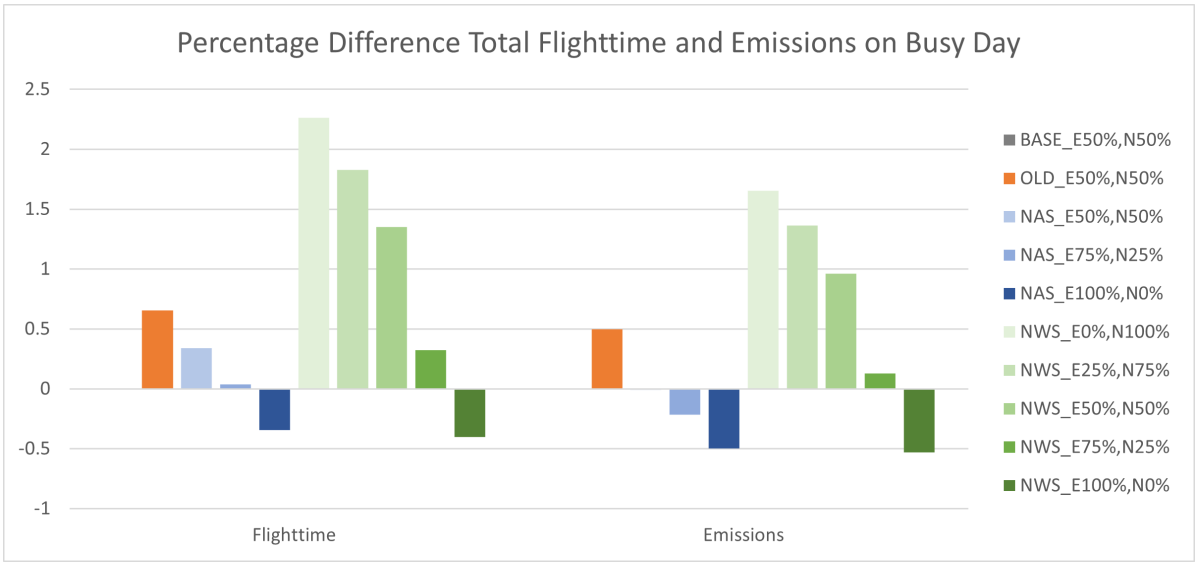

Figure G.6: Percentage Difference Total Flighttime and Emissions Compared to $BASE_{E50\%,N50\%}$ Scenario on a Busy Day (16 September 2019).

In general it can be stated that adding the 4th IAF results in a CO_2 reduction of 0.49% point, as seen by looking at the $BASE_{E50\%,N50\%}$ and $OLD_{E50\%,N50\%}$ scenario. When looking at the NAS scenarios it is seen that all have a lower or comparable amount of emissions compared to the $BASE_{E50\%,N50\%}$ scenario. The NWS scenarios clearly show more variation, with espacially $NWS_{E0\%,N100\%}$, $NWS_{E25\%,N75\%}$, and $NWS_{E50\%,N50\%}$ having a higher emission cost compared to both the $BASE_{E50\%,N50\%}$ and $OLD_{E50\%,N50\%}$ scenarios. The reason for this is simple since with adding more options comes the availability of choosing less noise costly routes, but at the cost of a longer flighttime and emission cost.

For the flighttime similar trends are found.

Runway and IAF selection

In figure G.7 and figure G.8 the IAF/runway combinations used by the various scenarios can be seen compared to the $BASE_{E50\%,N50\%}$ scenario. The Noise contours in appendix I.1 also give a good visual representation of the routes used for each scenario.

Adding the 4th IAF clearly has a large impact on the chosen routes as instead of 3 routes there are now 4 routes to a runway, resulting in shorter flight paths. A clear example for this is the usage of combinations RIVER/36R, ARTIP/36R, and IAF4/36R. Since in the $OLD_{E50\%,N50\%}$ scenario no aircraft was allowed to fly via IAF4 they needed to go via RIVER or ARTIP, but with IAF4 available in the $BASE_{E50\%,N50\%}$ scenario a shorter route became available for almost 150 aircraft. This is even more clearly illustrated in figure G.9 where in total a little over 250 aircraft found a shorter way via the new 4th IAF. Since no change is seen in SUGOL between

these scenarios it is clear that all these aircraft arrive from the South/South-East/East.
For the NAS scenarios it is clear that indeed it cannot use any IAF/runway combination violating the East-West separation, such as for example the combinations SUGOL/36R and IAF4/36C as seen in figure G.7 and figure G.8. One thing that stands out the most is the usage of IAF4/36R, which is clearly not only beneficial for noise, but also provides a shorter route since $NAS_{E100\%,N0\%}$ is only optimized for emission. Similarly, but with a smaller amount this also holds for combinations SUGOL/06, SUGOL/36C, and SUGOL/18R. This implies both for a considerable amount of traffic it is beneficial to fly via SUGOL emission wise, but it provides beneficial routes noise wise as well as can be seen by the behaviour of the $NAS_{E50\%,N50\%}$ and $NAS_{E75\%,N25\%}$ in figure G.9.
Looking at the same graphs it is clear the the East-West separation has a great influence on the IAF/runway selection, as the NWS scenarios follow a completely different trend than the NAS scenarios. The one thing that stands out the most is the combination of IAF4/06 which is used a lot by Noise Objective dominated $NWS_{E0\%,100N\%}$ and $NWS_{E25\%,N75\%}$, but not with Emission Objective dominated $NWS_{E75\%,25N\%}$ and $NWS_{E100\%,0N\%}$ scenarios. This implies that this approach is a very good approach to use when avoiding noise disturbance, but this comes at a higher emission cost. Interesting is also that the in high demand IAF4/36R for the NAS scenarios is not used that often for the Noise Objective dominated NWS scenarios $NWS_{E0\%,N100\%}$ and $NWS_{E25\%,N75\%}$. A lot of these flights instead use IAF4/36C or the earlier mentioned IAF4/06. This while clearly for the Emission dominated NWS scenarios IAF4/36R is still preferred.
In general for all scenarios it can be concluded that indeed all Western runways (06, 18R, and 36C) are less noise costly than the Eastern runways (36R and 27) as seen in figure G.9. Similarly this holds for IAF4 and SUGOL having less noise costly approaches on average compared to RIVER and ARTIP.

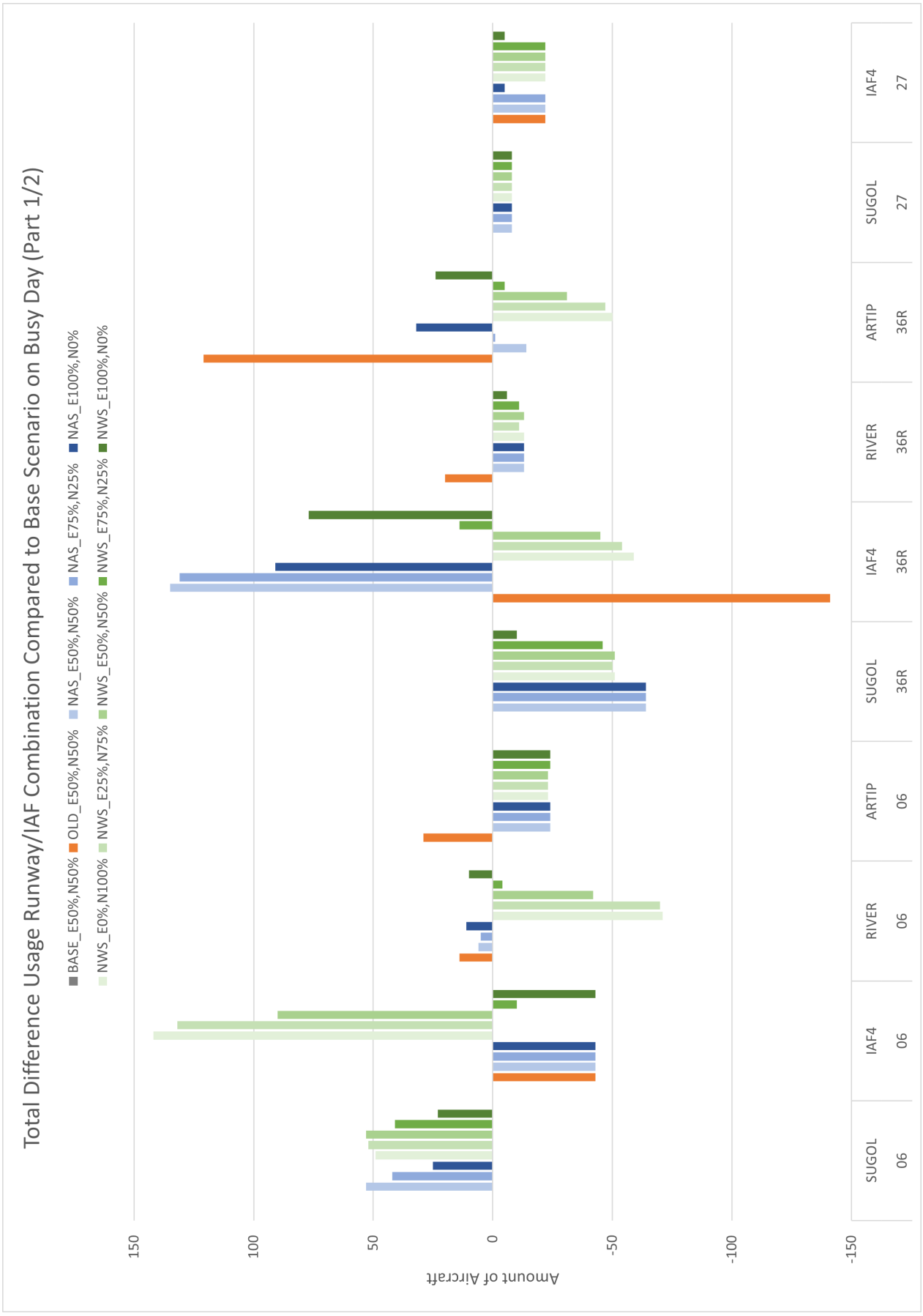

Figure G.7: Total Difference Usage IAF/Runway Combination Compared to $BASE_{E50\%,N50\%}$ Scenario on a Busy Day (16 September 2019) Part 1/2.

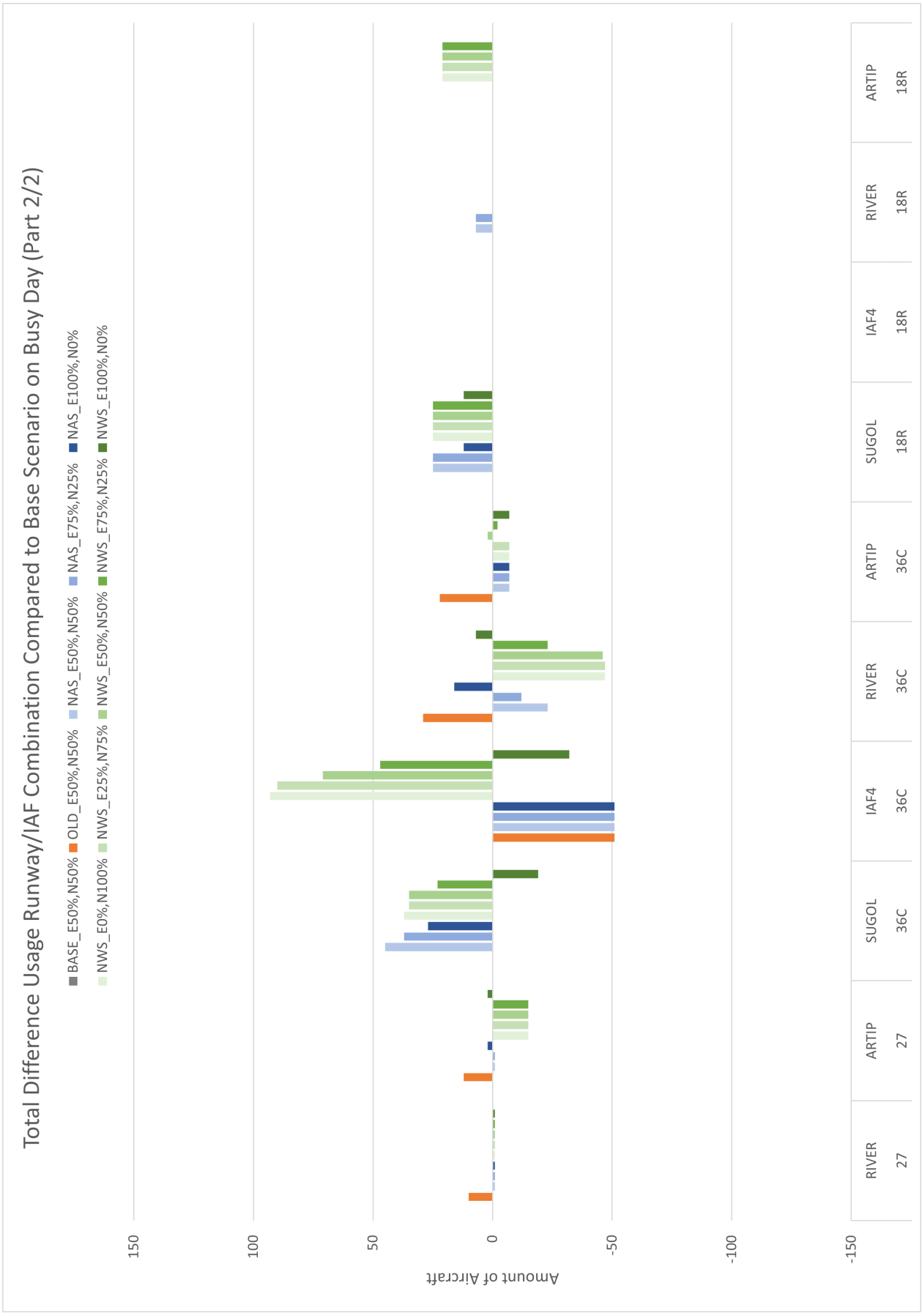

Figure G.8: Total Difference Usage IAF/Runway Combination Compared to $BASE_{E50\%,N50\%}$ Scenario on a Busy Day (16 September 2019) Part 2/2.

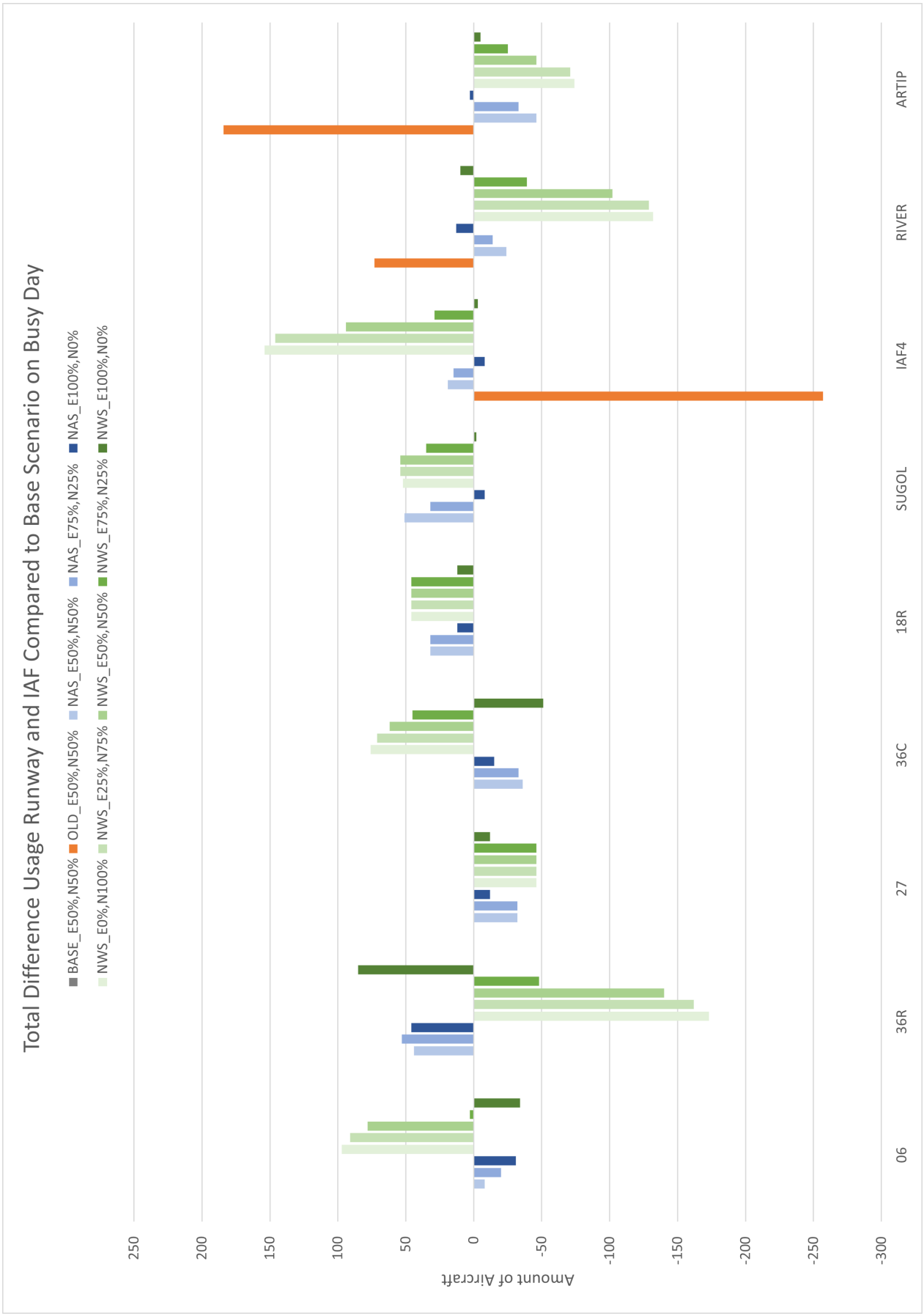

Figure G.9: Total Difference Usage Runway and IAF Compared to $BASE_{E50\%,N50\%}$ Scenario on a Busy Day (16 September 2019).

G.6.2. Average Day, 26 October 2019

Table G.30: Objective Costs for all Pareto Optimal Scenarios for 26 October 2019 compared to $BASE_{E50\%,N50\%}$ Scenario.

Average Day, 26 October 2019									
Scenario	Base	OLD	NAS	NAS	NWS	NWS	NWS	NWS	NWS
Emission	50%	50%	75%	100%	0%	25%	50%	75%	100%
Noise	50%	50%	25%	0%	100%	75%	50%	25%	0%
Emission Objective Cost	0%	+0.03%	+0.10%	-0.05%	+0.63%	+0.63%	+0.50%	+0.13%	-0.13%
Noise Objective Cost	0%	+0.99%	-11.78%	-3.96%	-23.28%	-23.18%	-22.91%	-21.78%	-3.73%
Total Objective Cost	0%	+0.53%	-5.48%	-1.79%	-7.30%	-7.28%	-8.04%	-10.11%	-1.82%

Table G.31: Supporting Statistics for all Pareto Optimal Scenarios for 26 October 2019.

Average Day, 26 October 2019									
Scenario	Base	OLD	NAS	NAS	NWS	NWS	NWS	NWS	NWS
Emission	50%	50%	75%	100%	0%	25%	50%	75%	100%
Noise	50%	50%	25%	0%	100%	75%	50%	25%	0%
Total Time Early Arrival [s]	4571	3657	4689	3735	3792	3707	4225	4251	3117
Total Time Late Arrival [s]	664	1353	4048	3193	41074	40843	32258	7723	2404
Total People Experiencing 48+ dB(A) [-]	2522630	2512645	2331508	2479248	1963022	1963626	1966642	1978213	2478201
Total People Experiencing 58+ dB(A) [-]	134667	136158	112833	122862	109224	109224	109109	115274	131976
Total Flighttime [s]	7432481	7436963	7472027	7448556	7529484	7528878	7516222	7472255	7440488
Total CO_2 Emitted [kg]	24039991	24047426	24063928	24028081	24191589	24190321	24159929	24070248	24009879

Delay

For the Delay Objective from table G.30 it is important to split the cost in Early Arrival and Late Arrival, as can be seen in table G.31. No aircraft is allowed to deviate more than 15 minutes from their arrival time. Given a total amount of flights for the Average Day of 677, this shows that the average amount of early arrival time per aircraft for all scenarios is between 4.6 and 6.8 seconds. This is relatively close to each other and a low number when taking the current planning horizon of 2 minutes into account. Similarly, the average late arrival time per aircraft for all scenarios is between 1.0 and 60.7 seconds. This is still well within the 2 minute window, but for some scenarios, especially the ones prioritizing the Noise Objective, the number is considerably higher than the average early arrival time.

Noise

From the Noise Objective costs as seen in table G.30 it is very clear that when the Noise Objective becomes more important the costs go down, which is exactly as expected. Looking at table G.31 and figure G.10 this also holds for the amount of people experiencing a certain threshold value.

An example on how the Noise contours look for each scenario for the Average day, the Noise contours of the $BASE_{E50\%,N50\%}$ scenario and the scenario with the lowest noise cost, $NWS_{E0\%,N100\%}$, are presented in figure G.11. From the noise contour it can be seen that especially over higher populated areas $NWS_{E0\%,N100\%}$ performs considerably better as it aims to stay away from these areas, which are indicated by the grey areas in the comparison figure. All noise contours for each scenario can be found in appendix I.2.

In general, it can be stated that all scenarios perform better than the $OLD_{E50\%,N50\%}$ Scenario. The addition of the 4th IAF alone can result in a decrease of 0.99% point as seen when comparing the $OLD_{E50\%,N50\%}$ Scenario with the $BASE_{E50\%,N50\%}$ Scenario. This does however come at the cost of a slightly increased amount of people that experience the average threshold level of 58+dB(A). The amount of people experiencing the threshold of 48+dB(A) decreases marginally.

Combining the extra IAF with NAS has the potential to further decrease the Noise Objective cost with 3.96% point to 11.78% point, while also decreasing the amount of people experiencing the threshold levels compared to the $OLD_{E50\%,N50\%}$ scenario, especially in the 58+dB(A) region.

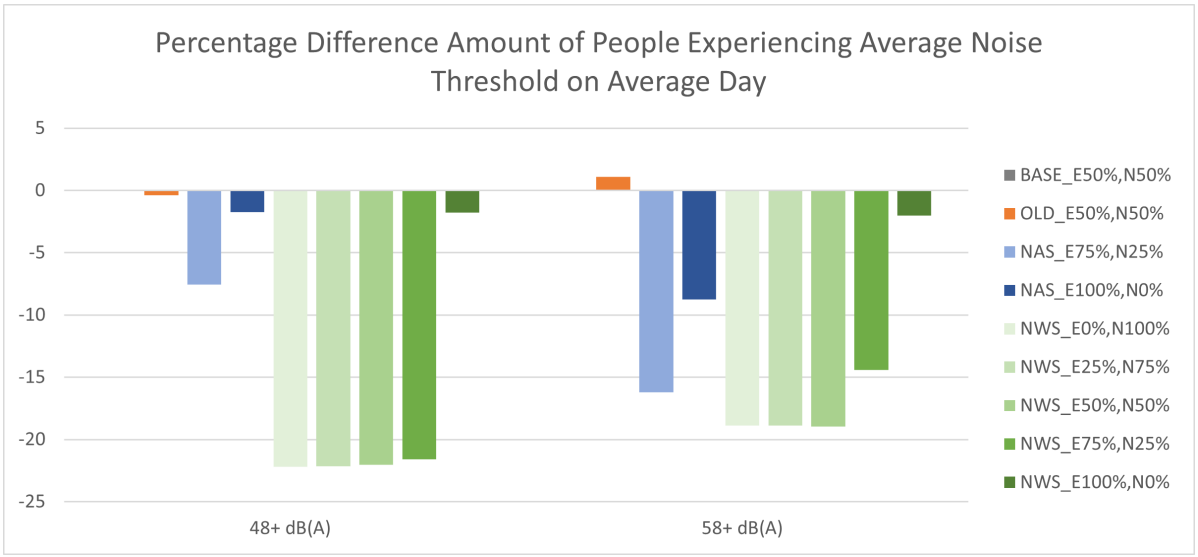

Figure G.10: Percentage Difference Amount of People Experiencing Average Noise Threshold Compared to $BASE_{E50\%,N50\%}$ Scenario on an Average Day (26 October 2019).

Looking at the NWS secenarios it is seen that an even bigger potential decrease can be achieved of 23.28% point when compared to the $BASE_{E50\%,N50\%}$ scenario, while scoring even better in the 48+dB(A) and 58+dB(A) threshold areas compared to the NAS scenarios. An important note to make here is that it is unlikely that the NWS scenarios are feasible for an average day as explained in appendix G.4.

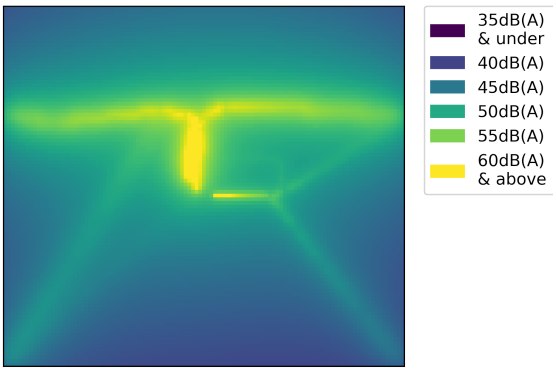

(a) L_{DEN} Average for $BASE_{E50\%,N50\%}$.

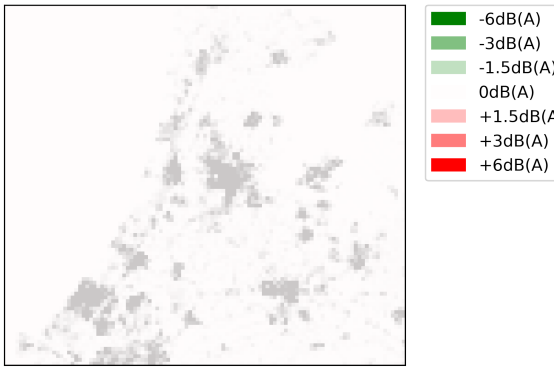

(b) Change in L_{DEN} Average Compared to $BASE_{E50\%,N50\%}$ for $BASE_{E50\%,N50\%}$.

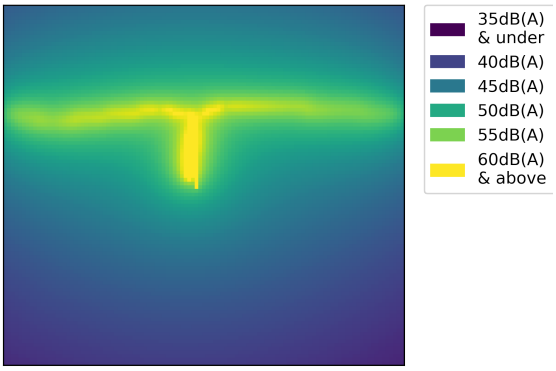

(c) L_{DEN} Average for $NWS_{E0\%,N100\%}$.

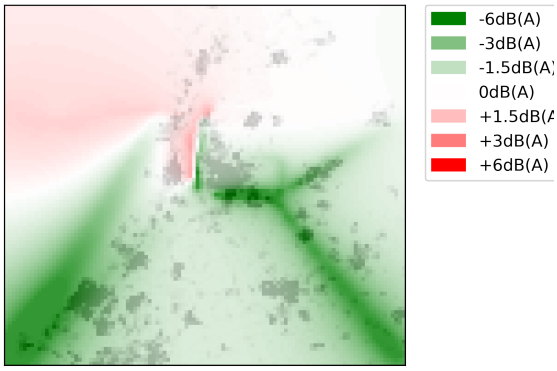

(d) Change in L_{DEN} Average Compared to $BASE_{E50\%,N50\%}$ for $NWS_{E0\%,N100\%}$.

Figure G.11: Example L_{DEN} Noise Contours for an Average Day, 26 October 2019.

Emissions and Flighttime

The Emission Objective costs can be found in figure G.2. Similar to the Noise Objective the costs go down when the objective becomes more important. From the indexed values it shows that the total difference in emitted CO_2 differs from 0.13% point ($NWS_{E100\%,N0\%}$) below the $BASE_{E50\%,N50\%}$ scenario to 0.63% point above it, as can also be seen in figure G.12. What also stands out from this graph is that the flighttime follows almost the same trend as the emissions, which of course is not very strange since if an aircraft flies longer it also uses more fuel, and thus emits more CO_2, since the Emission Objective is directly related to the fuel use of an aircraft.

The reason that the difference in Emission Objective cost between the various scenarios is limited compared to the Noise objective, is that where the full noise cost is calculated within the section between the IAF and the Runway, the emitted CO_2 is calculated for the whole flight. Thus resulting in smaller deviations in the final number. But, since the total amount of CO_2 emitted during a day, as seen in table G.29, is a high number this still has a considerable impact as a 1% point difference could mean an increase or decrease of the CO_2 emitted of approximately 240,000 kg on an average day.

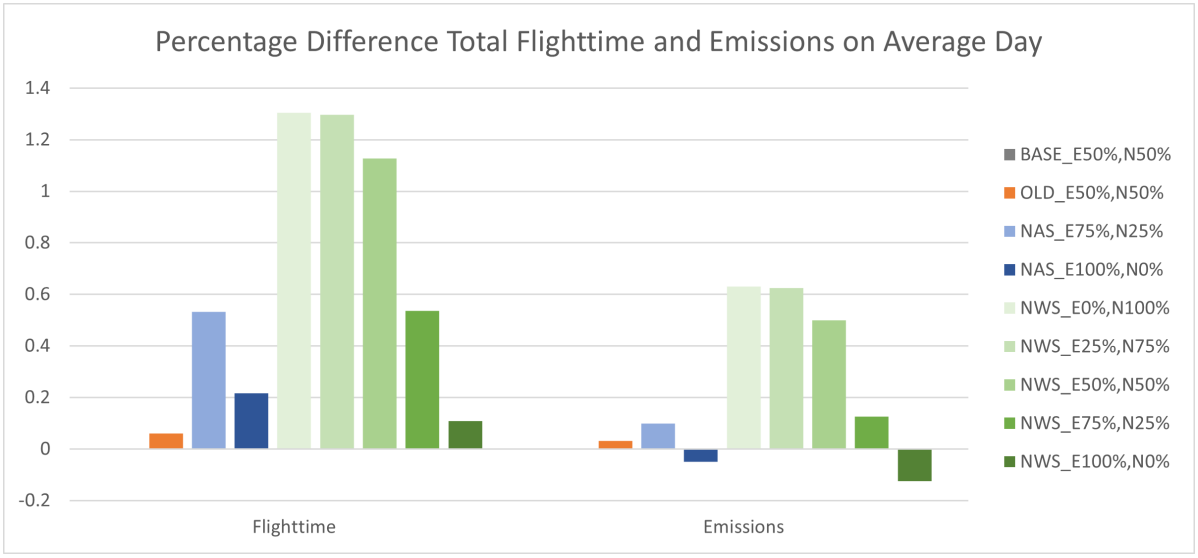

Figure G.12: Percentage Difference Total Flighttime and Emissions Compared to $BASE_{E50\%,N50\%}$ Scenario on an Average Day (26 October 2019).

In general it can be stated that adding the 4th IAF results in a CO_2 reduction of 0.03% point, as seen by looking at the $BASE_{E50\%,N50\%}$ and $OLD_{E50\%,N50\%}$ scenarios. When looking at the NAS scenarios it is seen that all have a comparable amount of emissions compared to the $BASE_{E50\%,N50\%}$ scenario. The NWS scenarios clearly show more variation with especially scenarios $NWS_{E0\%,N100\%}$, $NWS_{E25\%,N75\%}$, and $NWS_{E50\%,N50\%}$ having a higher emission cost compared to both the $BASE_{E50\%,N50\%}$ and $OLD_{E50\%,N50\%}$ scenarios. The reason for this is simple since with adding more options comes the availability of choosing less noise costly routes, but at the cost of a longer flighttime and emission cost.

For the flighttime similar trends are found.

Runway and IAF selection

In figure G.13 and figure G.14 the IAF/runway combinations used by the various scenarios can be seen compared to the $BASE_{E50\%,N50\%}$ scenario. The noise contours in appendix I.2 also give a good visual representation of the routes used for each scenario.

Adding the 4th IAF has little impact on the chosen routes for this Average Day as can be seen when comparing the $OLD_{E50\%,N50\%}$ scenario with the $BASE_{E50\%,N50\%}$ scenario. Only marginal changes can be seen since the $OLD_{E50\%,N50\%}$ scenario is not able to fly via the 4th IAF, but clearly for this day there were not a lot of aircraft that would have benefited from the extra IAF.

For the NAS scenarios the thing that stands out most is that aircraft who were scheduled originally to use ARTIP/18R and are no longer able to do so due to the East-West separation and are now diverted to ARTIP/18C, which is clearly less optimal noise wise. Similarly, but also because it is less noise costly, aircraft are

diverted from SUGOL/18C and RIVER/18R to SUGOL/18R. For the other combinations the difference with the $BASE_{E50\%,N50\%}$ and $OLD_{E50\%,N50\%}$ scenario are small.
For the NWS scenarios the combination ARTIP/18R stands out, as it is clearly favoured by the scenarios that also take noise into account, but is not favored by $NWS_{E100\%,N0\%}$ which only optimises for emission. Exactly the reverse can be seen for the ARTIP/18C combination, thus it can be concluded that the approach to 18R from ARTIP creates less noise disturbance, while ARTIP/18C provides a shorter route. The decrease in Emission Objective cost is marginal though since both runways are next to each other, which is thus also why all scenarios that take noise into account prefer to avoid it. What also stands out is that SUGOL is massively preferred by the scenarios that take noise into account. While these are avoiding RIVER, and SUGOL clearly also provides shorter routes as $NAS_{E100\%,N0\%}$ and $NWS_{E100\%,N0\%}$ also have a preference for this IAF.

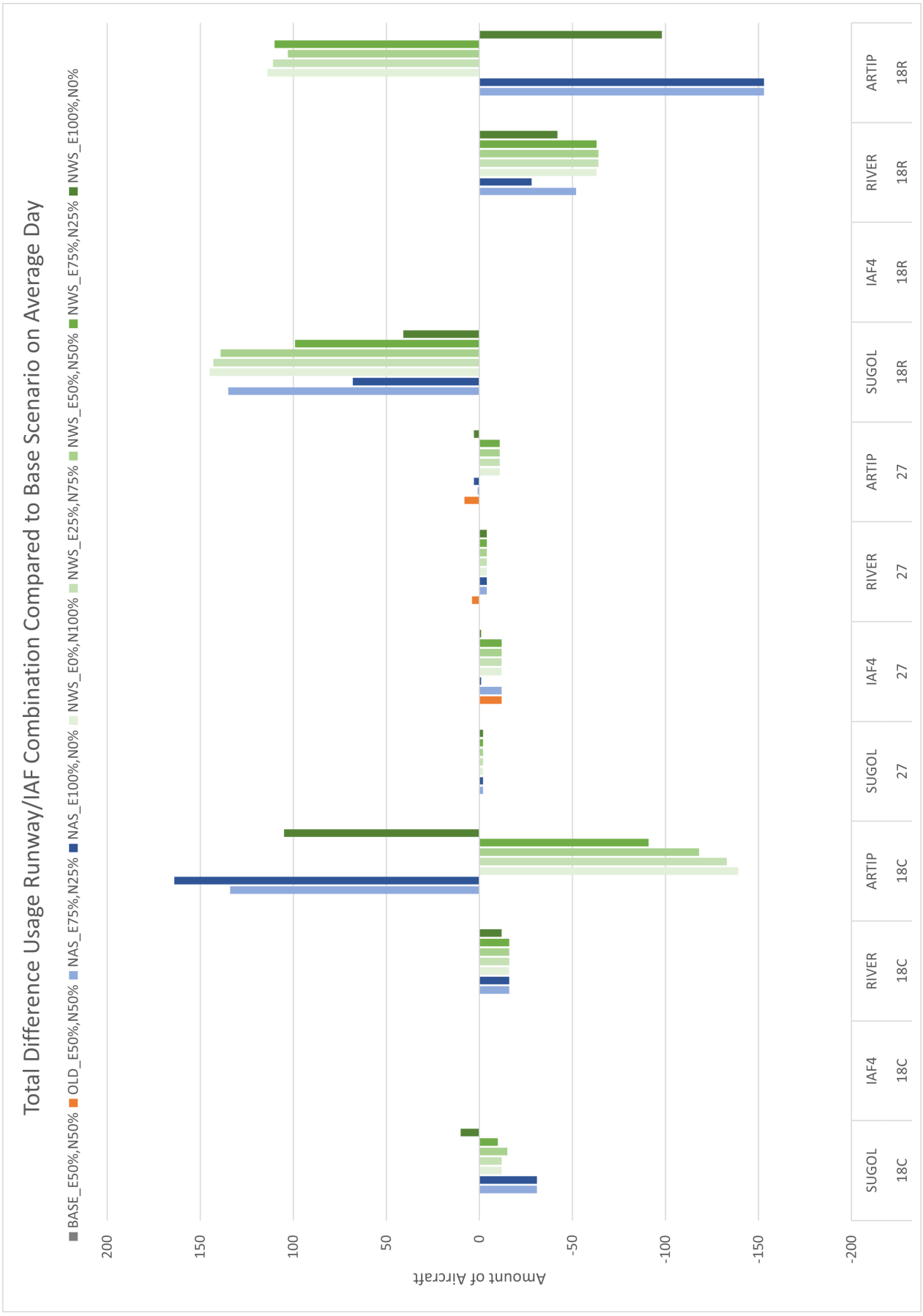

Figure G.13: Total Difference Usage IAF/Runway Combination Compared to $BASE_{E50\%,N50\%}$ Scenario on an Average Day (26 October 2019).

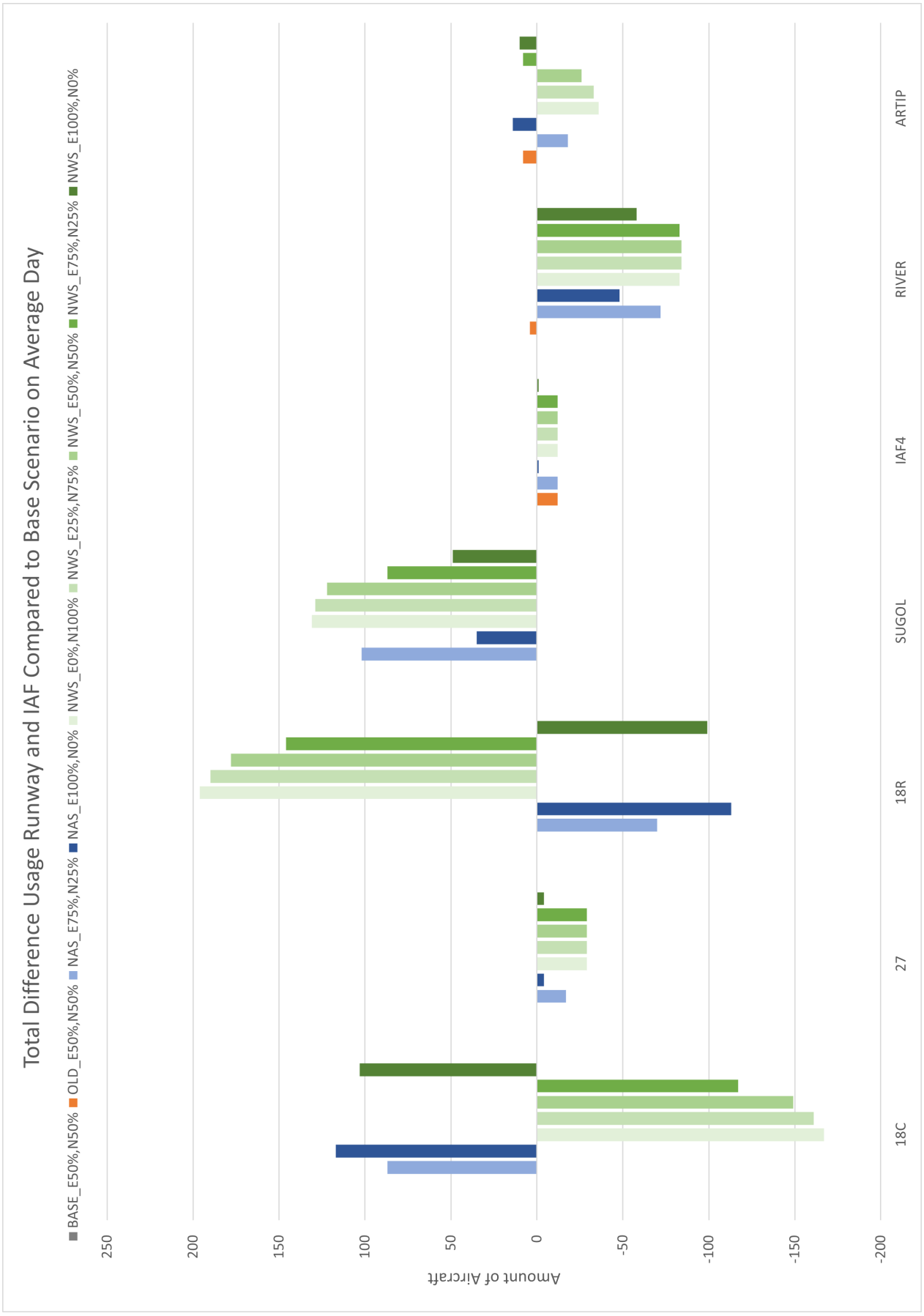

Figure G.14: Total Difference Usage Runway and IAF Compared to $BASE_{E50\%,N50\%}$ Scenario on an Average Day (26 October 2019).

G.6.3. Quiet Day, 21 March 2019

Table G.32: Objective Costs for all Pareto Optimal Scenarios for 21 March 2019 compared to $BASE_{E50\%,N50\%}$ Scenario.

Quiet Day, 21 March 2019								
Scenario	Base	OLD	NAS	NAS	NAS	NWS	NWS	NWS
Emission	50%	50%	100%/75%/50%	75%	100%	0% /25%/50%	75%	100%
Noise	50%	50%	0% /25%/50%	25%	0%	100%/75%/50%	25%	0%
Emission Objective Cost	0%	+0.01%	-0.36%	-0.41%	-1.10%	+0.02%	-0.03%	+1.1%
Noise Objective Cost	0%	+0.81%	+16.18%	+16.34%	+36.01%	-21.94%	-21.86%	+36.01%
Total Objective Cost	0%	+0.41%	+7.91%	+7.96%	+17.46%	-10.96%	-10.94%	+17.46%

Table G.33: Supporting Statistics for all Pareto Optimal Scenarios for 21 March 2019.

Quiet Day, 21 March 2019								
Scenario	Base	OLD	NAS	NAS	NAS	NWS	NWS	NWS
Emission	50%	50%	100%/75%/50%	75%	100%	0% /25%/50%	75%	100%
Noise	50%	50%	0% /25%/50%	25%	0%	100%/75%/50%	25%	0%
Total Time Early Arrival [s]	0	0	0	0	0	0	0	0
Total Time Late Arrival [s]	1	1	0	0	0	1	1	0
Total People Experiencing 48+ dB(A) [-]	2119864	2149169	2002261	2004180	2227301	1440142	1440625	2227301
Total People Experiencing 58+ dB(A) [-]	51806	51918	66747	65021	109884	34906	34906	109884
Total Flighttime [s]	5544589	5545126	5551118	5546658	5494970	5565312	5562323	5494970
Total CO_2 Emitted [kg]	18912309	18913618	18845444	18834140	18704508	18916433	18908179	18704508

Delay

For the Delay Objective from table G.32 it is important to split the cost in Early Arrival and Late Arrival, as can be seen in table G.33. No aircraft is allowed to deviate more than 15 minutes from their arrival time. But, as seen in these tables is that there is only a total of 1 second delay. This means that for the whole day there has only been 1 aircraft that needed to wait for 1 second for any scenario to use the most optimal routes available, and that no aircraft needed to arrive early. Therefore implying that on a Quiet Day there is so much available capacity that delay is no factor.

Noise

For the Noise Objective Cost as seen in table G.32, it is very clear that when the Noise Objective becomes more important the costs go down, which is exactly as expected. However when looking at table G.33 and figure G.15 this does not hold for the amount of people experiencing a certain threshold value. This is because the Noise Objective does not optimise for only these groups, but for all people affected by noise emitted around AAS. This could therefore mean that for the model it is beneficial to reduce noise for a large group that was already below the 48+dB(A) threshold at the cost of slightly more people inside the 48+dB(A) threshold area. One of the reasons for this is to prevent the model of allowing large amounts of people just below these threshold values.

An example of what this looks like can be seen in figure G.16. Here the $BASE_{E50\%,N50\%}$ scenario is shown with the scenario with the lowest noise cost, $NWS_{E0\%,N100\%}$, and how they compare to the $BASE_{E50\%,N50\%}$ scenario. From the noise contour it can be seen that especially over higher populated areas $NWS_{E0\%,N100\%}$ performs considerably better as it aims to stay away from these areas, which are indicated by the grey areas in the comparison figure. All noise contours for each scenario can be found in appendix I.3.

The addition of the 4th IAF results in a small reduction of Noise Objective cost of 0.81% point as seen when comparing the $OLD_{E50\%,N50\%}$ scenario with the $BASE_{E50\%,N50\%}$ scenario, while also decreasing the amount of people experiencing a certain average noise threshold slightly.

In contrary to previous findings for the Average and Busy Days when the 4th IAF is combined with the NAS scenario the Noise Objective cost actually increases with 16.18% point to 36.01% point instead of decreasing.

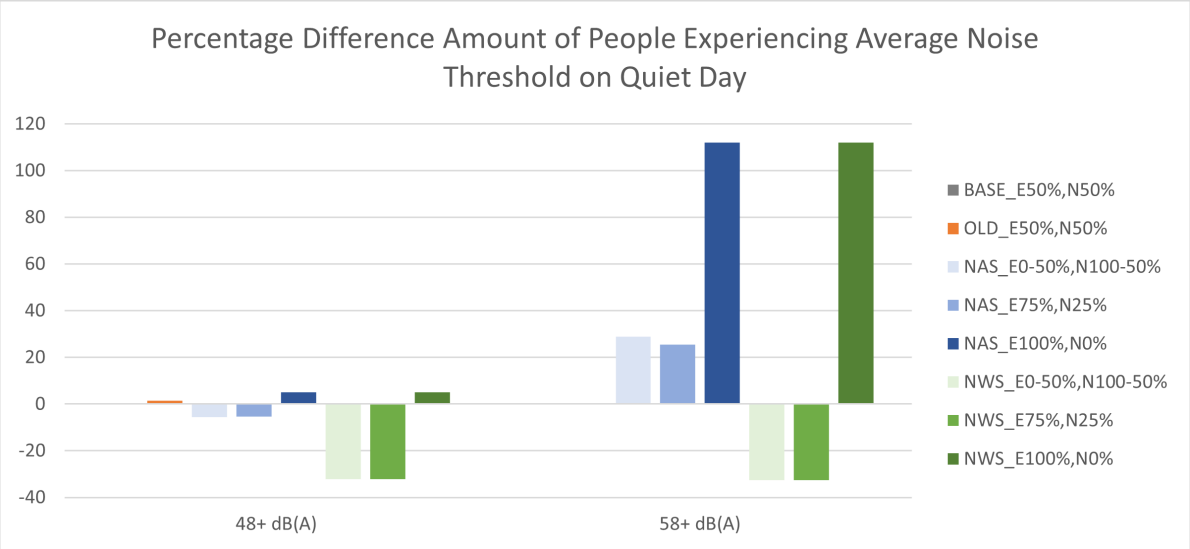

Figure G.15: Percentage Difference Amount of People Experiencing Average Noise Threshold Compared to $BASE_{E50\%,N50\%}$ Scenario on a Quiet Day (21 March 2019).

This implies that the strict East-West separation results in a worse situation noise wise than the current practice. For the amount of people experiencing a noise threshold of 48+dB(A) a slight decrease is seen for the NAS scenarios that take noise into account, and a slight increase for the Emission Objective optimized the $NAS_{E100\%,N0\%}$ scenario, but for the 58+dB(A) threshold a large increase for all NAS scenarios is seen.
For the NWS scenarios a wide range of Noise Objective costs can be seen, with $NWS_{E100\%,N0\%}$ being equal to the also only optimized on emission $NAS_{E100\%,N0\%}$ scenario. These scenarios both have an increase of the Noise Objective cost compared to the $BASE_{E50\%,N50\%}$ scenario of 36.01% point, with also a small increase in people experiencing the average threshold of 48+dB(A) and a large increase for the 58+dB(A) threshold. The other NWS scenarios all show a significant decrease in Noise Objective cost when compared to the $BASE_{E50\%,N50\%}$ scenario of 21.86% point to 21.94% point, combined with a significant decreased amount of people experiencing 48+dB(A) or 58+dB(A) threshold levels.

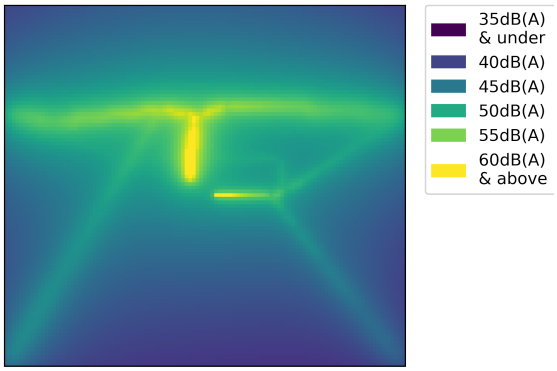

(a) L_{DEN} Average for $BASE_{E50\%,N50\%}$ Scenario.

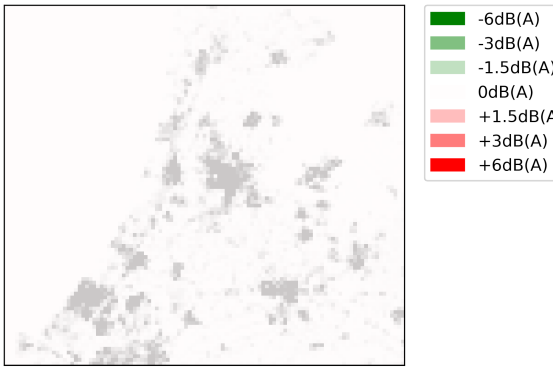

(b) Change in L_{DEN} Average Compared to $BASE_{E50\%,N50\%}$ for $BASE_{E50\%,N50\%}$.

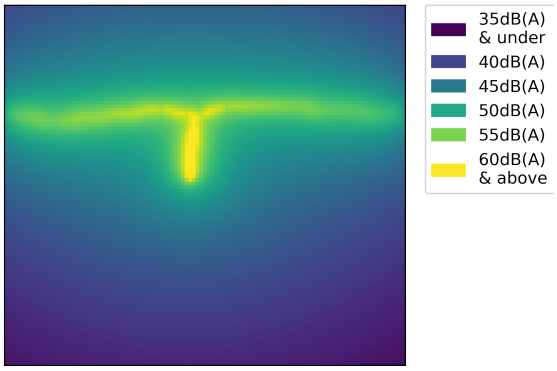

(c) L_{DEN} Average for $NWS_{E0\%,N100\%}$, $NWS_{E25\%,N75\%}$, and $NWS_{E50\%,N50\%}$.

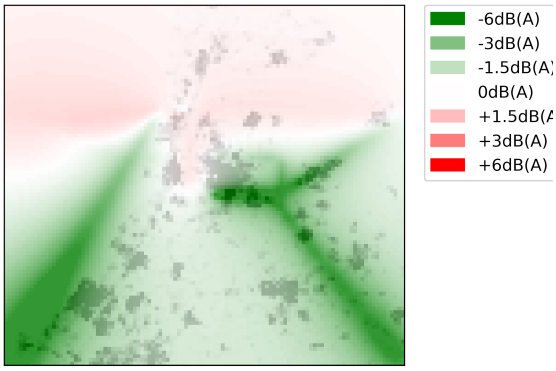

(d) Change in L_{DEN} Average Compared to $BASE_{E50\%,N50\%}$ for $NWS_{E0\%,N100\%}$, $NWS_{E25\%,N75\%}$, and $NWS_{E50\%,N50\%}$.

Figure G.16: Example L_{DEN} Noise Contours for a Quiet Day, 21 March 2019.

Emissions and Flighttime

The Emission Objective costs can be found in figure G.3. Similar to the Noise Objective the costs go down when the objective becomes more important. From the indexed values it shows that the total difference in emitted CO_2 differs from 1.10% point below the $BASE_{E50\%,N50\%}$ scenario to 0.02% point above it, as can also be seen in figure G.17.

The reason that the difference in Emission Objective cost between the various scenarios is limited compared to the Noise objective is that where the full noise cost is calculated within the section between the IAF and the Runway, the emitted CO_2 is calculated for the whole flight. This results in smaller deviations in the final number. But since the total amount of CO_2 emitted during a day, as seen in table G.29, is a high number this still has a considerable impact as a 1% point difference could mean an increase or decrease of the CO_2 emitted of approximately 189,000 kg on a quiet day.

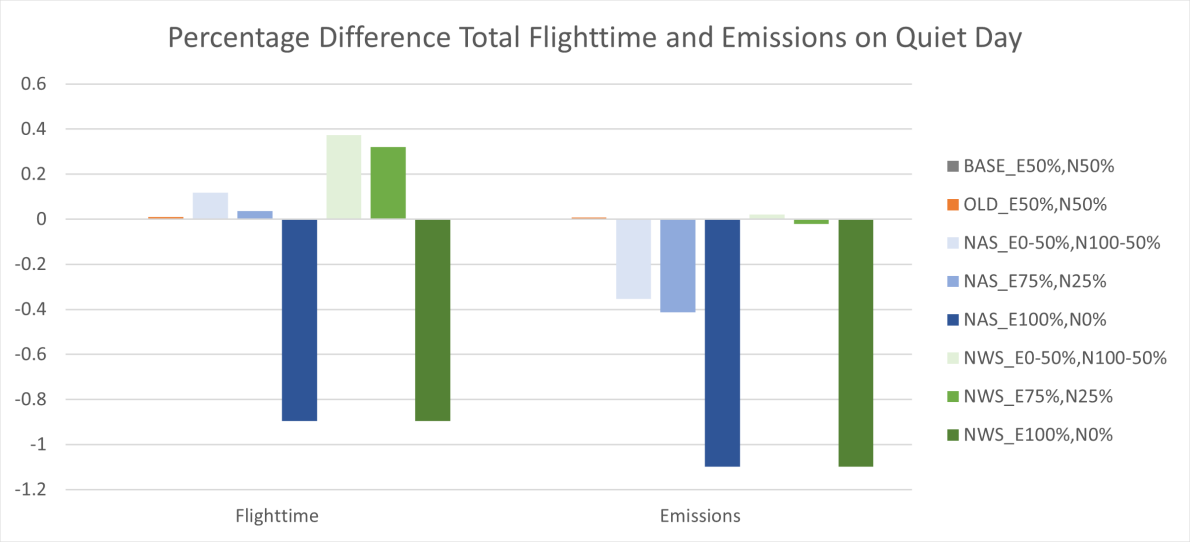

Figure G.17: Percentage Difference Total Flighttime and Emissions on a Quiet Day (21 March 2019).

In general it can be stated that adding the 4th IAF results in a CO_2 reduction of 0.01% point, as seen by looking at the $BASE_{E50\%,N50\%}$ and $OLD_{E50\%,N50\%}$ scenarios. When looking at the NAS scenarios it is seen that all have a lower or comparable amount of emissions compared to the $BASE_{E50\%,N50\%}$ scenario. For the $NWS_{E0\%,N100\%}$, $NWS_{E25\%,N75\%}$, and $NWS_{E50\%,N50\%}$ the Emission cost is highest for all scenarios, but with only an increase of 0.02% point compared to the $BASE_{E50\%,N50\%}$ scenario. $NAS_{E100\%,N0\%}$ and $NWS_{E100\%,N0\%}$, which are equal, both have the lowest Emission Objective cost with a decrease of 1.10% point compared to the $BASE_{E50\%,N50\%}$ scenario. These are also the only scenarios that show a reduction in flighttime.

Runway and IAF selection

In figure G.18 and figure G.19 the IAF/runway combinations used by the various scenarios can be seen compared to the $BASE_{E50\%,N50\%}$ scenario. The noise contours in appendix I.3 also give a good visual representation of the routes used for each scenario.

Adding the 4th IAF has little impact on the chosen routes for this Quiet Day as can be seen when comparing the $OLD_{E50\%,N50\%}$ scenario with the $BASE_{E50\%,N50\%}$ scenario. Only marginal changes can be seen since the $OLD_{E50\%,N50\%}$ scenario is not able to fly via the 4th IAF, but clearly for this day there were not a lot of aircraft that would have benefited from the extra IAF.

For the NAS scenarios that take noise into account, it is clear that since they are not able to fly from an Eastern IAF to a Western runway all traffic that goes via ARTIP/18R in the $BASE_{E50\%,N50\%}$ scenario now is redirected via ARTIP/27 or SUGOL/18R, and that traffic coming via RIVER/18R in the $BASE_{E50\%,N50\%}$ scenario is also redirected to ARTIP/27 or SUGOL/18R for these scenarios.

$NAS_{E100\%,N0\%}$ and $NWS_{E100\%,N0\%}$ both have the same solution, what stands out for these solutions is that also $NWS_{E100\%,N0\%}$ only uses Eastern IAFs with Eastern runways, and similar for Western, basically adhering voluntarily to the East-West separation $NAS_{E100\%,N0\%}$ is confined upon. This does makes sense since due to the little amount of traffic there is plenty of capacity and runways and IAFs that are on the same side have

a shorter approach and therefore use less fuel and thus less CO_2 emissions. The reason why for these two the usage of runway 18R decreases significantly is because in the $BASE_{E50\%,N50\%}$ and $OLD_{E50\%,N50\%}$ scenarios runway 27 is not available for most flights, while from an emission perspective this would have been beneficial. This is also the reason why all NWS scenarios except $NWS_{E0\%,N100\%}$ differ very little from the $BASE_{E50\%,N50\%}$ and $OLD_{E50\%,N50\%}$ scenario, since runway 18R is the least Noise Objective costly runway of the two. It must be noted that the approach via RIVER/18R is also not preferred from a noise perspective, and therefore these scenarios instead use SUGOL/18R.

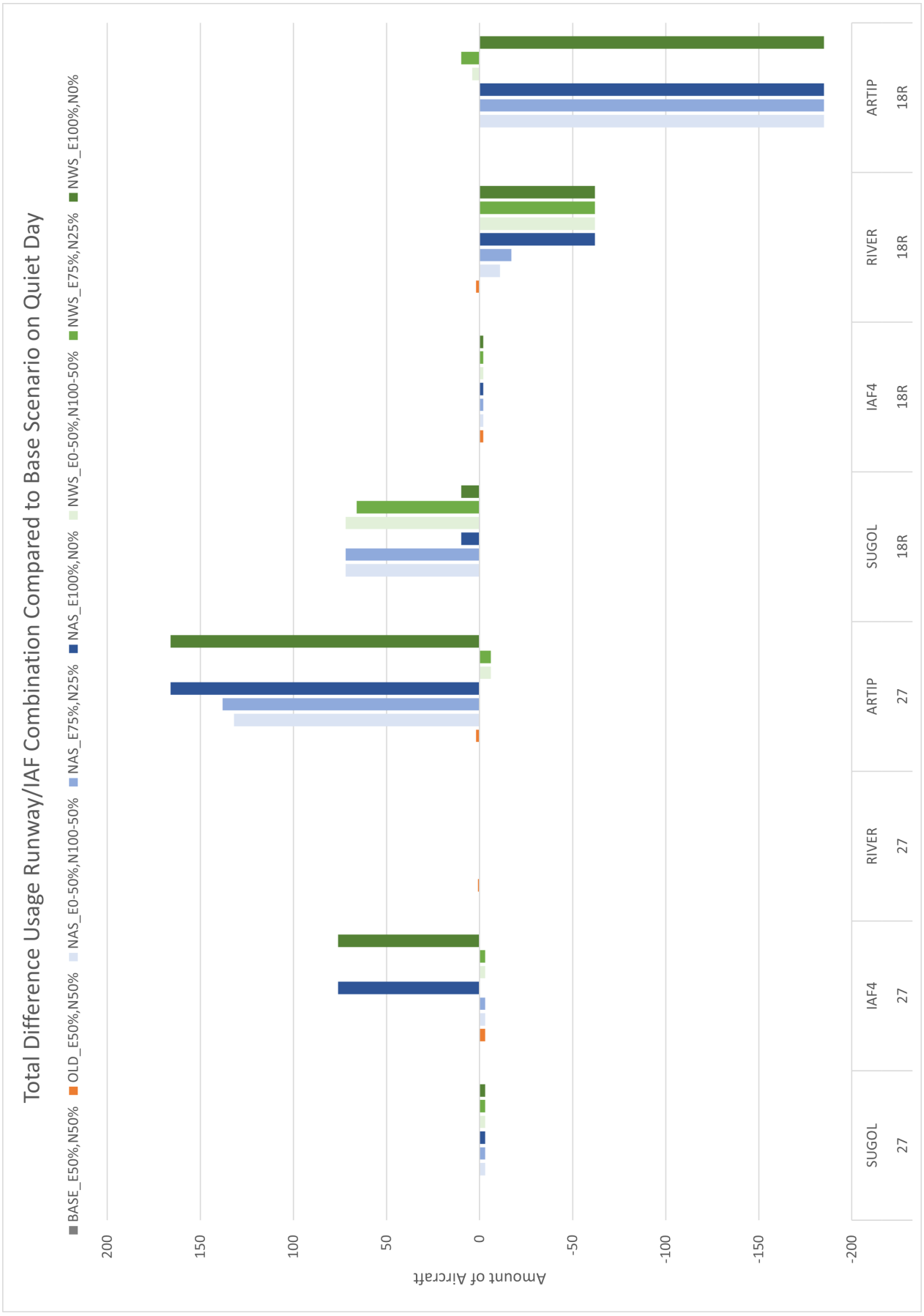

Figure G.18: Total Difference Usage IAF/Runway Combination Compared to $BASE_{E50\%,N50\%}$ Scenario on a Quiet Day (21 March 2019).

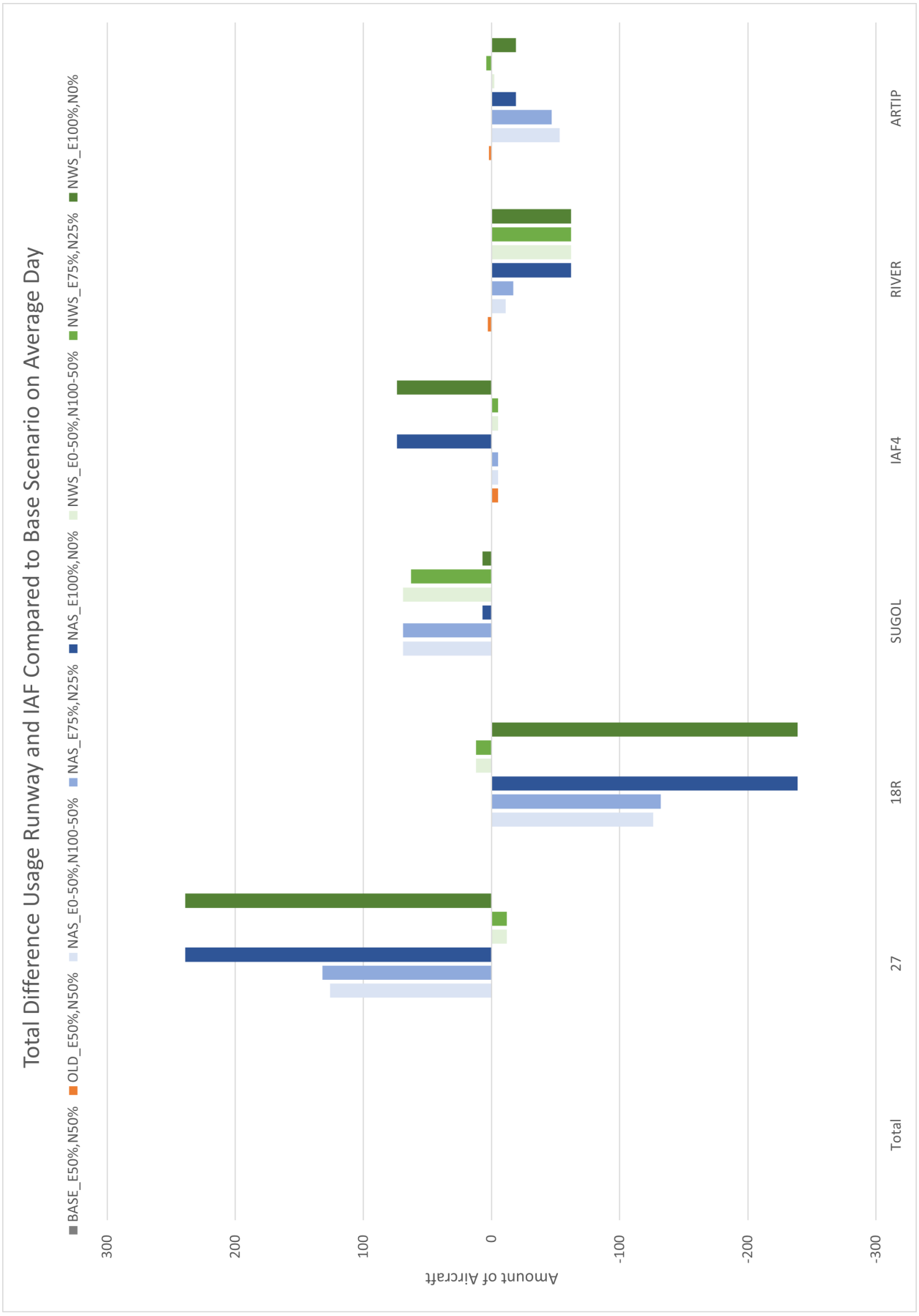

Figure G.19: Total Difference Usage Runway and IAF Compared to $BASE_{E50\%,N50\%}$ Scenario on a Quiet Day (21 March 2019).

H

Verification & Validation IAF Optimization Model

H.1. Verification

To verify that the IAF selection model performs as expected, the model is subjected to unit testing. Each formula used in the code of the model is checked by hand calculation, and for each constraint random sub-constraints were selected and checked if the constraint performs as expected. Since the model is split to run multiple increments for each day, each of the outcomes of these increments were checked if the outcome was as expected. This brought to light that there is one specific increment in scenario $NWS_{E100\%,N0\%}$ for the date 16 September 2019 between 13:35 and 14:20, which does not produce a solution. Closer investigation of the problem did not provide a reason of the failure, however replicating the situation proved that the failure to produce a solution was not an one time error, as the problem occurred also then, but still only for this specific increment, date, and scenario. Other scenarios for that day, and other days for the same scenario did produce a solution. Fortunately, the increments are chosen in a way that they have overlap with the previous and next increments, and since the increment before and after do produce a solution it was decided to not put more resources into finding the root of the problem. Instead it was decided that manually validating the outcome of the previous and next increment would prove that the total solution for the entire day would still be valid for all constraints. This is done in appendix H.2. In table H.3 an example of the final outcome of an increment can be seen. For a full day this would be similar.

H.2. Validation

For the validation of the IAF selection model random aircraft combinations were selected and checked if they comply to all the constraints. This process is very similar for all constraints, therefore it was decided to only show the validation of the increment that did not produce a solution.

The designed model failed to produce a solution while running the following settings:

Table H.1: Settings for increment that failed to produce a solution.

Constant	**Value**	**Description**
$date$	16Sep	Date run is 16 September 2019
$Starttime$	48900	Amount of seconds from start of the day (00:00) for the beginning of this increment.
$Stoptime$	51600	Amount of seconds from start of the day (00:00) for the end of this increment.
C_{NOISE}	9.370314942239448	Normalization constant for Noise Objective
$C_{EMISSION}$	0.12362506744787292	Normalization constant for Emission Objective
C_{DELAY}	1	Normalization constant for Delay Objective
$EMISSION$	100%	Importance Emission Objective compared to Noise Objective $EMISSION + NOISE = 100\%$
$NOISE$	0%	Importance Noise Objective compared to Emission Objective $EMISSION + NOISE = 100\%$
$EastWestSeparation$	$False$	If True: Strict East-West Separation meaning no aircraft can fly from a Western IAF to the Eastern runway and vice versa. If False: No East-West Separation is maintained.
$FixedRunway$	$False$	If True: Aircraft are fixed to the runway they originally landed on on the specific date run. If False: Aircraft have free choice of available runways.
$IAF4$	$True$	If True: Aircraft are allowed to fly via the 4th IAF. if False: The 4th IAF is not available

This means that no solution was found for the case where no East-West separation is enforced, the choice of available runways is free, the optimisation is purely on emission and delay, thus neglecting noise, the date was the 16th of September 2019 between 13:35 and 14:20. From the previous run already an optimal solution was found for the arriving aircraft before 14:05, leaving the gap of 15 minutes between 14:05 and 14:20. The unassigned flights are the following:

Table H.2: Unassigned flights.

Callsign	Flight ID	ADEP	DEST	ICAO_ACT	RECAT-EU	Original Arrival Time
KLM67W	20553545	EGPE	EHAM	E75L	E	14:05:38
KLM36U	20553521	EGCC	EHAM	E190	E	14:07:04
KLM1386	20553560	UKBB	EHAM	B738	D	14:08:41
KLM1846	20553555	LOWW	EHAM	B738	D	14:10:53
KLM1976	20553565	LHBP	EHAM	B737	D	14:15:25
CAI5B	20553574	LTAI	EHAM	B738	D	14:18:41

Running the next part of the optimization, the part between 14:05 and 14:50, did produce a solution for these aircraft. Since there is no overlapping of the two optimizations since the run between 13:35 and 14:20 failed, there is a chance that constraints are violated. To confirm this is not the case it was checked manually if the separation constraints are met for all aircraft. Since the solution for the aircraft between 14:05 and 14:20 is found in the run between 14:05 and 14:50 it is already guaranteed that all aircraft after 14:05 adhere to the constraints between each other. Therefore only the aircraft before 14:05 need to be checked with those after 14:05. No aircraft is allowed to be more than 15 minutes early or late, thus the time frame that needs to be checked is between 13:50 and 14:20. All aircraft in this window and their assigned time, runway and IAF are shown in table H.3.
It is thus already known that all aircraft before 14:05 (50700 seconds) and all aircraft after 14:05 adhere to the constraints and are an optimal combination. Therefore only these two sets need to be checked. This is easily done by checking the latest aircraft landing on a runway before 50700 seconds with the earliest aircraft landing on that runway after 50700 seconds. Since there are two runways this results in the following pairs.

Table H.3: Assigned Flights Between 13:50 and 14:20 on 16 September 2019 for $NWS_{E100\%,N0\%}$.

Callsign	Flight ID	ADEP	DEST	ICAO_ACT	RECAT-EU	Original Arrival Time [s]	Assigned Arrival Time [s]	Assigned Runway	Assigned IAF
KLM18M	20553513	ENGM	EHAM	E190	E	49807	49762	06	SUGOL
ICE4E	20553526	BIKF	EHAM	B752	C	49834	49827	06	SUGOL
KLM90Z	20553479	LPPT	EHAM	B738	D	49886	49921	06	RIVER
SIA7343	20553552	HKJK	EHAM	B744	B	49940	49874	36R	IAF4
KLM52X	20553506	EDDT	EHAM	B737	D	49994	49972	36R	IAF4
BEE6CP	20553568	EGHI	EHAM	DH8D	E	50086	50086	06	SUGOL
KLM26K	20553529	LOWG	EHAM	E75L	E	50086	50041	36R	IAF4
KLM78T	20553514	LIPE	EHAM	E190	E	50168	50131	36R	IAF4
AMC386	20553556	LMML	EHAM	A20N	D	50175	50176	06	RIVER
KLM20M	20553478	ESSA	EHAM	B738	D	50240	50225	36R	ARTIP
KLM1052	20553518	EGGD	EHAM	E190	E	50270	50270	06	SUGOL
KLM80A	20553512	LKPR	EHAM	B738	D	50335	50329	36R	IAF4
KLM70H	20553546	EGSH	EHAM	E75L	E	50374	50374	06	SUGOL
KLM1334	20553446	EKYT	EHAM	E190	E	50422	50419	36R	ARTIP
EJU53JD	20553564	LIRN	EHAM	A319	D	50447	50464	06	RIVER
KLM1756	20553527	EDDW	EHAM	E75L	E	50526	50514	36R	ARTIP
EJU68WE	20553542	EGPF	EHAM	A319	D	50559	50559	06	SUGOL
KLM14X	20553544	EKCH	EHAM	B737	D	50616	50604	36R	ARTIP
KLM50L	20553507	LSZH	EHAM	E190	E	50647	50649	06	RIVER
KLM67W	20553545	EGPE	EHAM	E75L	E	50738	50738	06	SUGOL
KLM36U	20553521	EGCC	EHAM	E190	E	50824	50824	06	SUGOL
KLM1386	20553560	UKBB	EHAM	B738	D	50921	50921	36R	IAF4
KLM1846	20553555	LOWW	EHAM	B738	D	51053	51053	36R	IAF4
KLM1976	20553565	LHBP	EHAM	B737	D	51325	51325	36R	IAF4
CAI5B	20553574	LTAI	EHAM	B738	D	51521	51521	36R	IAF4

Runway 36R
For runway 36R the aircraft that need to be checked are the KLM14X and KLM1386.

Table H.4: Assigned Flights KLM14X and KLM1386.

Callsign	Flight ID	ADEP	DEST	ICAO_ACT	RECAT-EU	Original Arrival Time [s]	Assigned Arrival Time [s]	Assigned Runway	Assigned IAF
KLM14X	20553544	EKCH	EHAM	B737	D	50616	50604	36R	ARTIP
KLM1386	20553560	UKBB	EHAM	B738	D	50921	50921	36R	IAF4

Since they are both from the D RECAT-EU category they need a minimum of 2.5 nautical miles separation. Since both aircraft have an estimated approach speed of 147 knots, equation (B.1) shows that the time required between the aircraft is $2.5/147 = 0.017$ hours = 61.2 seconds. Also taking into account equation (B.2) with the AROT of 45 seconds this thus results in:

$$T_{ij} = max(\mu_1, \mu_2) = max(61.2, 45) = 61.2 \text{ seconds} \tag{H.1}$$

With the time between the two assigned arrival times of the aircraft being $50921 - 50604 = 317$ seconds it can be concluded that these two aircraft adhere to the constraints.

Runway 06
For runway 06 the aircraft that need to be checked are the KLM50L and the KLM67W.

Table H.5: Assigned Flights KLM50L and KLM67W.

Callsign	Flight ID	ADEP	DEST	ICAO_ACT	RECAT-EU	Original Arrival Time [s]	Assigned Arrival Time [s]	Assigned Runway	Assigned IAF
KLM50L	20553507	LSZH	EHAM	E190	E	50647	50649	06	RIVER
KLM67W	20553545	EGPE	EHAM	E75L	E	50738	50738	06	SUGOL

Since they are both from the E RECAT-EU category they need a minimum of 2.5 nautical miles separation. Since both aircraft have an estimated approach speed of 131 knots, equation (B.1) shows that the time required between the aircraft is $2.5/131 = 0.019$ hours = 68.7 seconds. Also taking into account equation (B.2) with the AROT of 45 seconds this thus results in:

$$T_{ij} = max(\mu_1, \mu_2) = max(68.7, 45) = 68.7 \text{ seconds} \tag{H.2}$$

With the time between the two assigned arrival times of the aircraft being $50738 - 50647 = 91$ seconds it can be concluded that these two aircraft adhere to the constraints.

Therefore it can be concluded that the solution found is both optimal and viable. As to the question why in one case the model did not produce a solution no answer was found. Since a workaround is easily created, it is the only time it occurs, and it can be easily proven that an optimal solution is found no further resources are allocated to find the root of the problem.

I

Noise Contours

Table I.1: Scenario descriptions. More detailed description can be found in appendix G.

Scenario	**Description**
$BASE_{E50\%,N50\%}$	Base scenario, with $EMISSION = 50\%$ and $NOISE = 50\%$
$OLD_{E50\%,N50\%}$	Old scenario, with $EMISSION = 50\%$ and $NOISE = 50\%$
$NAS_{E0\%,N100\%}$	NAS scenario, with $EMISSION = 0\%$ and $NOISE = 100\%$
$NAS_{E25\%,N75\%}$	NAS scenario, with $EMISSION = 25\%$ and $NOISE = 75\%$
$NAS_{E50\%,N50\%}$	NAS scenario, with $EMISSION = 50\%$ and $NOISE = 50\%$
$NAS_{E75\%,N25\%}$	NAS scenario, with $EMISSION = 75\%$ and $NOISE = 25\%$
$NAS_{E100\%,N0\%}$	NAS scenario, with $EMISSION = 100\%$ and $NOISE = 0\%$
$NWS_{E0\%,N100\%}$	NWS scenario, with $EMISSION = 0\%$ and $NOISE = 100\%$
$NWS_{E25\%,N75\%}$	NWS scenario, with $EMISSION = 25\%$ and $NOISE = 75\%$
$NWS_{E50\%,N50\%}$	NWS scenario, with $EMISSION = 50\%$ and $NOISE = 50\%$
$NWS_{E75\%,N25\%}$	NWS scenario, with $EMISSION = 75\%$ and $NOISE = 25\%$
$NWS_{E100\%,N0\%}$	NWS scenario, with $EMISSION = 100\%$ and $NOISE = 0\%$

I.1. Busy day, 16 September 2019

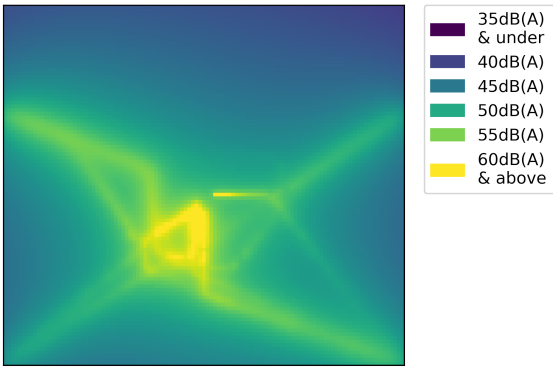

(a) L_{DEN} Average for $BASE_{E50\%,N50\%}$.

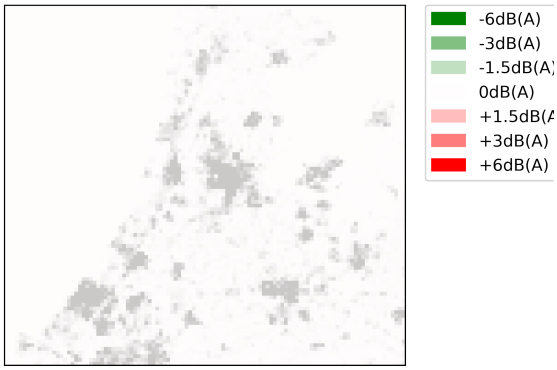

(b) Change in L_{DEN} Average Compared to $BASE_{E50\%,N50\%}$ for $BASE_{E50\%,N50\%}$.

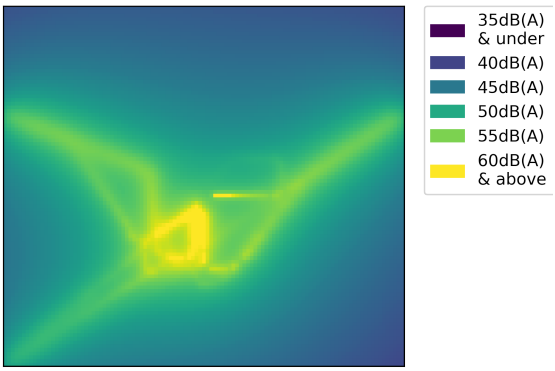

(c) L_{DEN} Average for $OLD_{E50\%,N50\%}$.

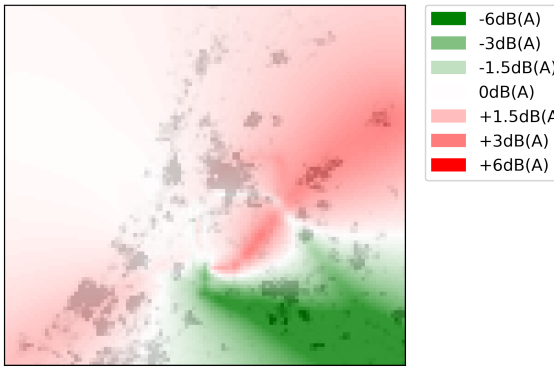

(d) Change in L_{DEN} Average Compared to $BASE_{E50\%,N50\%}$ for $OLD_{E50\%,N50\%}$.

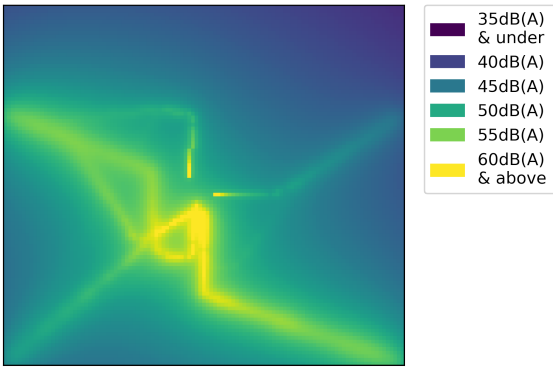

(e) L_{DEN} Average for $NAS_{E50\%,N50\%}$.

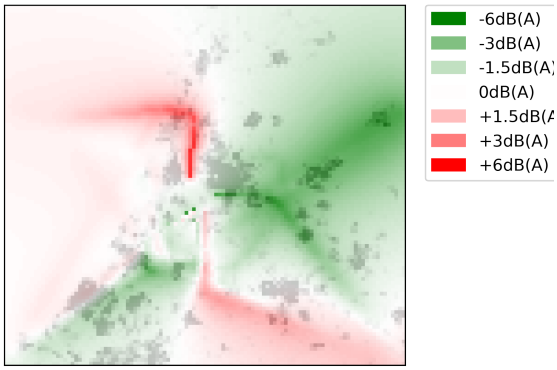

(f) Change in L_{DEN} Average Compared to $BASE_{E50\%,N50\%}$ for $NAS_{E50\%,N50\%}$.

Figure I.1: L_{DEN} Noise Contours for a Busy Day, 16 September 2019, Part 1/4.

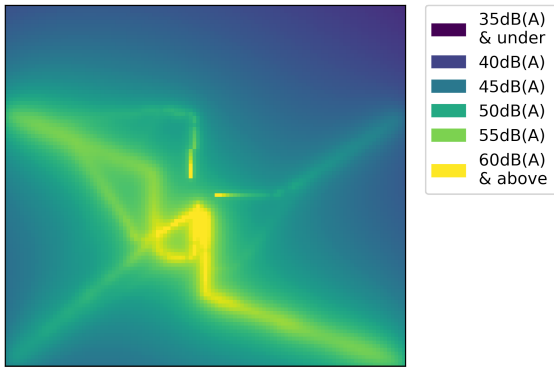

(a) L_{DEN} Average for $NAS_{E75\%,N25\%}$.

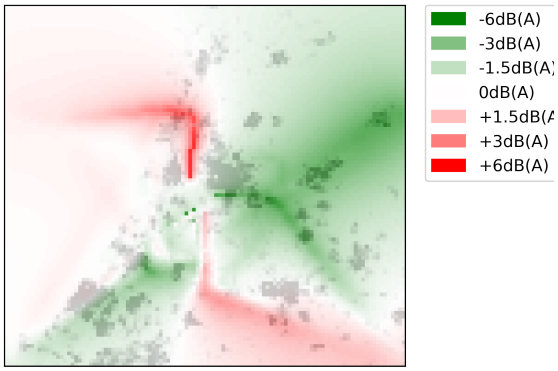

(b) Change in L_{DEN} Average Compared to $BASE_{E50\%,N50\%}$ for $NAS_{E75\%,N25\%}$.

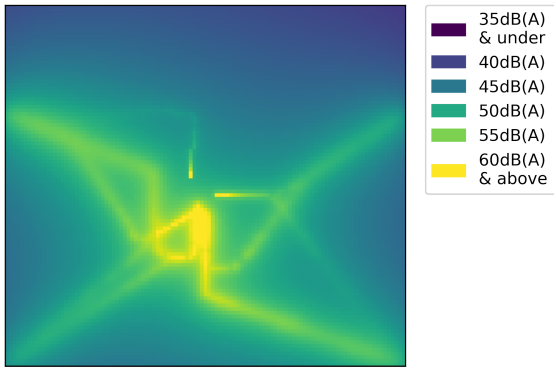

(c) L_{DEN} Average for $NAS_{E100\%,N0\%}$.

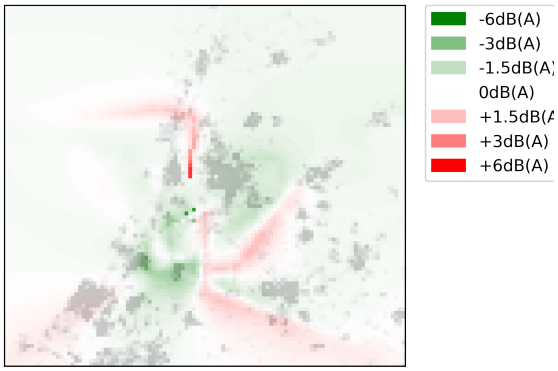

(d) Change in L_{DEN} Average Compared to $BASE_{E50\%,N50\%}$ for $NAS_{E100\%,N0\%}$.

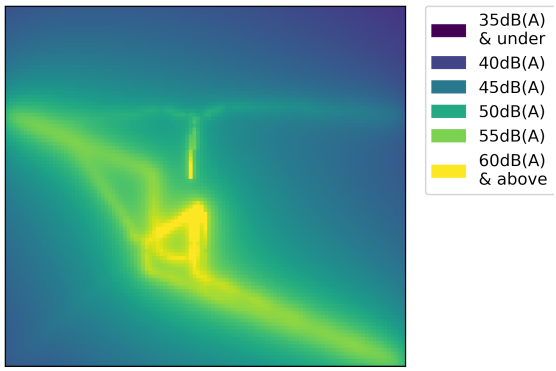

(e) L_{DEN} Average for $NWS_{E0\%,N100\%}$.

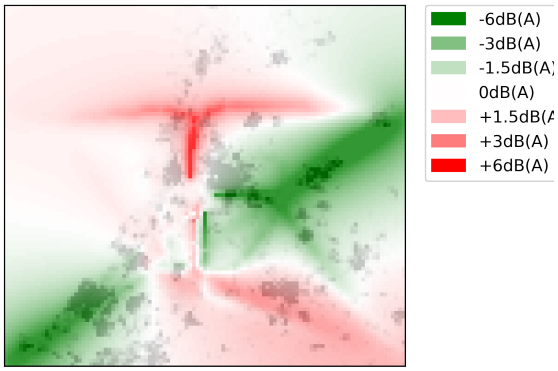

(f) Change in L_{DEN} Average Compared to $BASE_{E50\%,N50\%}$ for $NWS_{E0\%,N100\%}$.

Figure I.2: L_{DEN} Noise Contours for a Busy Day, 16 September 2019, Part 2/4.

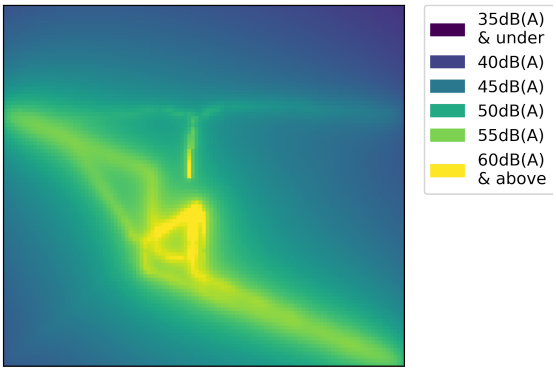

(a) L_{DEN} Average for $NWS_{E25\%,N75\%}$.

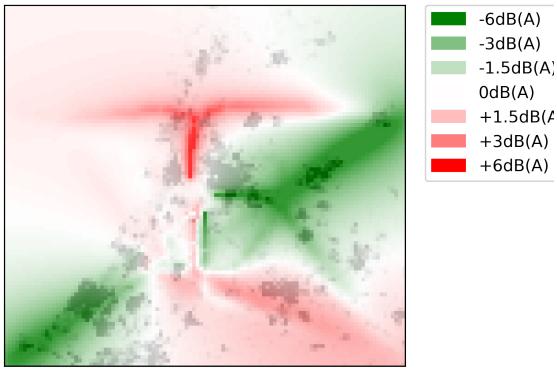

(b) Change in L_{DEN} Average Compared to $BASE_{E50\%,N50\%}$ for $NWS_{E25\%,N75\%}$.

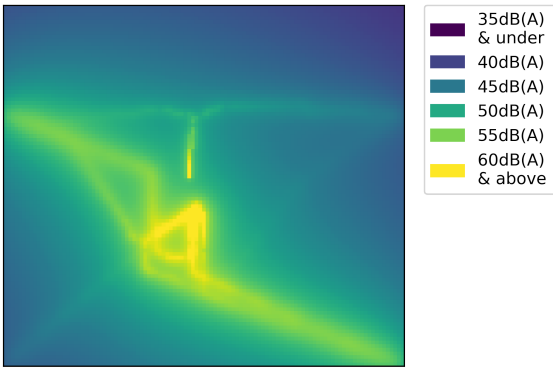

(c) L_{DEN} Average for $NWS_{E50\%,N50\%}$.

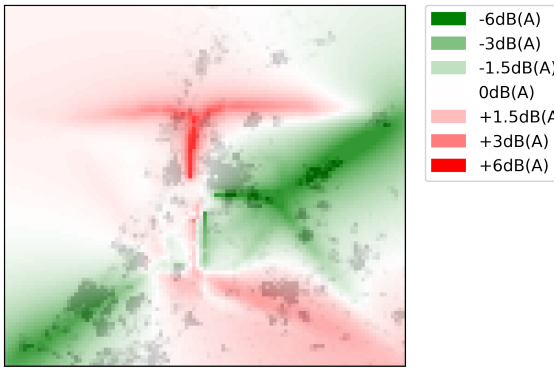

(d) Change in L_{DEN} Average Compared to $BASE_{E50\%,N50\%}$ for $NWS_{E50\%,N50\%}$.

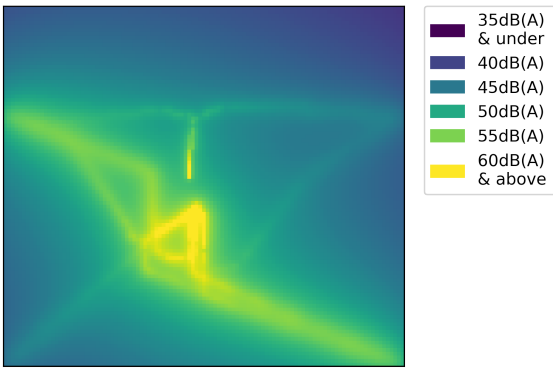

(e) L_{DEN} Average for $NWS_{E75\%,N25\%}$.

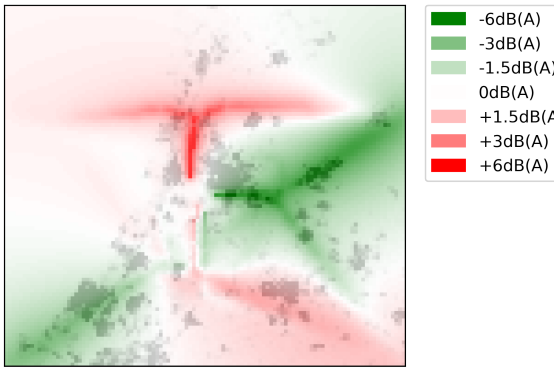

(f) Change in L_{DEN} Average Compared to $BASE_{E50\%,N50\%}$ for $NWS_{E75\%,N25\%}$.

Figure I.3: L_{DEN} Noise Contours for a Busy Day, 16 September 2019, Part 3/4.

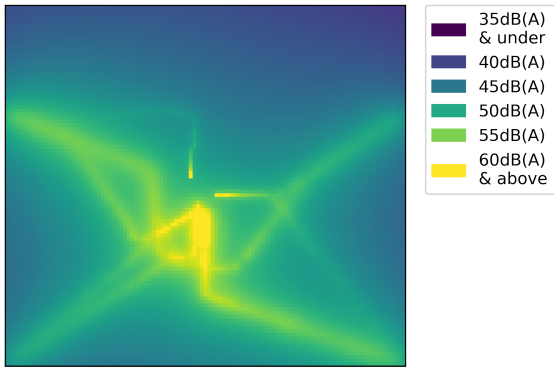

(a) L_{DEN} Average for $NWS_{E100\%,N0\%}$.

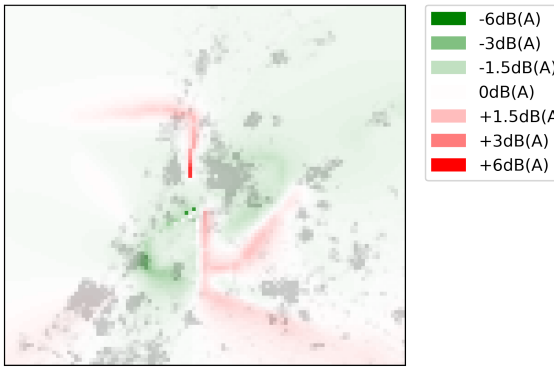

(b) Change in L_{DEN} Average Compared to $BASE_{E50\%,N50\%}$ for $NWS_{E100\%,N0\%}$.

Figure I.4: L_{DEN} Noise Contours for a Busy Day, 16 September 2019, Part 4/4.

I.2. Average Day, 26 October 2019

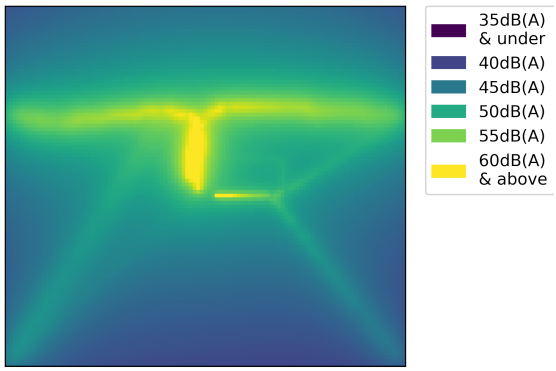

(a) L_{DEN} Average for $BASE_{E50\%,N50\%}$.

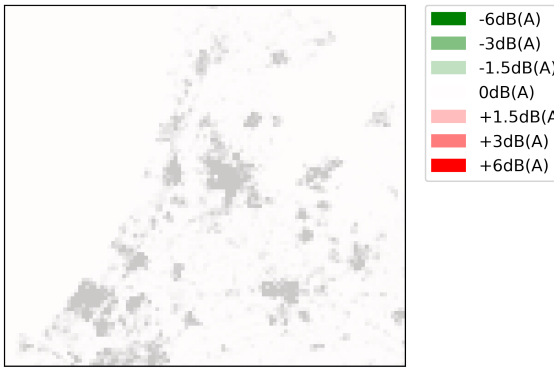

(b) Change in L_{DEN} Average Compared to $BASE_{E50\%,N50\%}$ for $BASE_{E50\%,N50\%}$.

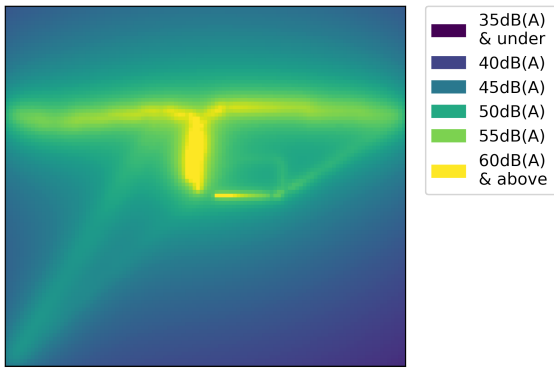

(c) L_{DEN} Average for $OLD_{E50\%,N50\%}$.

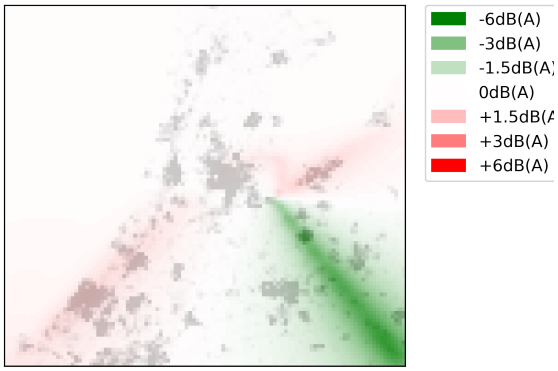

(d) Change in L_{DEN} Average Compared to $BASE_{E50\%,N50\%}$ for $OLD_{E50\%,N50\%}$.

Figure I.5: L_{DEN} Noise Contours for an Average Day, 26 October 2019, Part 1/4.

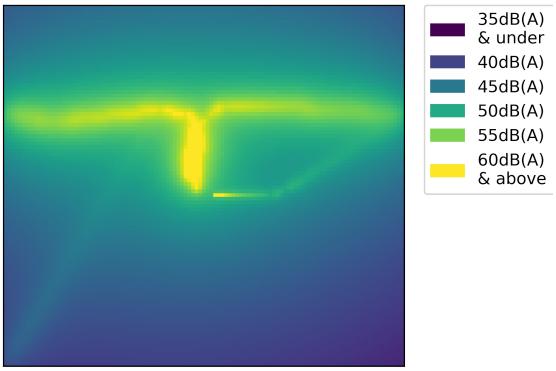

(a) L_{DEN} Average for $NAS_{E75\%,N25\%}$.

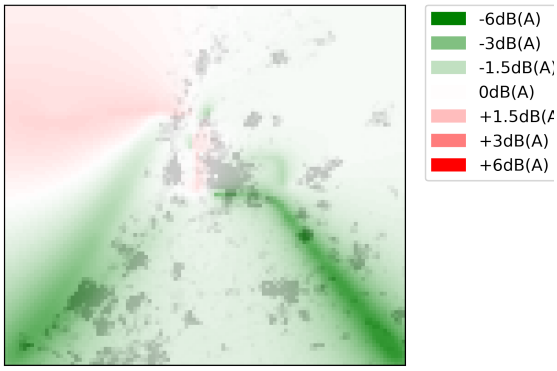

(b) Change in L_{DEN} Average Compared to $BASE_{E50\%,N50\%}$ for $NAS_{E75\%,N25\%}$.

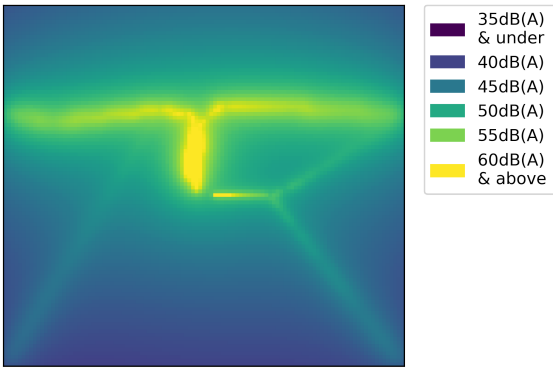

(c) L_{DEN} Average for $NAS_{E100\%,N0\%}$.

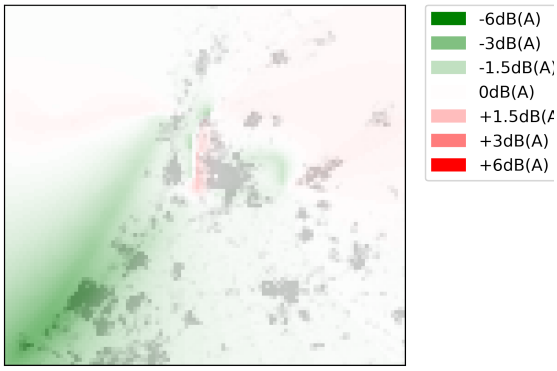

(d) Change in L_{DEN} Average Compared to $BASE_{E50\%,N50\%}$ for $NAS_{E100\%,N0\%}$.

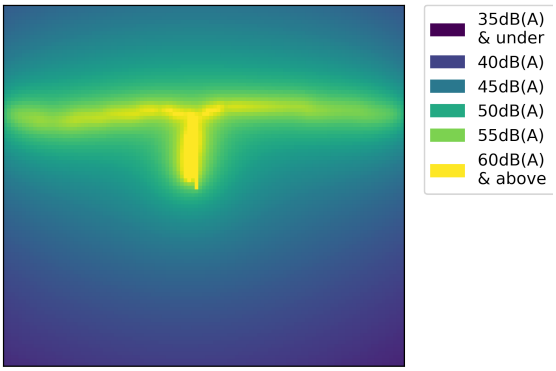

(e) L_{DEN} Average for $NWS_{E0\%,N100\%}$.

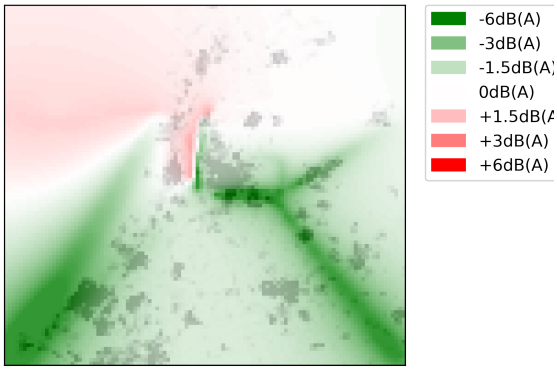

(f) Change in L_{DEN} Average Compared to $BASE_{E50\%,N50\%}$ for $NWS_{E0\%,N100\%}$.

Figure I.6: L_{DEN} Noise Contours for an Average Day, 26 October 2019, Part 2/4.

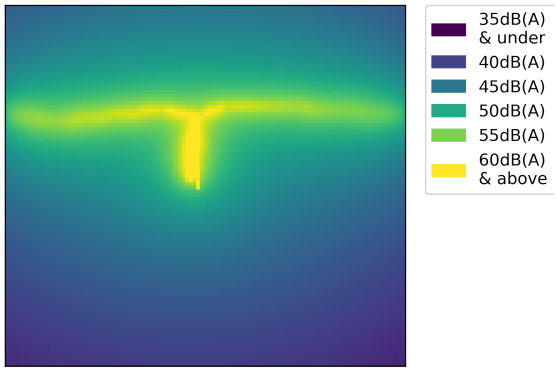

(a) L_{DEN} Average for $NWS_{E25\%,N75\%}$.

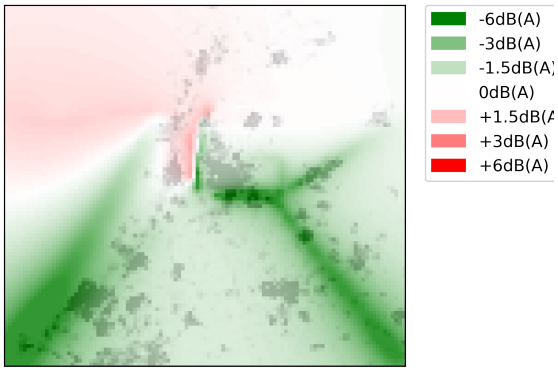

(b) Change in L_{DEN} Average Compared to $BASE_{E50\%,N50\%}$ for $NWS_{E25\%,N75\%}$.

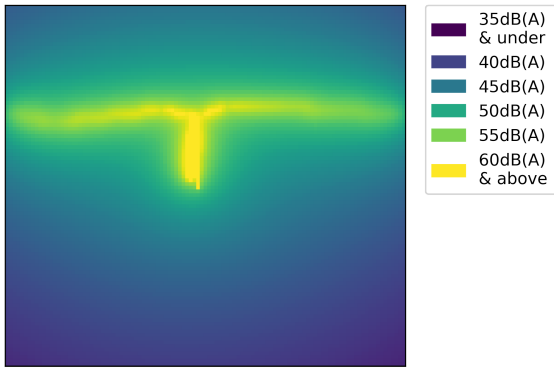

(c) L_{DEN} Average for $NWS_{E50\%,N50\%}$.

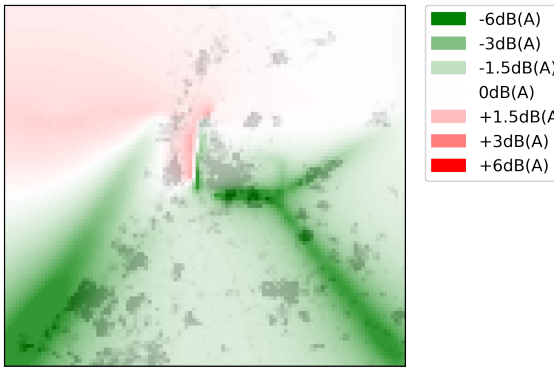

(d) Change in L_{DEN} Average Compared to $BASE_{E50\%,N50\%}$ for $NWS_{E50\%,N50\%}$.

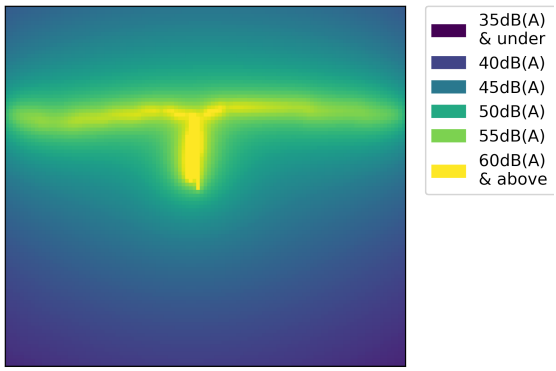

(e) L_{DEN} Average for $NWS_{E75\%,N25\%}$.

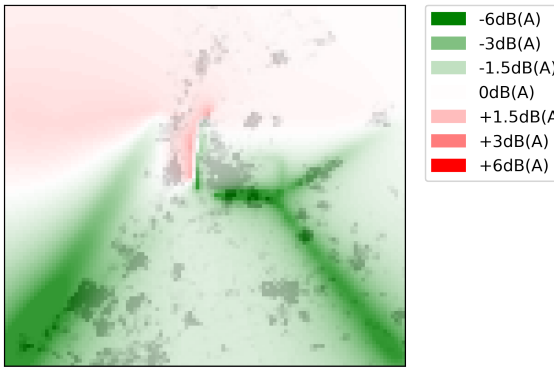

(f) Change in L_{DEN} Average Compared to $BASE_{E50\%,N50\%}$ for $NWS_{E75\%,N25\%}$.

Figure I.7: L_{DEN} Noise Contours for an Average Day, 26 October 2019, Part 3/4.

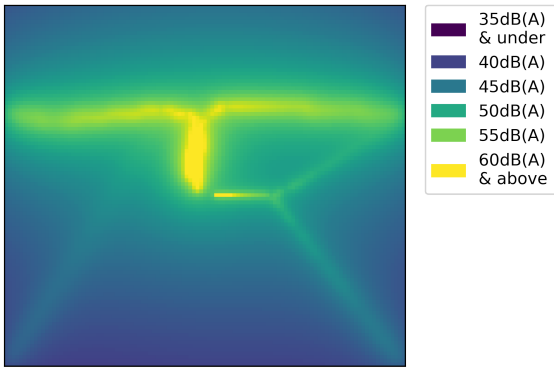

(a) L_{DEN} Average for $NWS_{E100\%,N0\%}$.

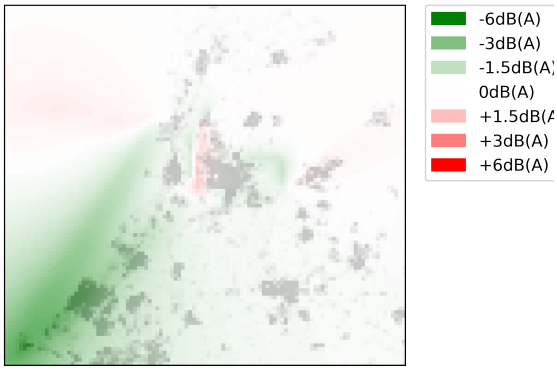

(b) Change in L_{DEN} Average Compared to $BASE_{E50\%,N50\%}$ for $NWS_{E100\%,N0\%}$.

Figure I.8: L_{DEN} Noise Contours for an Average Day, 26 October 2019, Part 4/4.

I.3. Quiet day, 21 March 2019

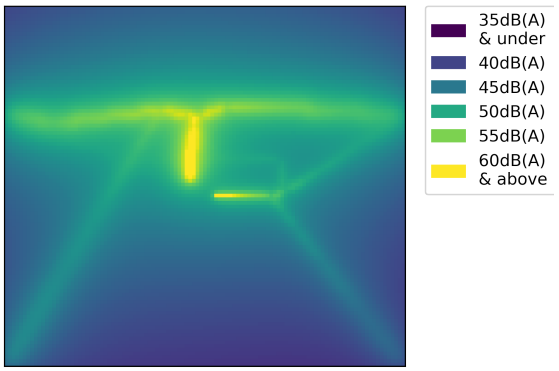

(a) L_{DEN} Average for $BASE_{E50\%,N50\%}$.

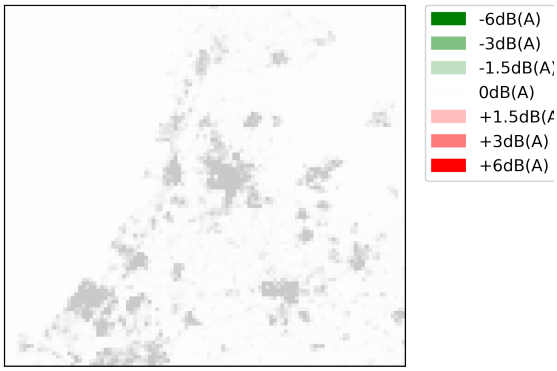

(b) Change in L_{DEN} Average Compared to $BASE_{E50\%,N50\%}$ for $BASE_{E50\%,N50\%}$.

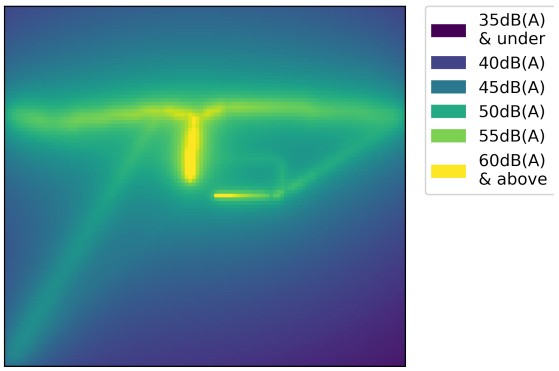

(c) L_{DEN} Average for $OLD_{E50\%,N50\%}$.

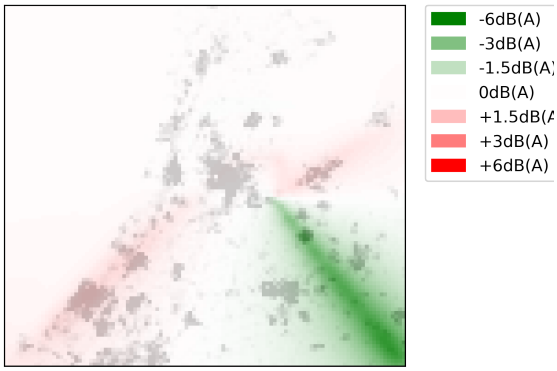

(d) Change in L_{DEN} Average Compared to $BASE_{E50\%,N50\%}$ for $OLD_{E50\%,N50\%}$.

Figure I.9: L_{DEN} Noise Contours for a Quiet Day, 21 March 2019, Part 1/3.

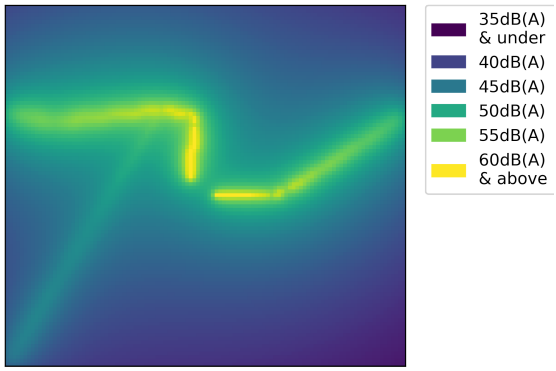

(a) L_{DEN} Average for $NAS_{E0\%,N1000\%}$, $NAS_{E25\%,N75\%}$, and $NAS_{E50\%,N50\%}$.

(b) Change in L_{DEN} Average Compared to $BASE_{E50\%,N50\%}$ for $NAS_{E0\%,N1000\%}$, $NAS_{E25\%,N75\%}$, and $NAS_{E50\%,N50\%}$.

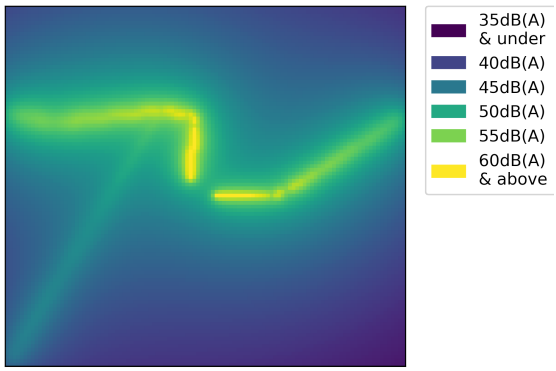

(c) L_{DEN} Average for $NAS_{E75\%,N25\%}$.

(d) Change in L_{DEN} Average Compared to $BASE_{E50\%,N50\%}$ for $NAS_{E75\%,N25\%}$.

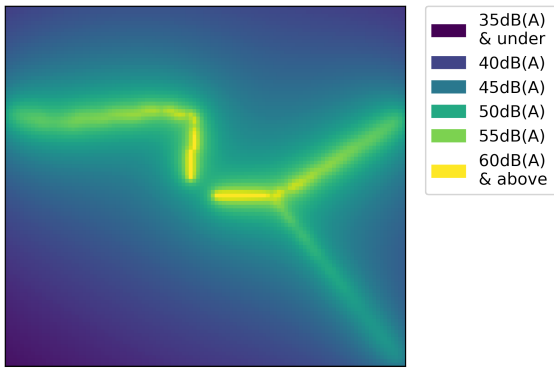

(e) L_{DEN} Average for $NAS_{E100\%,N0\%}$.

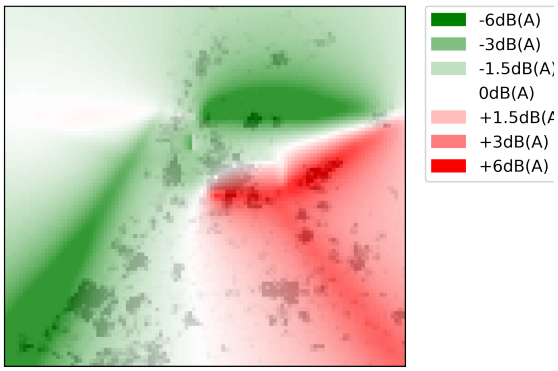

(f) Change in L_{DEN} Average Compared to $BASE_{E50\%,N50\%}$ for $NAS_{E100\%,N0\%}$.

Figure I.10: L_{DEN} Noise Contours for a Quiet Day, 21 March 2019, Part 2/3.

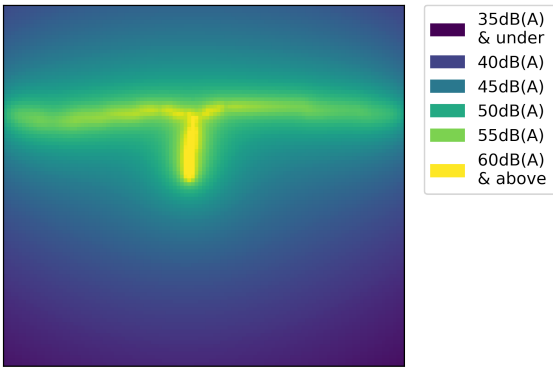

(a) L_{DEN} Average for $NWS_{E0\%,N1000\%}$, $NWS_{E25\%,N75\%}$, and $NWS_{E50\%,N50\%}$.

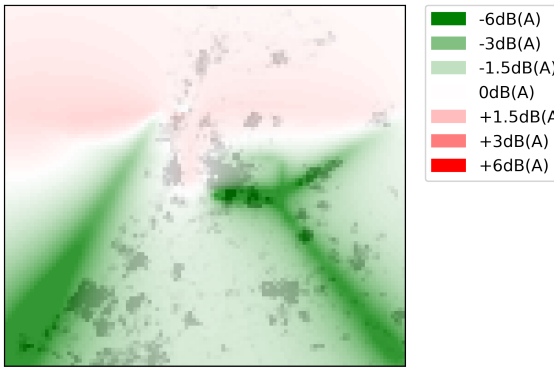

(b) Change in L_{DEN} Average Compared to $BASE_{E50\%,N50\%}$ for $NWS_{E0\%,N1000\%}$, $NWS_{E25\%,N75\%}$, and $NWS_{E50\%,N50\%}$.

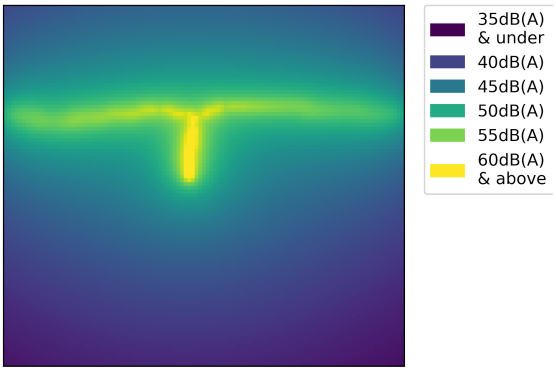

(c) L_{DEN} Average for $NWS_{E75\%,N25\%}$.

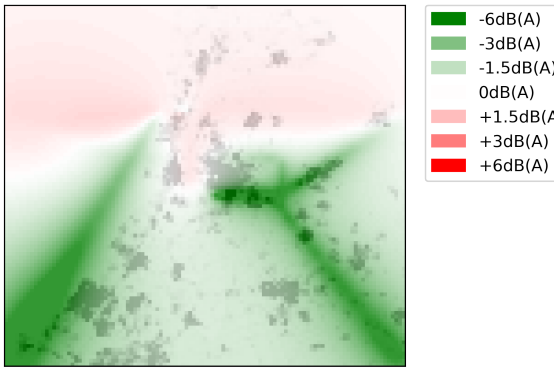

(d) Change in L_{DEN} Average Compared to $BASE_{E50\%,N50\%}$ for $NWS_{E75\%,N25\%}$.

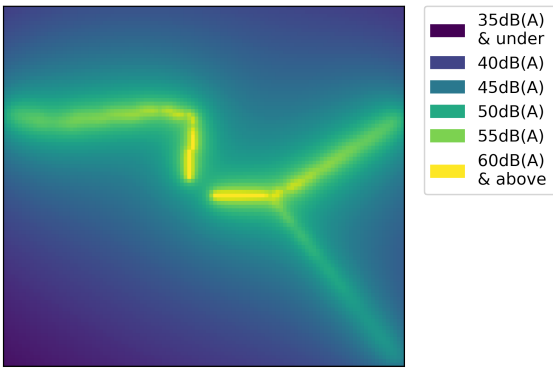

(e) L_{DEN} Average for $NWS_{E100\%,N0\%}$.

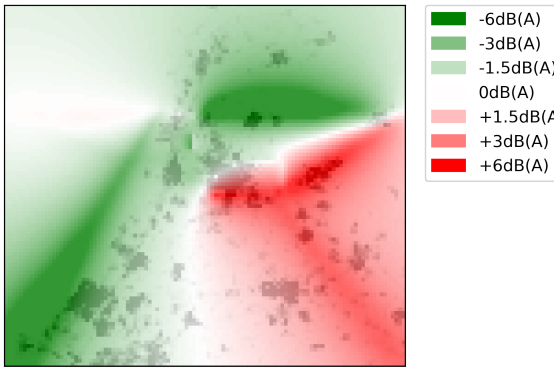

(f) Change in L_{DEN} Average Compared to $BASE_{E50\%,N50\%}$ for $NWS_{E100\%,N0\%}$.

Figure I.11: L_{DEN} Noise Contours for a Quiet Day, 21 March 2019, Part 3/3.